GA–A28213

DEVELOPMENT OF ASTM STANDARD FOR SiC-SiC JOINT TESTING

Final Report

by
Project Staff

Prepared for the
U.S. Department of Energy
under Grant No. DE-NE0000612

DATE PUBLISHED: OCTOBER 2015

GENERAL ATOMICS

DISCLAIMER

GA–A28213

DEVELOPMENT OF ASTM STANDARD FOR SiC-SiC JOINT TESTING

Final Report

by
Project Staff

Prepared for the
U.S. Department of Energy
under Grant No. DE-NE0000612

GENERAL ATOMICS PROJECT 30403
DATE PUBLISHED: OCTOBER 2015

GENERAL ATOMICS

TABLE OF CONTENTS

LIST OF FIGURES

LIST OF TABLES

1. EXECUTIVE SUMMARY

As the nuclear industry moves to advanced ceramic based materials for cladding and core structural materials for a variety of advanced reactors, new standards and test methods are required for material development and licensing purposes. For example, General Atomics (GA) is actively developing silicon carbide (SiC) based composite cladding (SiC-SiC) for its Energy Multiplier Module (EM^2), a high efficiency gas cooled fast reactor. Through DOE funding via the advanced reactor concept program, GA developed a new test method for the nominal joint strength of an endplug sealed to advanced ceramic tubes, Fig. 1-1, at ambient and elevated temperatures called the endplug pushout (EPPO) test. This test utilizes widely available universal mechanical testers coupled with clam shell heaters, and specimen size is relatively small, making it a viable post irradiation test method. The culmination of this effort was a draft of an ASTM test standard that will be submitted for approval to the ASTM C28 ceramic committee. Once the standard has been vetted by the ceramics test community, an industry wide standard methodology to test joined tubular ceramic components will be available for the entire nuclear materials community.

Fig. 1-1. A SiC-SiC tube joined with a monolithic SiC Endplug

In addition to the standard itself, several key innovations came from this work. A large number of purposely misaligned specimens were tested and guidelines developed for alignment that is expected to be applicable to a number of advanced ceramic tube test methods. Finite Element Modeling (FEM) was used to show that the EPPO test correlated well to pressure burst testing over a wide range of specimen geometry and compositions. Investigation of joining SiC to nickel superalloy based metals was required as part of the high temperature test methodology and several viable active brazes were identified for metal to SiC bonding. During testing, GA demonstrated that its GA-HSiC joint material maintains its strengths at test temperatures up to 800 °C, the operating temperature for the EM^2 reactor, Fig. 1-2. Statistical analysis showed a statistical spread for GA-HSiC consistent with a low porosity ceramic based joint material (Weibull Modulus = 7.8). Post test fractography was combined with FEM to help understand failure stresses and improvements to endplug design were made based on these analyses. This data will be used in modeling efforts to help further EM^2 as well as eventual licensing of SiC as a reactor core material.

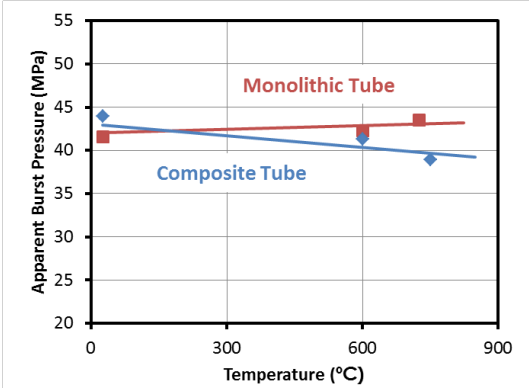

Fig. 1-2. Strength as measured with the EPPO test as function of temperature for SiC tube

2. SUMMARY OF ACCOMPLISHMENTS

For each of the project objectives listed below a summary of the qualitative and quantitative results are provided. These objectives are based off project deliverables and multiple project tasks contributed to each objective:

1) **A well-defined and experimentally validated methodology for gripping and alignment of joined specimens at room temperature.**
    - Investigated active and passive gripping and determined that passive gripping is the best choice for EPPO test methodology.
    - Identified high shear strength epoxies for testing up to 300ºC and brazes for testing up to 800ºC.
    - Investigated three different types of misalignment in the system and determined guideline for allowable bending (<20% imbalance as measured via strain).
    - Defined a set of dimensional tolerances that define a valid test without the use of strain gauges during testing.
    - Identified that fracture must occur in joint region for a test to be determined valid.
    - Performed increasingly complex FEM to help determine that the test is ideal for quality control, material comparison, and specification purposes.

2) **Validate room temperature test methodology by testing a variety of joint types and specimen geomoetries and by testing a large specimen set for statistical analysis.**
    - Tested a set of 30 specimens using GA-HSiC joint material and obtained characteristic nominal burst strength of 48 MPa and a Weibull modulus of 3.8.
    - Performed XCT of specimens to correlate failure with joint structure and inform statistical spread.
    - Demonstrated the versatility of test by testing a variety of specimens including different joint types, tube diameter, and endplug geometry.
    - Evaluated the use of Bilinear Isotropic Hardening as a means to model composite behavior to add versatility to the model.
    - Used experimental results both with and without a chamfer on the endplug to validate the FEM.

3) **Comparison and correlation of data with a second geometrically relevant test method via hydrostatic burst pressure testing.**
    - Performed hydrostatic burst testing on three joint candidates for experimental comparison to EPPO.
    - Utilized FEM to compare internal pressurization versus axial force only for a large set of boundary conditions including wall thickness, joint/tube modulus, and others.
    - Brought together FEM and experimental data to demonstrate that EPPO testing typically results in higher strengths than hydrostatic burst testing, and the results correlate to each other.

- Defined conditions where this correlation may need further evaluation, such as when residual processing stress is present in the specimens.

4) **A statistically significant data set for testing of tube-endplug assemblies at elevated temperature.**
   - Modified the room temperature test method for high temperature use including identification of high temperature fixture materials.
   - Identified brazes for use in passive bonding that allow test temperatures up to 1200ºC.
   - Developed a methodology for high temperature strain gauge application and in-test measurement.
   - Demonstrated the versatility of EPPO test by performing high temperature testing on a variety of specimens and temperatures up to 800ºC
   - Tested a set of 25 specimens of GA-HSiC at 600ºC and obtained characteristic nominal burst strength of 46 MPa and a Weibull modulus of 7.8.
   - Explained the failure behavior observed in the set of 25 specimens using the previously developed FEM.
   - Used FEM to evaluate the effects of residual stress on the grip regions due to CTE mismatching of brazes.

5) **Drafting and submittal of an ASTM standard for high temperature testing of SiC/SiC joints via the endplug pushout test.**
   - Worked with C28 ceramics committee to keep them updated on progress of standard and anticipated submission date.
   - Collaborated with Steve Gonczy, an expert in ASTM ceramic test standards, for writing of standard.
   - Wrote draft standard of the EPPO test entitled “Standard Test Method for the Nominal Joint Strength of End-Plug Joints in Advanced Ceramic Tubes at Ambient and Elevated Temperatures”, see Appendix C
   - Formalized commitment to submit the standard by obtaining a work item number from the ASTM C28 committee
   - Pre-balloting review of the standard is currently being performed and formal submittal will occur before the end of the year.

3. PROJECT ACTIVITIES

3.1. Background

The development of ceramic matrix composite (CMC) technology, including accurate and reliable test methods for measuring the mechanical properties of CMCs, is an important area of enabling research and development (R&D) for advanced nuclear reactors. Silicon carbide (SiC) fiber-reinforced SiC matrix CMCs (SiC-SiC) are a particularly attractive material for fuel rod cladding in advanced reactor concepts such as General Atomics’ gas-cooled fast reactor (EM^2),

liquid metal reactors, and advanced molten salt reactors. SiC-SiC is also being looked at for use as accident tolerant fuel in current generation light water reactors (LWR). The capability to fabricate high-strength, radiation-tolerant, impermeable joints between tubular SiC-SiC cladding and a monolithic SiC or SiC-SiC endplug that seals the fuel inside the cladding is essential to the use of SiC-SiC for this purpose, and General Atomics (GA) and others are currently developing the requisite SiC joining technology. While planar joint standards are available[1], a standard for tubular geometries is not. The lack of a standard test method for measuring the mechanical strength of the joint between the SiC-SiC cladding and endplug is an impediment to development and licensing of SiC-SiC fuel rod cladding.

DOE funded GA under its advanced reactor concept program (DOE-NE0000612) to address this critical need and what follows is a final report on the work performed. During the period of performance, GA has developed a robust, reliable test method named the Endplug Pushout (EPPO) test. This test is used for measuring the mechanical strength of endplug seals to tubular SiC-SiC cladding that can meet the rigorous requirements for an ASTM International (ASTM) standard. To have widespread applicability across the nuclear and ceramics communities, the test method was designed to be versatile, and functional over a wide range of temperatures. The test methodology uses existing test equipment and relatively small sized specimens, making it capable of testing irradiated specimens. Versatility was addressed by ensuring that the method is applicable for a variety of endplug geometries and for different joining techniques such as metal brazing, reaction bonding, and pre-ceramic polymers. Most importantly, the test was developed for use at elevated temperatures relevant to a variety of advanced reactor designs. This was very critical to the success of the project as testing at elevated temperatures is impractical using more conventional methods like hydrostatic burst testing or internal pressurization burst testing. Development of the method has culminated in a draft of an ASTM standard for the test method, and the resulting data from testing will be used to gain approval of the ASTM standard and to develop joint criteria for codes and specifications for use in reactor design and licensing.

In the EPPO test specialized fixturing is used to hold the specimen in place while an axial load is applied using a universal mechanical tester. This fixture features a load rod, a support block, and a split conical collet. A schematic of the test fixture are shown in Fig. 3-1. The mechanical load rod connects to the load train of the test frame via clevis pin. The specimen is held in place using an active or passive gripping mechanism, being careful to minimize induced damage in the tube portion of the specimen. The specimen is held in the support block with the endplug on the bottom, and the open end of the specimen on the top. The mechanical load rod inserts into the open end of the cladding tube and is lowered until it is incident on the inside surface of the endplug before conducting the test. A force is then applied directly to the endplug via the mechanical load rod, until failure occurs.

[1] ASTM C1469 “Standard Test Method for Shear Strength of Joints of Advanced Ceramics at Ambient Temperature”, ASTM International, Westhconshoken, NY (2015)

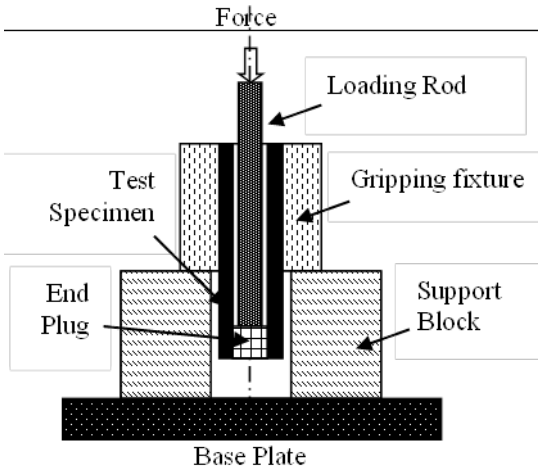

Fig. 3-1. Overview of the fixturing associated with the EPPO test

This project was built on previous work by General Atomics in which an endplug pushout test, Fig 3-2. was used at room temperature to examine GA fabricated joints. During this background work, a fixture that relies on passive gripping of the test piece was designed and fabricated under INL contract BEA PO 128790[2]. Test data using passive gripping was obtained on monolithic and composite joints using a scarf geometry endplug. For the monolithic material, an average load at failure was 1544 N with a standard deviation of 506 N was obtained. For composite material an average load of 2292 N with a standard deviation of 448 N was obtained. The typical load versus extension graph for composite material, as seen in Fig. 3-3, show a near linear increase in load with a roll off near the failure point. This roll off is expected and due to crack formation in the joint before full failure occurs.

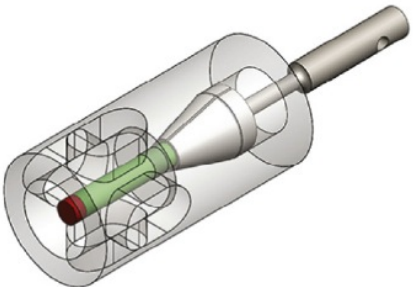

Fig. 3-2 (left). Fixturing used for the initial EPPO test work.

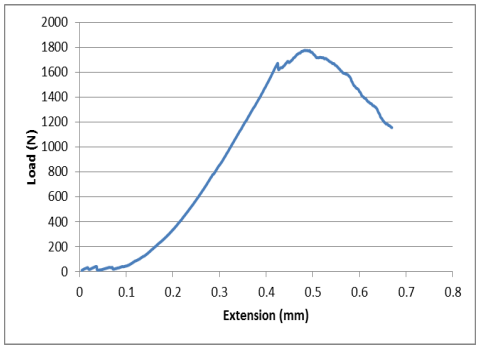

Fig. 3-3 (right). Typical load versus extension plot for a composite endplug pushout test.

This background work effectively demonstrated the utility of the method, but also demonstrated key areas where additional development was required. In that work, the focus was

[2] Khalifa, Hesham "Technology for Joining Silicon Carbide Ceramic Matrix Composites for Nuclear Fuel Cladding" Final Report Prepared for the Battelle Energy Alliance, LLC (BEA, GA document # GA-C27672 (2013).

on evaluation of joint strength for different endplug geometries and little method development took place. All testing was performed at room temperature and neither the reproducibility nor versatility of the method was demonstrated. In addition, minimal attempt was made to compare results of this test method to more commonly available test methods, such as pressure burst testing. In order to develop this work into a test method of sufficient quality to be considered an ASTM standard, these topics were addressed in the work performed.

3.2. Room Temperature Test Methodology

Development of the room temperature method was performed before transitioning to the more time intensive and difficult high temperature testing. Focus was placed on gripping of the specimen and alignment of the specimen in the test fixture. Alignment and gripping are two of the most important factors in test methods for ceramics and ceramic composites as damaging of the specimen prior to testing and bending of the specimen during testing has been shown to cause drastic reduction in measured strengths.

3.2.1. Gripping

Initial investigation focused on how to grip onto a ceramic tube both at room temperature and at elevated temperature. The method must not damage the component and yet remain functional at the high temperatures the joints will experience during testing. Investigation of gripping focused on the critical decision point between active and passive gripping methods with the maximum load that can be applied to the endplug using different gripping options being the key decision point. The goal was to make the resulting ASTM standard as widely encompassing as possible, so the applied axial load must be large enough that a wide range of joint designs and materials can be tested. Based on available literature on SiC joint strength and GA measurements on its own joining approach, shear strength as measured on planar joints can be in excess of 250 MPa, although more typical values are 100 MPa[3]. Calculating load for tubular geometry for LWR sized tubing based on this shear strength suggests that axial loading in excess of 25,000 N could be required to push out endplugs, although more typical loads were found to be <10,000 N.

3.2.1.1. PASSIVE GRIPPING

Passive gripping utilizes an adhesive to bond the test specimen to the fixture. The benefit of this approach is it eliminates the possibility of specimen damage as a result of gripping. At room temperature this method is very straight forward and easy to setup, however, adhesives typically cannot sustain elevated temperatures. Investigation of several high temperature adhesives for the passive bonding of the tube onto the test fixture was performed. Although the ultimate goal for the proposed work was testing at 800 ºC, tests were also performed with lower temperatures.

[3] S. Bragg-Sitton, "Status of Silicon Carbide Joining Technology Development" *US DOE Report# INL/EXT-13-30286*, **2013.**

For passive bonding, a fixture was used where the specimen is held between the split conical collet, Fig. 3-4, and for room temperature testing a high strength epoxy is used to bond the specimen to the collet. The angle of the collet helps to self-align the test specimen as well as apply a small amount of normal force to the tube to aide in grip strength. During testing, the load rod inserts into the open end of the cladding tube and load is applied onto the endplug until failure occurs.

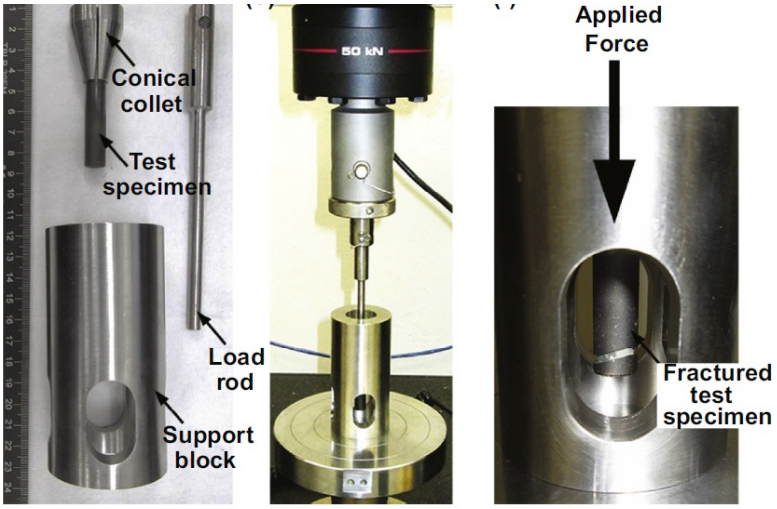

Fig. 3-4. Fixturing and application of load used during EPPO test when using passive gripping

In order to test the high temperature capability of these adhesives, residual strength was measured at room temperature after taking to use temperatures suggested by the manufacturers, Table 3-1. The adhesives were applied to a 1" section of tube and bonded onto the stainless steel collets, Fig. 3-5. Each adhesive was cured according to the directions given by the manufacturer. Adhesives were then heat treated by taking to the use temperature listed in table 3-1 for 30 minutes. The specimens were cooled back down to room temperature at which point residual strength was measured by compressing the joint/fixture specimen against platens in a mechanical testing unit. Three to four tests were performed for each adhesive.

Table 3-1. Measured strengths at room temperature after exposing joint for 30 minutes to the maximum temperature recommended for use

Adhesive	Type	Use Temp (°C)	Measured Residual Load (N)
Masterbond EP46HT	Epoxy	280	30,000
Epotec H74	Epoxy	280	4,000
Aremco 890	Glass	700	500
Morgan Incusil	Braze	730	16,000

Ceramabond 668	Ceramic	850+	500
Saureisen #1	Ceramic	850+	1000
Morgan Ticuni	Braze	1000	200

Fig. 3-5. Bonded monolithic tube to stainless steel collets using Morgan Incusil Braze.

Results from this testing show that for temperatures up to 280 °C commercially available high temperature epoxies, such as Masterbond EP46HT, are able to meet the needs of the test as load values above 30,000 N are sufficiently large to test a large variety of joint materials. At temperatures above 280 °C epoxies begin to degrade and can no longer be used. Above 280 ° C, commercially available glass and ceramic filler adhesives such as Saureisen #1 are known to be effective, but for this application, they were shown to have poor strength in the residual load test, likely because these adhesives work best for bonding to porous ceramics and not dense SiC. Thus for these higher temperatures, metal brazes were found to be the best candidate. Several compositions of active brazes were explored and average residual strengths of up to 16,000 N has been obtained for the Morgan Ceramics Incusil braze.

3.2.1.2. ACTIVE GRIPPING

Active gripping holds the specimen in the test fixture through use of applied force perpendicular to the direction of the axial load during testing. The benefits of this approach are it has a quick set up time and a direct pathway towards use at high temperature. Due to stress at the grip contact points, application of excess force can result in the crushing of the cladding and must be avoided. One of the critical questions that needed to be answered to decide the suitability of the active gripping approach is determination of what maximum gripping force can be applied during the endplug pushout test while avoiding damage to the composite. Once this gripping force is obtained, the maximum applied axial load to the endplug without the specimen slipping in the grips can be determined.

The initial study of active gripping was performed using a set of Wyoming Test Fixture tensile grips with v-groove inserts (see Fig 3-6). These inserts are designed to hold LWR

diameter material and are tungsten carbide coated to improve gripping. Through tightening of the fixture, increasing force is applied normal to the specimen.

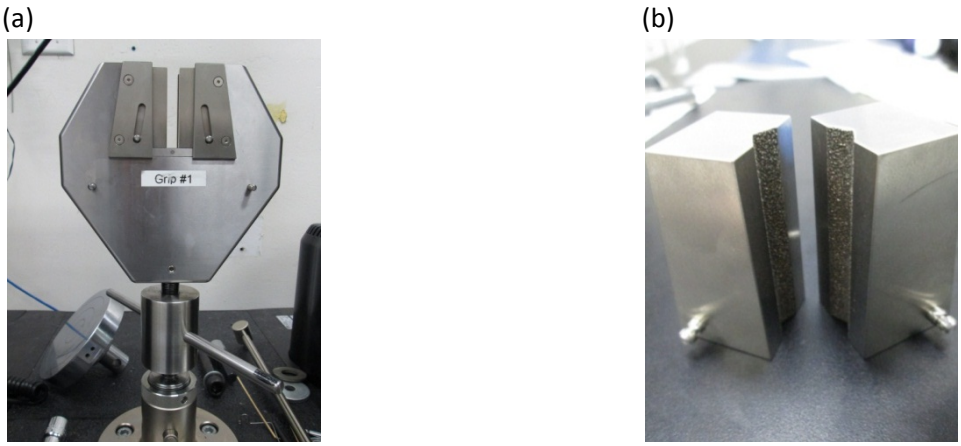

Fig. 3-6. Active gripping fixtures: (a) Wyoming Test Fixtures tensile grips with (b) v-groove inserts.

Tests were performed to determine maximum grip force that can be applied and maximum axial load at this gripping force for the active v-groove grip approach. In order to find the maximum applied axial load for the Wyoming Test Fixtures grips, pieces of monolithic and composite tube with no endplug/joint were loaded into the grips and compressive load applied until the load leveled off or began to drop, Fig. 3-7. The gripping region was standardized at 1" long for this study. When the load levels off, it indicates the piece is slipping and is no longer being held in place. This is the maximum axial load that can be applied to the endplug during testing. The experiment was repeated for various amounts of applied gripping force, Fig. 3-8, and the specimens were monitored for damage in the gripping region using optical microscopy and SEM. Specifically, the presence of cracking and out of roundness was monitored on the specimens.

Fig. 3-7 (left). Mechanical test of maximum applied load for active gripping.

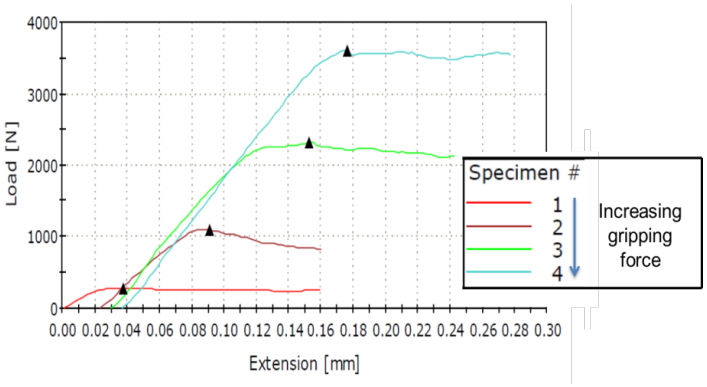

Fig. 3-8 (right). Applied axial load vs. extension for increasing amounts of gripping force. The maximum amount of load that could be applied during the endplug pushout test is the point where the load levels off for each plot.

Several different factors including compressive grip force, tube surface roughness, and presence of a compliant layer between the grips and ceramic tube were investigated in the course of this experiment. Maximum axial load that can be applied to a specimen was found to be heavily influenced by these factors. The highest load, approximately 4,000 N was measured on a composite with high O.D. roughness and with use of a thin layer of copper foil as a compliant layer, Table 3-2. For a smooth material, such as monolithic SiC, a maximum load of 2100 N was measured. Loads of 2100-4000 N are larger than the measured GA joint load as found using passive gripping methods, although fall short of the calculated 25,000 N benchmark . To ensure a broad ASTM standard is developed, additional grip strength is desired. Maximum loads are typically 500-1000 N lower without the compliant layer present. The use of a compliant layer and a rough outer surface both appear beneficial to grip strength.

Table 3-2. Max useable load for active grip based approach; two or more specimens were tested for each approach.

Active Grip Type	Tube	Measured Max Useable load (N)
V-Notch	Monolithic	2,100
V-Notch	Composite	4,000
Split Collet	Monolithic	2,300
Split Collet	Composite	4,600

To improve upon the v-notch grips, a split collet was designed and fabricated, Fig. 3-9. A split collet design allows increased contact area and a more even distribution of force over the entire tube area. Grips were fabricated so that the collet diameter was closely matched to the outer diameter of the composite. Tests were performed to determine maximum grip force that can be applied and maximum axial load at this gripping force for the active split-collet grip approach. The test process was repeated that was used for the v-groove approach.

Results for the split collet test show improvement over the v-notch approach, but still loads fall short of required grip strength. A small improvement for the split collet design, 4,600 N for composite tube, was obtained versus the v-notch grips, 4,000 N, but it is still well short of 25,000 N loads required for the endplug pushout test.

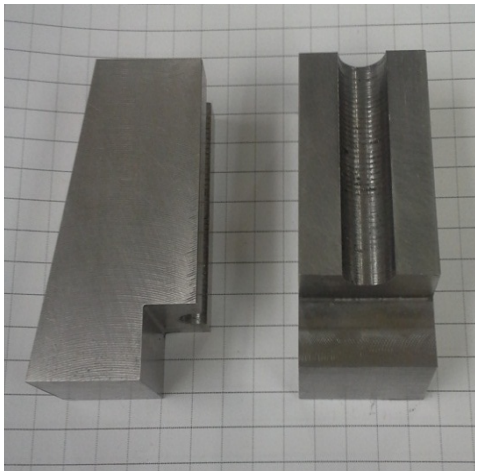

Fig. 3-9. Split collet design for use with standard tensile grip fixtures.

3.2.1.3. Grips Conclusion

Based on the available data, the decision was made to focus on passive based gripping mechanism for the remainder of the project. For the active gripping method the force required to grip onto the tube so that it does not

slip or otherwise shift during testing results in damage of the specimen. Testing using active gripping is considered non-valid as failure occurs at the grips instead of at the desired endplug joint. Multiple designs for active gripping were investigated and all suffered from this problem. Passive joining does not suffer this issue and coupled with the identification of high temperature epoxies for use in the 300 ºC range and brazes for use up to 800 ºC range, the decision was made to focus on passive joining.

3.2.2. Alignment

Ensuring proper alignment of specimens is critical during ceramic testing, much more so than during testing of metals and other materials with lower elastic modulus[4]. Misalignment can induce bending of the specimen during testing, resulting in lower measured strengths than would otherwise be expected. In the endplug pushout test there are several sources for potential misalignment, shown in Fig. 3-10. The specimen itself may be a source of misalignment, such as in the case where the endplug is tilted on a slight angle compared to the tube or in the case where the inside surface of the endplug where force is applied during the test has excess adhesive so that load is not being applied to a flat surface. In addition, there can be misalignment in how the specimen is mounted into the test fixture. The fixture is designed to try and minimize this potential misalignment by using self-aligning collets, but the collets must be correctly mounted to the specimen.

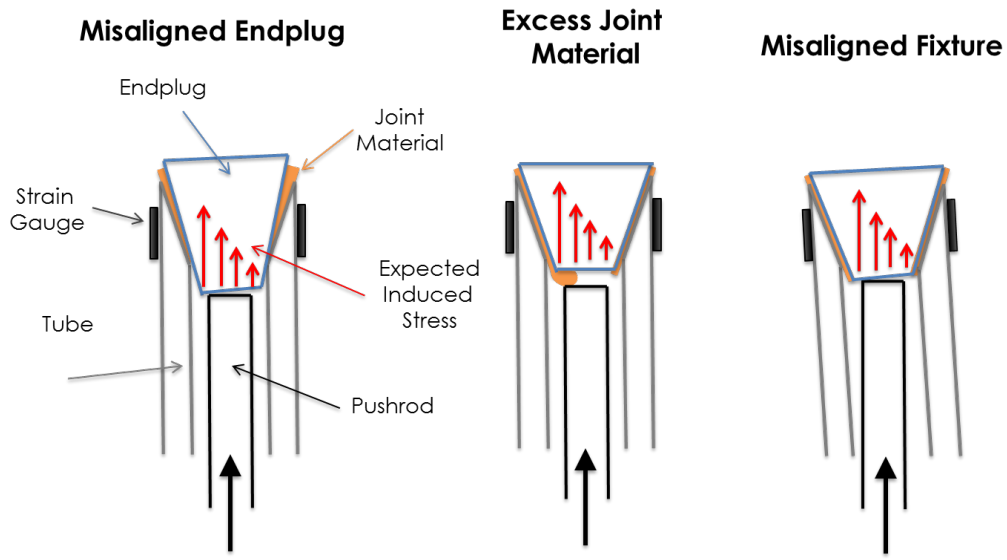

Fig. 3-10. The three potential sources of misalignment being investigated

In all three cases of misalignment, the pushrod preferentially pushes on one side of the endplug causing a bending moment in the sample. Observation during the first two quarters of the project showed that misalignment of the specimen in the fixture tended to be small if care was taken during pretest specimen preparation and that excess adhesive on the push side of the

[4] Wachtman, W. ed. "Mechanical Properties of Ceramics" John Wiley & Sons, Hoboken, NJ (2009)

endplug can be eliminated during fabrication. However, misalignment due to the endplug being bonded at a slight angle relative to the ceramic tube was more prevalent and slightly more difficult to control. Coupled with the fact that this type of misalignment is easily to quantify by measurement of the angle of the endplug, it made it an ideal test case study.

3.2.2.1. Endplug Alignment

Endplugs were purposely misaligned during fabrication so that a variety of tilts was represented. Actual endplug misalignment was measured using X-ray analysis for each specimen tested, Fig. 3-11. A range from no misalignment (zero degrees) to approximately four degrees of misalignment was investigated. Strain during testing was monitored by mounting two strain gauges 180 degrees from each other in the plane of maximum misalignment, Fig. 3-12. Care was taken during testing and fabrication to ensure misalignment from excess adhesive or fixturing was not a factor.

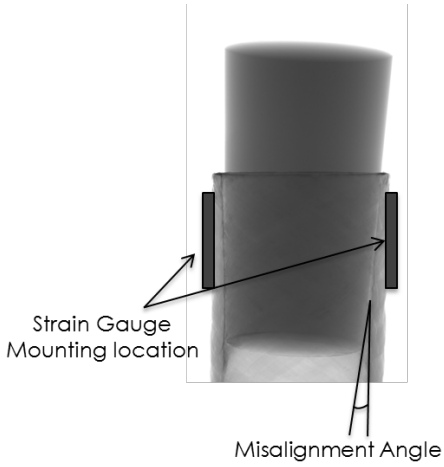

Fig. 3-11. X-Ray analysis of a misaligned endplug. An angle of misalignment of 2.2 degrees was measured based on this image.

Fig. 3-12. Specimen ready for testing with strain gauges and collet installed.

When the test is performed on well aligned specimen the strain is balanced in close to a 1:1 ratio as would be expected when there is no misalignment present, Fig. 3-13. With misaligned endplugs a bending motion is introduced into the specimen and the axial strain near where the pushrod preferentially makes contact increases relative to the side where no contact is made, Fig. 3-14. While some random spread in the test results exist, an overall trend can be seen as angle of misalignment increases, the ratio between the two strain gauges increases as well, Fig. 3-15. This difference also causes an effect on the overall measured strength, Fig. 3-16. As the angle of misalignment increases, a drop in strength occurs that seems to follow a linear relationship with misalignment. At very large angles of misalignment, failure in the composite as opposed to failure in the joint region can occur. This observed linear trend shows that drop in strength can be 10% or more due to even moderate misalignment and indicates a potential source of error in the test that should be corrected if possible.

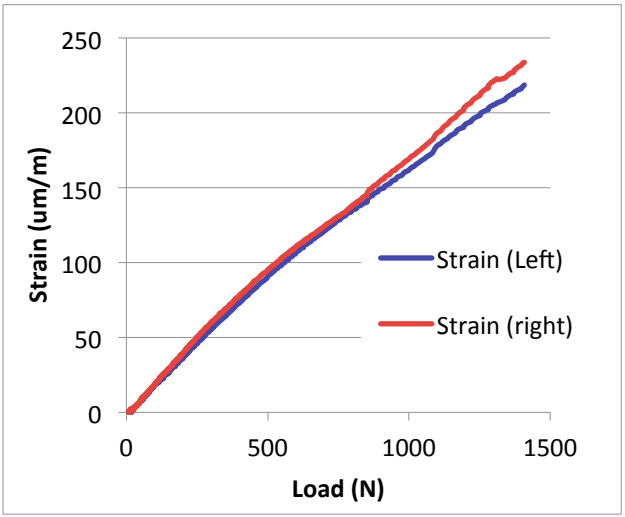

Fig. 3-13 (left). Strain versus load for well aligned specimen.

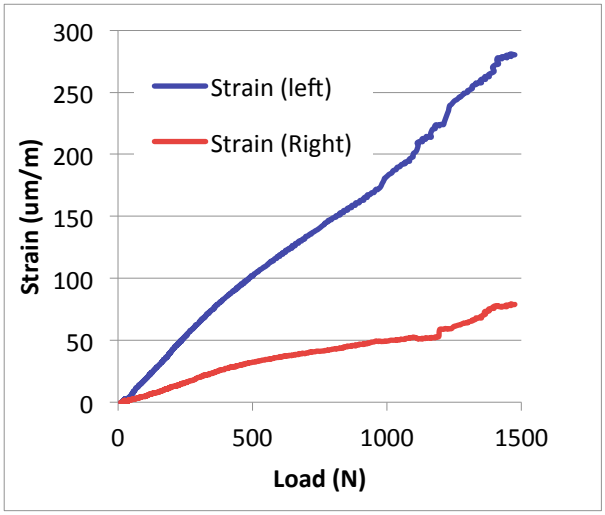

Fig. 3-14 (right). Strain versus load for an endplug with a 1.45 degree misalignment.

In order to correct for small misalignments in the endplug use of a compliant layer at the push rod/endplug interface was explored. Use of compliant layers is common way to deal with misalignment and rough surfaces during ceramics testing. Two compliant layers were explored, the use of thin <0.005" copper foil and the use of <0.0625" layer of grafoil. In general copper is used to correct for small amounts of misalignment and has minimal effect on the crosshead displacement. Grafoil is thicker and softer meaning it can help in cases with more severe misalignment and roughness, but due to the thickness often makes the displacement readings more ambiguous.

In addition, an alternative method of alignment correction is observed in some ASTM standards where a hemispherical load plate is used to minimize errors associated with misalignment, Fig. 7. The advantage of this method is that 360° of freedom are present right at the endplug push surface which can allow improved alignment in the case of a misaligned specimen/endplug. Also explored was the use of a u-joint on the push rod to allow for increased degrees of freedom for the push rod. This was predominately used in combination with compliant layer.

Initial data was obtained using a copper compliant layer or using a u-joint. Use of copper at an endplug misalignment of 1-2 degrees gave strain ratios on the order of 2:1 or more and slightly reduced strengths relative to the case of perfect alignment, Fig. 3-15 and 3-16. When u-joint only tests were performed in the same 1-2 degrees offset region gave a strain ratio of 3:1 or more and again slightly reduced strengths relative to the case of perfect alignment. Based on this data it was decided that the thicker, softer grafoil was necessary and that a u-joint alone was not enough to correct for all but the smallest of misalignments. A summary of this data can be found in Table 3-3.

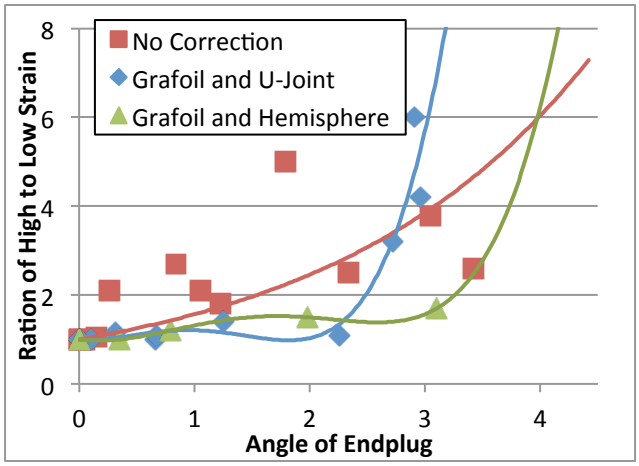

Fig. 3-15 (left). Strain ratio versus angle of misalignment for as is specimens and for specimens with Grafoil and U-Joint as a misalignment correction.

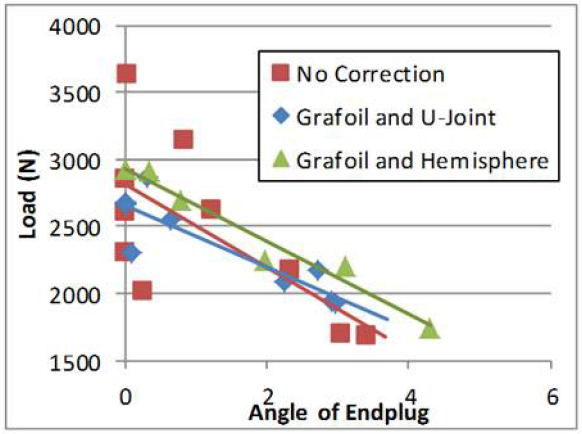

Fig. 3-16 (right). Strength versus angle of misalignment for as is specimens and for specimens with Grafoil and U-Joint as a misalignment correction.

When both a U-joint and grafoil layer is used or hemispherical correction is used the ratio of the high and low strain stays close to 1:1 for misalignments up to about 2 degrees, at which point a rapid increase in strain ratio is observed, Fig. 3-15. The rapid increase in strain occurs due to the misalignment exceeding the ability to be corrected. This serves as guidance as to what misalignment must be kept below. In addition, the overall measured strength seems slightly higher for a given misalignment when compared to the case of no correction being used, although strength still appears to drop with increasing angle of misalignment. More notable is that the spread in data is considerably less in the case when alignment correction is used. For reliable test methods, it is important to eliminated test induced variations in strength and this is considered an important result.

Table 3-3. Alignment correction techniques attempted and results of test for the case of endplug misalignment

Alignment Correction	Results
none	Only acceptable in case of perfect alignment
Copper Compliant Layer	Good for small misalignment <0.5 °
Grafoil Compliant Layer	Good for larger misalignment <1 °
U-Joint	Inadequate without compliant layer
Grafoil and U-Joint	Best results obtained, misalignment <1.5 °
Hemisphere	Best results obtained, misalignment <2 °

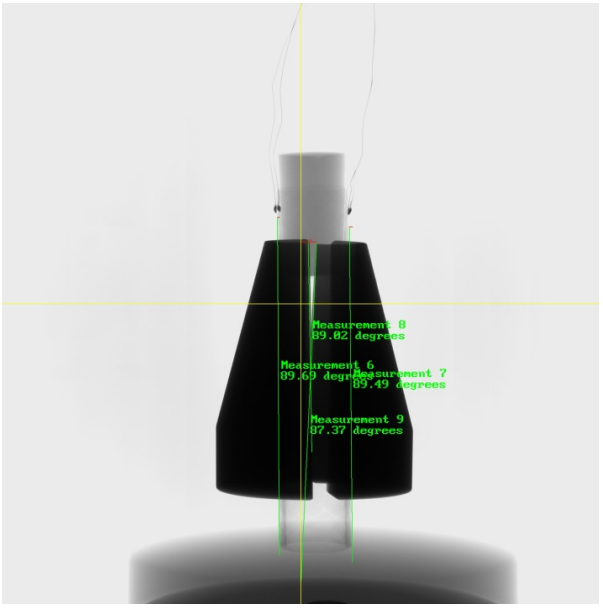

Fig. 3-17 (left). X-Ray analysis of a misaligned collet. Angle measurements used to quantify misalignment are shown in green on the image.

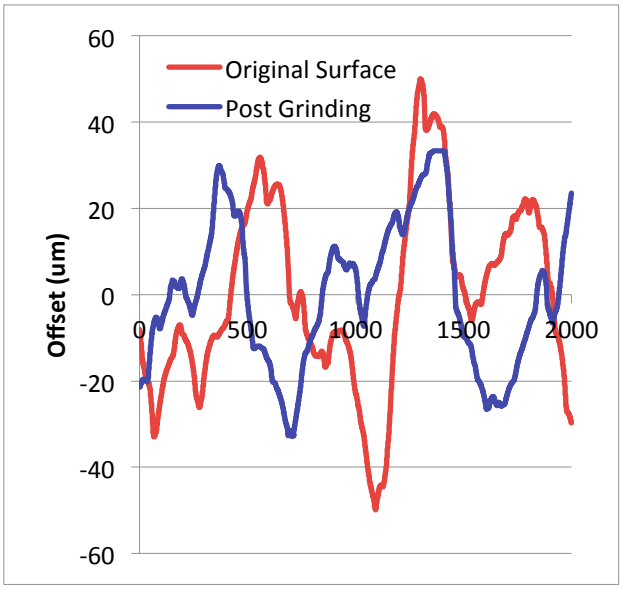

Fig. 3-18 (right). Surface roughness profile of composite before and after machining removing ~20 um of material. Material is removed only from the largest peaks and valleys.

Based on this data, even with grafoil and u-joint or hemispherical correction, total misalignment in the endplug should be no more than 1.5 degrees so that the strain ratio is kept at or below a 1:1.2 ratio. At this 1.5 degree angle though, measured strength may be up to 5% lower than the true value, underscoring the necessity of using fabrication practices that allow good endplug alignment, rather than trying to correct the problem during testing.

3.2.2.2. Specimen alignment

Alignment of the specimen in the fixture is a second source of misalignment. For the fixture being used, a conical feature is built into the fixture so that the collets attached to the specimen will self-align into the fixture. The specimen will only be properly aligned however if the collets are bonded onto the specimen with proper alignment. In order to investigate this misalignment, a procedure similar to the method used to analyze endplug misalignment was used where the specimen was misaligned, measured using x-ray analysis, Fig. 3-17, and tested for strength and strain ratio.

The results of these tests were similar to that obtained from the endplug misalignment tests, although the test appears to be less sensitive to fixture misalignment. With the use of a grafoil and u-joint on the push rod a maximum allowable misalignment of approximately 3 degree before the strain ratio drifted significantly away from the ideal 1:1 ratio was obtained. Strength did not appear to as strongly correlate with misalignment; misalignment of 2 to 3 degrees can be tolerated before a several percent drop in load is experienced. It is believe to be the case that having a push rod on the u-joint is particularly valuable for fixture misalignment as the push rod can align itself in the direction of the specimen misalignment and push along the axis of misalignment. This means that even though the specimen is misaligned relative to the fixture, the load is being applied near uniformly onto the endplug surface.

In addition to use of the compliant layer, care should be taken during specimen preparation to minimize collet misalignment. This is best accomplished by closely matching the collet ID to the specimen OD. When the ID of the collet is a slip fit to the specimen it was observed that misalignment tended to be very small, <0.20 degrees. When composite tubes are being used this can be more challenging due to the inherent roughness of the composite as a result of fiber architecture. Lightly machining the specimen, in which < 50 um of material was removed, was investigated as a means of improving the fit of the specimen in the collet by removing some of the larger peaks in the roughness profile, Fig. 3-18. Alignment of the composite in the collets was compared for the original as is composite surfaces versus machined surfaces. For the as is surface, misalignment was observed from 0 to 0.4 degrees. With a light machining this was reduced and maximum misalignment was found to be 0.2 degrees or less.

3.2.2.3. Excess Adhesive

For these experiments endplugs were bonded with good alignment. Excess epoxy with an additive to improve contrast during x-ray analysis was applied to the bottom of the endplug. 2D x-ray imaging was used to observe and quantify the excess adhesive, Fig. 3-19. Excess adhesive was applied so that a variety of different quantities and locations could be studied.

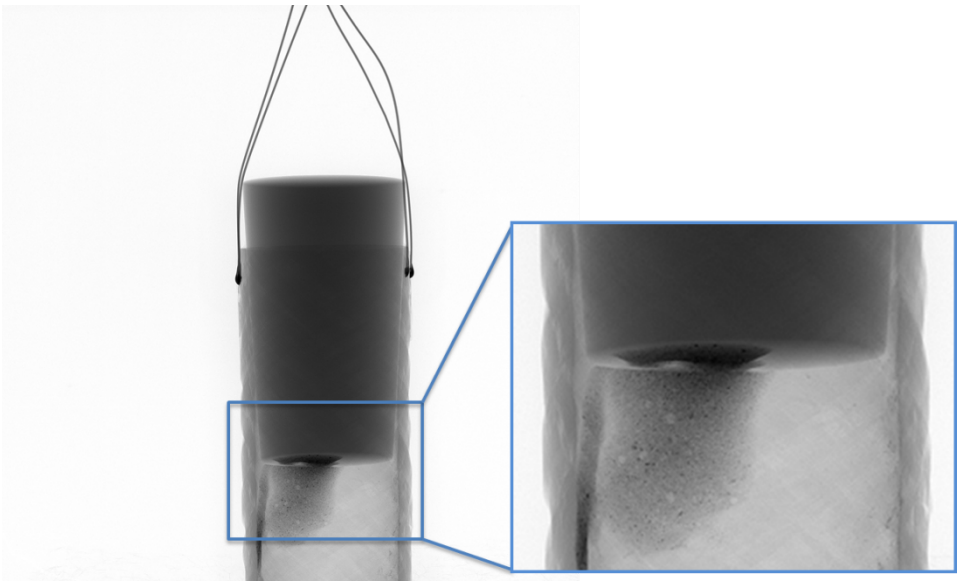

Fig. 3-19. 2D X-ray scans of endplug pushout specimens with the presence of excess adhesive on the push surface of the endplug.

As expected, excess adhesive does cause bending in the tube, Table 3-4. Even relatively thin layers of excess adhesive can cause alignment issues without the use corrective actions, as in the case of 13380-16-2. While it might be expected that the worst case would occur when the adhesive is at the very edge of the tube, 13380-16-3, it actually occurs when the adhesive is slightly offset from the center of the rod, such in specimen 13380-16-4. This is due to the fact that the push rod is typically ~20% smaller than the ID of the tube so that excess adhesive on the very edge of the tube may not in fact contact the pushrod.

With the addition of alignment correction, the strain ratio improves dramatically and bending stress is reduced. Typical strain ratios tend to be no more than 1.5:1 with the addition of a graphfoil compliant layer and a u-joint. While the addition of the graphfoil and u-joint is useful, care should be taken to remove excess joint material from the surface of the endplug during fabrication of the joints. Small amounts of misalignment can be corrected for, but properly fabricated specimens are required to keep bending to a minimum.

Table 3-4. Illustrative results of alignment investigation for the case of excess adhesive on the endplug surface

Specimen	2D x-ray of Endplug Surface	Alignment correction	Strain Ratio	Measured Load (N)
13380-16-2	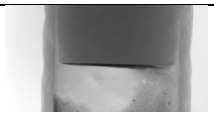	None	1.8:1	4507
13380-16-3	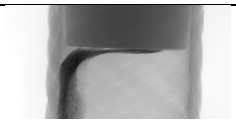	None	3:1	4020
13380-16-4	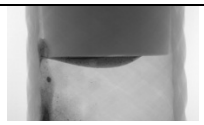	None	3.5:1	4861
13380-18-1	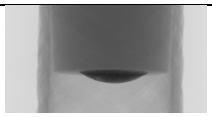	Graphfoil & U-Joint	1.1:1	4440
13380-18-3	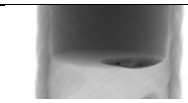	Graphfoil & U-Joint	1.5:1	4785
13380-20-2	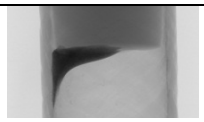	Graphfoil & U-Joint	1.3:1	4244

3.2.3. Validity of Test Specimens

Having fully completed the first milestone, a more thorough discussion can be made on determining the validity of a given test specimen. Alignment and posttest failure criteria are the primary means in which specimens may be considered non-valid.

In order to develop a stronger ASTM standard, guidelines for specimen alignment have been developed. This becomes particularly important at high temperature where the use of high temperature strain gauges can be costly and time intensive. By following these guidelines, valid

test data will be gathered, even without the use of additional strain gauges to confirm alignment. These guidelines were developed through use of pretest analysis of the alignment via X-ray tomography and comparing these measurements to resulting strain measurements. By comparing valid versus non-valid tests, as defined by strain gauge data, threshold values for alignment were developed. More universally available methods besides XCT for quantifying specimen dimensions and alignment are currently being evaluated.

A test will be considered valid if the guidelines seen in Table 3-5 are met. If the test specimen does not meet these guidelines, it may still be valid, but strain gauges or other means of monitoring strain during testing should be used in order to evaluate percent bending during testing. For a test to be considered valid with use of strain gauges, the percent bending as observed in the strain gauges must be kept under 20%. This 20% value is based on the experimental alignment data for all three cases of misalignment studied. This data shows that deviations in strength due to alignment at percent bending less than 20% appears to have little to no impact on measured strength. As misalignment increases past this value, measured strengths become considerably lower than expected. Percent bending for four axial strain gauges mounted in 90 degree intervals can be calculated using the following equation[5]:

$$\%B = \frac{\varepsilon_B}{\varepsilon_o}(100)$$

where ε_o is the average strain and $\varepsilon_B = \left[\left(\frac{\varepsilon_1-\varepsilon_2}{2}\right)^2 + \left(\frac{\varepsilon_3-\varepsilon_4}{2}\right)^2\right]^{1/2}$

Table 3-5. Specifications to be met for a valid test to occur

Part(s)	Specification	Rationale
Tube	Concentricity of 0.2 mm along center axis of tube	Tube self-aligns into collets if it is a close fit to collet surface
Tube	Surface roughness of Ra of 30 µm	Ensures good tube/collet alignment
Endplug	Endplug push surface shall be free of adhesive features thicker than 0.1 mm	Ensures uniform push rod contact
Endplug	The push surface shall be parallel with the top surface of the endplug within 0.01 mm	Allows easier determination of alignment of specimen
Endplug/tube	Endplug push surface and tube wall should be perpendicular to within 1.5 degrees	Minimized bending moment due to endplug misalignment
Tube/collets	Collet ID/OD shall be parallel with surface of the tube to 3 degrees	Minimize bending moment due to fixture misalignment

[5] ASTM C1773 "Standard Test Method for Monotonic Axial Tensile Behavior of Continuous Fiber-Reinforced Advanced Ceramic Tubular Test Specimens at Ambient Temperature" ASTM International, Westhconshoken, NY (2015)

Tube/Collets	ID of Collets shall be within 0.3 mm of OD of tube	Excess gap between collet and tube can lead to poor gripping and misalignment

A test may also be considered non-valid based on post-test analysis. Breakage must occur in or near the joint region to be considered a valid test. If a joint is sufficiently strong, or in the presence of induced stresses due to fixturing the test specimen may break in the tube away from the joint region. When this occurs, the test results should be considered non-valid as breakage is occurring away from the region of maximum stress. This data should not be included in any kind of statistical analysis, however, it is suggested these results should still be reported.

While breakage in the tube away from the joint region is considered non-valid, breakage does not necessarily need to be entirely in the joint itself. Cracking of the tube in the joint region may occur due to residual stresses during processing or in the case of angled scarf joints; the strength of the tube may be exceeded in thin walled sections of the tube. Because the endplug pushout test is focused on the tube-endplug geometry and is not trying to measure fundamental properties of the adhesive itself, this type of breakage is still considered a valid test and should be included in calculation and results.

3.2.4. Room Temp FEM

FEM was used to help understand the stresses present during EPPO testing as well as to help in method development. FEM was first started on a more simplified geometry to test examine algorithms and gridding. Increasingly complicated geometries were used until a model representative of the EPPO test was obtained. In all cases ANSYS was used for FEM with boundary conditions based on SiC properties presented in the literature or obtained by GA[6]. For this models all material, including the joint itself, are considered to be monolithic or variations on monolithic SiC and elastic modulus and Poisson's ratio are kept constant for all features. More details on model setup can be found in section 5.

As an initial, simple to model test case, single lap offset (SLO) testing was chosen due to GA having a large body of data on the test, making it an ideal way to validate the FEM being used. For the SLO model the top SiC bar is fixed on the left and load is applied on the bottom SiC bar, Fig. 3-20. The pressure load is incremented from 0 MPa increasing in 0.1 MPa increments. The contact is a line between the topside and bottom side bars with 40 equal element increments across the 12 mm width. The bonded contact elements were individually checked for the tension and shear force values which are provided in ANSYS results. A failure criteria of 3 MPa maximum shear stress for each contact element was selected for the analysis as shear stress common for many epoxies. If shear stress exceeded the 3 MPa limit for any individual contact element, that element was "killed", meaning the element was removed from the calculation, and the stress distribution recalculated for the remaining intact elements.

[6] Snead et. al. Handbook of SiC Properties for Modeling, *J. Nuc. Mat.*371, 329-377, (2007)

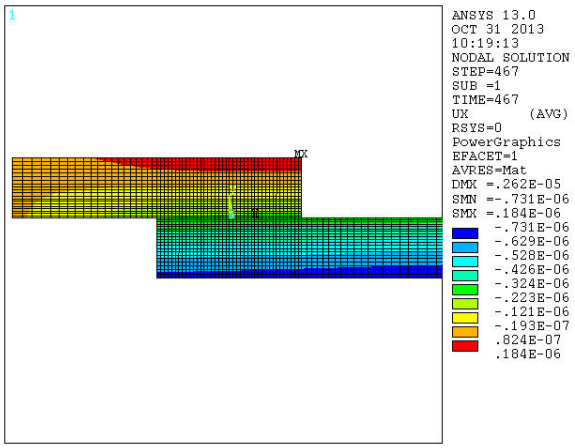

Fig. 3-20. Stress contour plot derived from the SLO FEM.

For a shear stress of 3 MPa, there was no failure of any contact elements until 1.2 MPa of applied load and it was only one of the 40 contact elements that exceeded the maximum allowed shear stress. It occurred on the left side in Fig. 3-21, where the highest concentration of shear stress was calculated. Indeed in all cases of these type of offset joint tests, including the endplug pushout test, a stress concentrator exists which keeps the measurement from being a pure sheer stress, and instead an apparent stress is measured. Once this initial element fails, stress redistributes and the remaining stresses on each element stays below the 3 MPa limit. However, when load is increased to 1.3 MPa, the crack propagates through the remaining elements and failure occurs. The reason that the failure load is below the shear stress of 3 MPa is due to the fact that the test does not induce a pure shear stress, but instead a bending moment is introduced. This bending moment can be observed in the stress plot calculated in ANSYS seen in Fig. 3-20.

When this modeling is repeated with a shear strength value of 97 MPa, which is shear strength of the GA hybrid polymer/CVD joint material as obtained by torsion testing, the expected stress at failure from the FEM is 40 MPa. Actual SLO data has been measured to be in the 35-40 MPa range, matching well with the model. Note that there is some dependency based on size of the meshing. This becomes particularly apparent when larger meshes are used. GA chose a mesh size appropriate with what is in the literature and where additional decrease in mesh seems to have limited effects on the stress distribution.

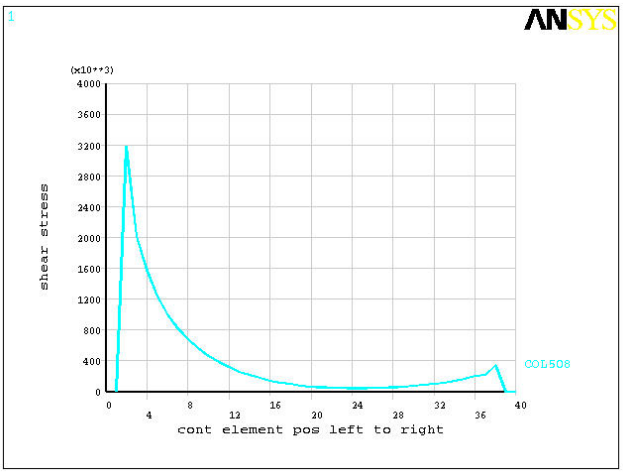

Fig. 3-21. Shear stress distribution between the 40 elements at a loading of 1.2 MPa.

The SLO model was then extended into an axisymmetric based model that more closely resembles the geometry for the endplug pushout test, Fig. 3-22. For this model an outer tube with an inner solid rod are drawn out in two dimensions and then rotated around the center axis in ANSYS to model the tubular geometry. An analysis similar to that used in the SLO test was performed on this new model and solved successfully. However, no experimental data was available for verification so the model was quickly progressed to a more advanced state. The geometry of the endplug was altered to more closely match the scarf geometry commonly used during actual testing. Both a 2d axisymmetric model and a 3d model were investigated in which a monolithic tube is bonded onto an endplug with an 8 degree scarf angle, Fig. 3-23.

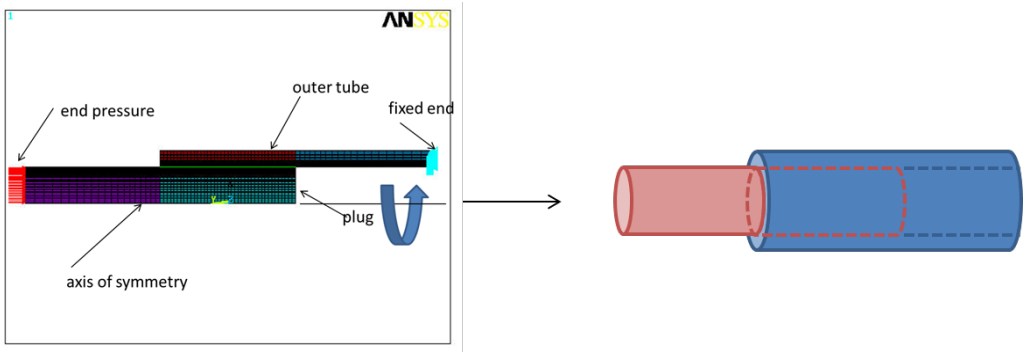

Fig. 3-22. Simplified axisymmetric model.

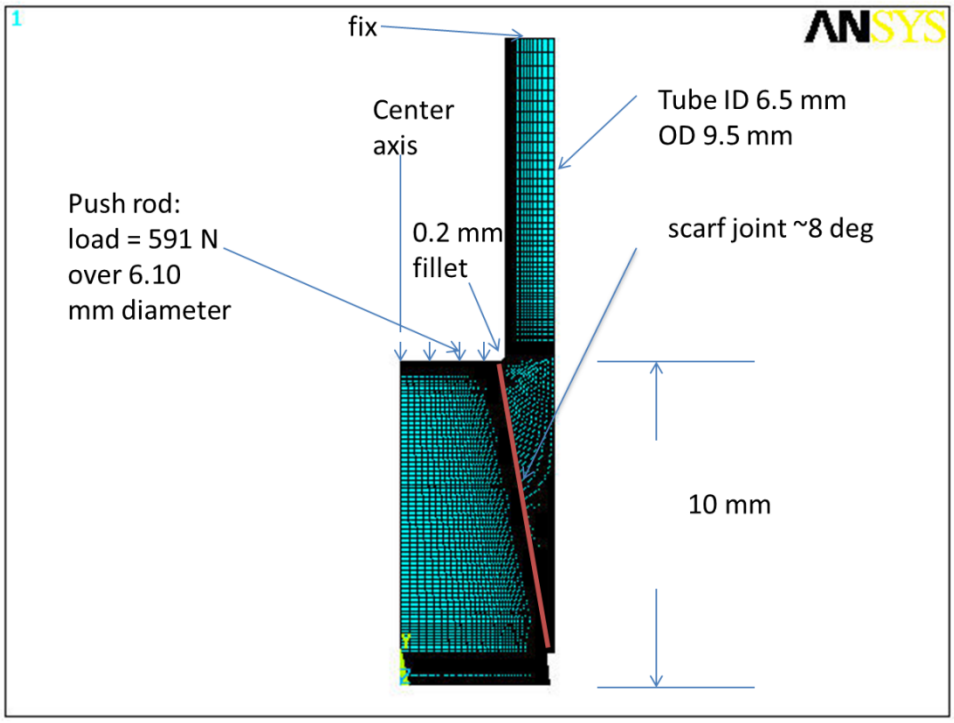

Fig. 3-23. ANSYS Mesh of a monolithic of a joined specimen with an 8 degree scarf angle.

The resulting finite element models suggest that there is a large stress concentrator at the junction of the tube and endplug, Fig. 3-24 and 3-25. Use of a fillet at this junction, which represent a small amount of excess adhesive that bridges the endplug and tube, does help to reduce the stress concentration. However, this stress concentration it is still present even with a large fillet and is expected to be the location of crack initiation during testing. This fact reinforces, as already suspected, that the endplug pushout test will not give pure shear strength and therefore should not be used to try and obtain fundamental shear strength of a given adhesive. Instead, the test is meant to be a geometrically relevant test that can be used to compare loads and apparent strength for a variety of test samples as long as test methodology is kept constant. The use of the test for measuring apparent strengths only is in line with the original stated purpose for developing this test, that being to "develop a robust, reliable test method for measuring the mechanical strength of endplug seals to tubular SiC-SiC cladding".

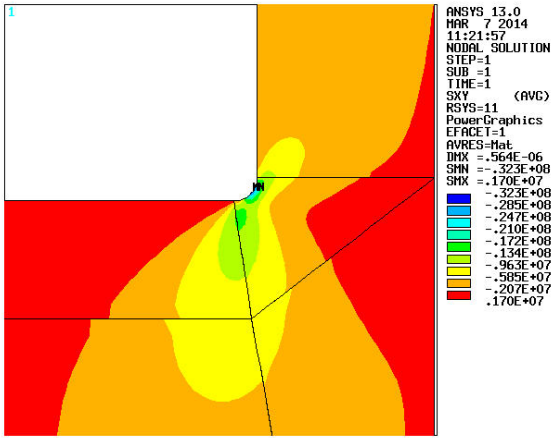

Fig. 3-24 (left). ANSYS model of shear stress along the joint as a result of ~600 N of load.

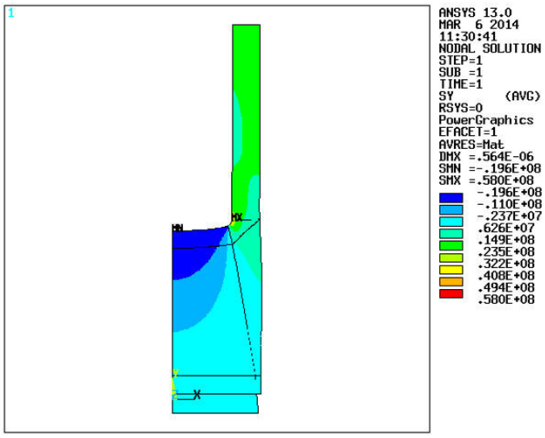

Fig. 3-25 (right). ANSYS model of axial stress in the specimen as a result of ~600 N of load.

For the 2d model, an applied load of 600 N on the endplug surface, a maximum stress of 58 MPa is obtained. For the 3D model, Fig. 3-26, an applied load of 600 N, yields a maximus stress of 54 MPa. In both cases, due to the relative softness of the epoxy the maximum stress, is located at the composite wall. Less than 20 MPa of stress is experienced in the epoxy. However, the composite is much stronger than the epoxy and is still the location of expected failure. Results of the 3d model are similar to that of the 2d model, with small difference believed to be due to difference in meshing between the two models. Due to the reduced run times and relative ease of use of the 2D model, subsequent work made use of this 2D model.

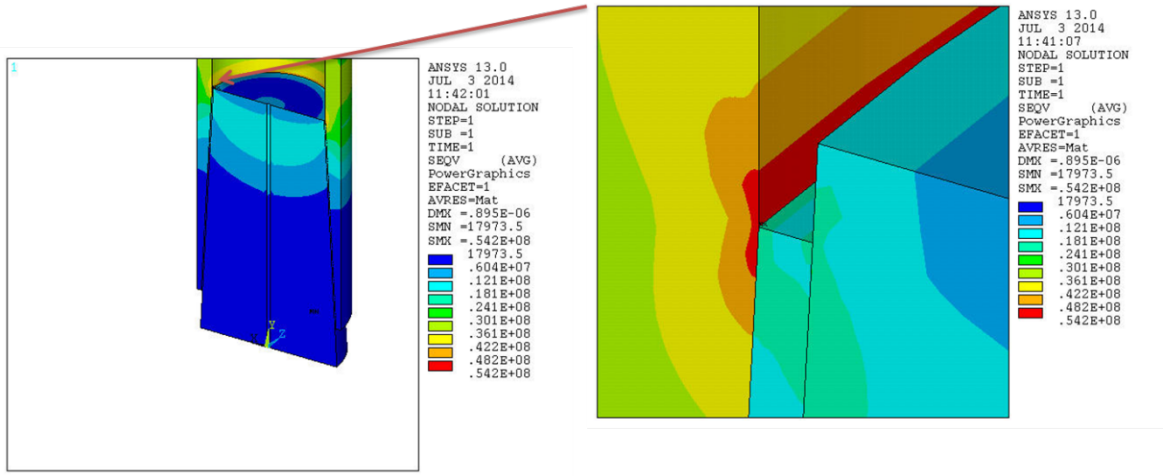

Fig. 3-26. Stress profile for the case of 0 degree offset (perfect alignment)

3.3. Repeatability and Versatility

ASTM standards typically should be written such that the standard can test a wide variety of materials and can do so with good precision and accuracy. The test method should be able to be used with a wide variety of materials. However, more important is that the specimens show

good repeatability between testing and that the test does not introduce errors during repeat testing of materials. Statistical analysis must be used to show a high quality test method.

3.3.1. Repeatability

A repeatability study was performed on a set of 30 joints, Fig. 3-27, in order to both analyze the repeatability of the test method as well as to obtain a statistically significant data set on GA hybrid polymer/CVD joint process.

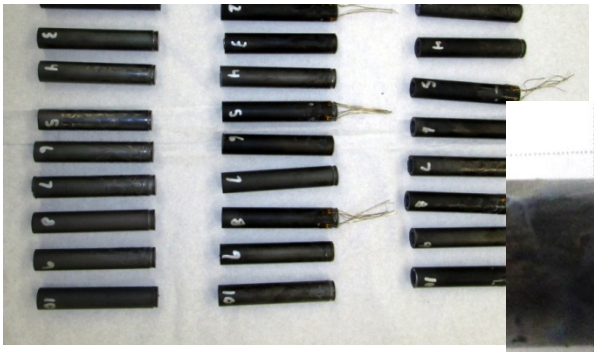

Fig. 3-27. Full set of joint specimens for repeatability test. Strain gauges have been mounted on some specimens.

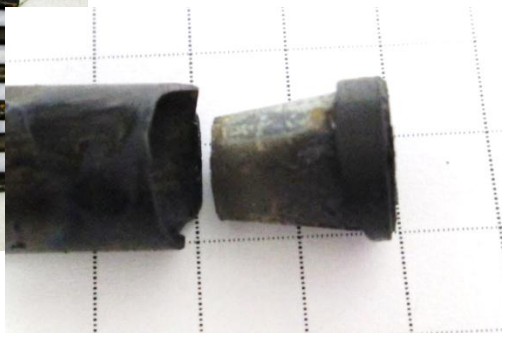

Fig. 3-28. Post-test fracture showing a primary failure in the joint with partial failure in the monolithic tube.

The complete data set for the set of 30 can be found in Appendix A. The procedure outlined in the previous section using passive gripping and alignment corrections was used. Post failure analysis showed a common mechanism of failure, Fig. 3-28, where cracking was observed to take place primarily in the joint layer with a small amount of cracking in the monolithic tube near the tip. Even though failure did not occur fully in the joint itself, because failure did take place in the joint region and specimens are considered valid.

Of the 30 total specimens, only 25 specimens were included in statistical analysis. Four specimens were deemed non-valid due to excessive bending based on strain gauge readings. Based on x-ray imaging, the primary cause of this misalignment was due to excess adhesive on the push surface of the endplug. However, most specimens were well aligned and the strain gauge readings matched well to each other, Fig. 3-29. One additional specimen was deemed non valid due to a crack near the joint during visual pretest inspection of the joints. This gives a testing efficiency of about 85%, which is typical of ceramic materials.

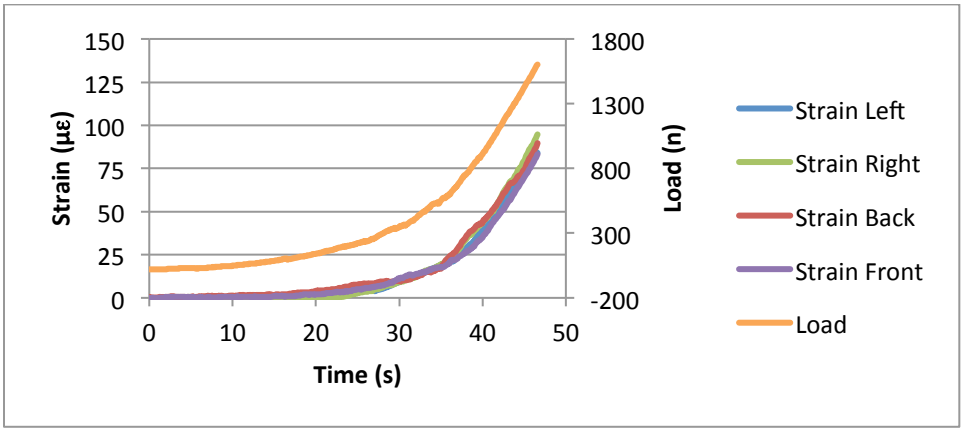

Fig. 3-29. Plot of strain versus time during endplug pushout testing. Four strain gauges are mounted in 90 degree intervals and show good alignment with little bending in tube.

For the 25 valid tests, the average load is 1344 N, nominal burst strength is 42 MPa, and when normalized to joint contact area an average apparent strength of 6.60 MPa is measured. While this average apparent strength appears low, it should be noted that this strength does not represent a fundamental property of the adhesive nor joint itself due to the stress distribution during testing, but is rather an apparent strength to be used for comparison purposes between samples tested using the same methodology.

Weibull data for the 25 valid specimens is shown in Fig. 3-30. A characteristic load of 1492 N is obtained and a Weibull modulus of 4.2. For the case of nominal burst strength, characteristic strength is 48 MPa and Weibull modulus is 3.8. For the case normalized to joint area characteristic strength equals 6.24 MPa and Weibull modulus is 4.4. The relatively good fit of this data suggests that there is only a single predominate failure mechanism. The Weibull modulus is somewhat lower than that obtained during torsion testing (~6.0) performed and reported in Khalifa et al, although within the range typically seen for ceramic materials[7],[8]. The slightly lower Weibull modulus can be attributed to difference in specimen layup and joint porosity. These differences are the primary reasons that evaluation by a test dependent on the geometry of the joint, such as the endplug pushout test, is critical. For torsion joints two flat plates are bonded together under pressure. However, pressure in the tube geometry necessitates the use of scarf angles on the tube and endplug and can be more difficult to apply uniform pressure. These fabrication differences need to be accounted for in the measuring of joint parameters.

[7] Khalifa, H.E.; Deck, C.P.; Gutierrez, O.; Jacobsen, G.M.; Back, C.A. "Fabrication and Characterization of Joined Silicon Carbide Cylindrical Components for Nuclear Applications," Journal of Nuclear Materials, 457, (2015), 227-240.

[8] Snead et. al. Handbook of SiC Properties for Modeling, *J. Nuc. Mat.*371, 329-377, (2007)

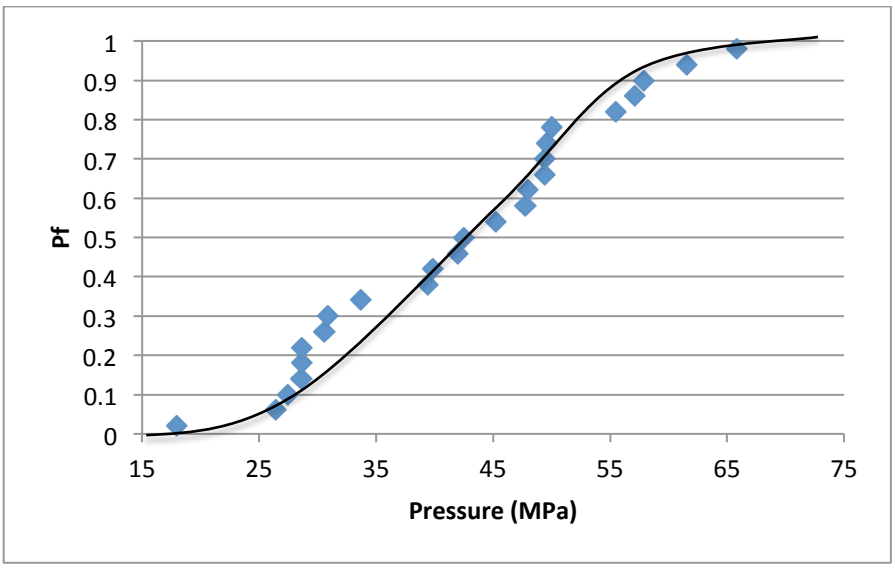

Fig. 3-30. Weibull data for all valid tests based on nominal burst strength at failure

3.3.2. Versatility

In order to show the versatility of the joining method several different types of specimens have been analyzed. To show the test can be used with a variety of joint materials, joints using epoxy, metal brazes, and ceramic based adhesive have been tested. To show it can be used for different ceramic tube types, both composite and monolithic tubing has been used. To show it can be used on a variety of tube sizes, tube sized appropriate for LWR material (9.5-10.5 mm O.D.) and a larger tube closer to that appropriate for use in GA's Energy Multiplier Module (21 mm O.D.), Fig. 3-31, have been tested.

Test results for these tests can be seen in Table 3-6. These tests were performed on a minimum set of five specimens each and the average and standard deviation is included. In all cases only valid tests were used for these calculations. No unanticipated issues or problems were encountered while performing these tests and the test is applicable and valid for different joint types and materials.

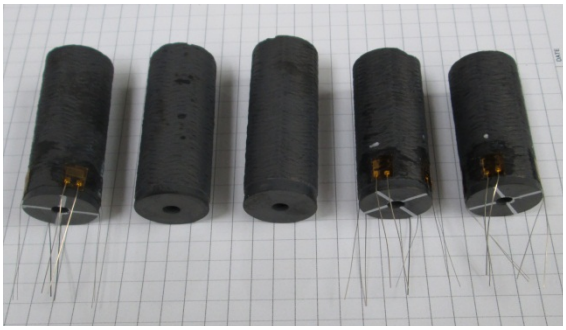

Fig. 3-31. EM^2 sized GA Hybrid joined test specimens with hole in endplug to vent fission products. Three of the specimens have been mounted with strain gauges.

Table 3-6. EPPO test data for a diverse set of tube and joint materials

Tube Type	Tube Size	Joint Geometry	Joint Material	Load (N)	Std. Dev. (N)
Monolithic	LWR (9.5 mm OD)	Scarf	Tuff Bond Epoxy	1589	209
Monolithic	LWR (9.5 mm OD)	Scarf	Incusil Braze	749	211
Monolithic	LWR (9.5 mm OD)	Scarf	Lucas Milhaupt Braze	672	158
Monolithic	LWR (9.5 mm OD)	Scarf	GA Hybrid SiC	1356	367
Monolithic	LWR (9.5 mm OD)	Butt	GA Glass	998	125
Composite	LWR (10.5 mm OD)	Scarf	Tuff Bond Epoxy	2609	214
Composite	LWR (10.5 mm OD)	Chamfered Scarf	Tuff Bond Epoxy	3773	404
Composite	LWR (10.5 mm OD)	Scarf	Incusil Braze	880	266
Composite	LWR (10.5 mm OD)	Scarf	GA Hybrid SiC	2092	269
Composite	EM^2 (21 mm OD)	Scarf	GA Hybrid SiC	2135	274

3.3.3. Finite Element Modeling

3.3.3.1. FEM OF EPPO TEST WITH COMPOSITE BEHAVIOR

During initial modeling of the EPPO test, composite behavior of the tube was treated as liner elastic as a simplifying assumption. This was used during method development in order to simplify the initial modeling. However, the stress strain behavior of ceramic composite materials is much more complex, Fig. 3-32. In order to better represent the behavior observed

for composites during the versatility study, more advanced composite modeling was incorporated into the existing EPPO FEM, Fig. 3-33.

A 3D model for the tube, joint and endplug was created in SolidWorks 2014 and the file was transferred to ANSYS. A Bilinear Isotropic Hardening (BISO) module was used in ANSYS to better represent composite behavior of the tube. In BISO an elastic modules is used until the yield stress (proportional limit stress for composites) and tangent modulus is used post PLS, Fig. 10. Values for these moduli were taken from experimental data obtained by GA on the composite tubes.

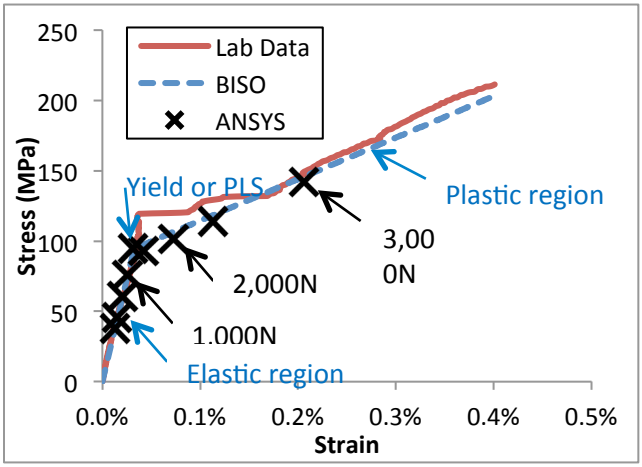

Fig. 3-32. (Left) Stress versus strain for a SiC Composite showing experimental data as well as the approximation used in the FEM.

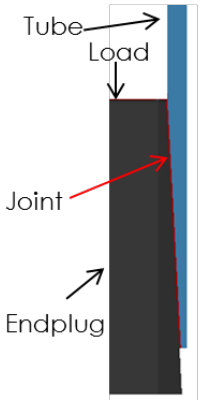

Fig. 3-33. (Right) The geometry of the axisymmetric FEM model of the EPPO test.

In this model, load was applied to the endplug in three different amounts: 1000 N, 2000 N, and 3000 N. The calculated stress on the composite tube using these three different values gives good insight into the effect of using BISO. At 1000 N, linear elastic behavior is still anticipated as seen in Fig. 3-32 and the model does not differ from earlier efforts. At 2000 N, some deviations can be seen in the measured axial strain, Fig. 3-34, as this loading is located just past the PLS in the composite stress/strain curve. At 3000 N, the stress/strain on the tube is well into the plastic region, and a large increase in calculated strain in the tube is observed. If the joint material is not able to plastically deform with the tube, interface debonding between the joint and tube can occur.

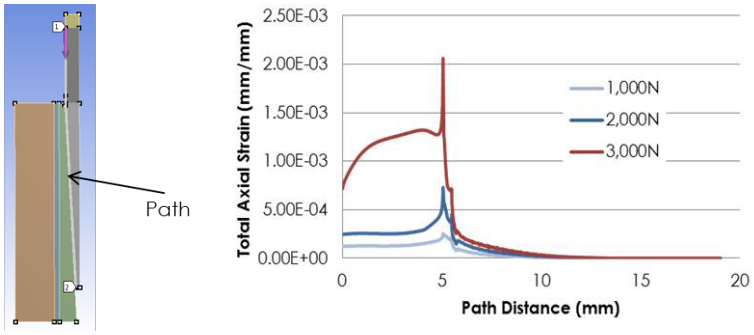

Fig. 3-34. Calculated Axial strain in the composite tube for EPPO loads of 1000, 2000, and 3000 N along the designated pathway.

3.3.3.2. MODEL VERIFICATION USING CHAMFERED ENDPLUGS

Experimental data on chamfered endplugs, Fig. 3-35, was compared to the finite element model prediction in order to validate the FEA. In previous modeling efforts of the EPPO test and similar single lap offset test methods, a stress concentrator is observed, Fig. 3-36. This stress concentration is a real feature of endplug-tube bonding and GA attempted to reduce this stress concentration through use of a chamfer on the endplug. This also allowed an opportunity to verify the model by comparing results of the model to experimentally measured strengths for specimens with and without a chamfer.

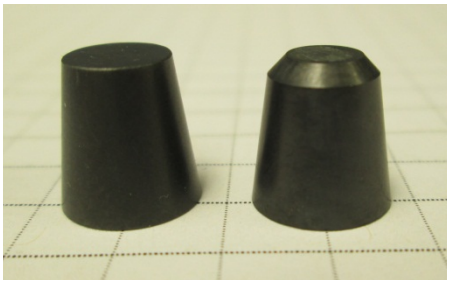

Fig. 3-35 (Left). CVD SiC Endplug both with and without a 45°, ~2.5 mm chamfer.

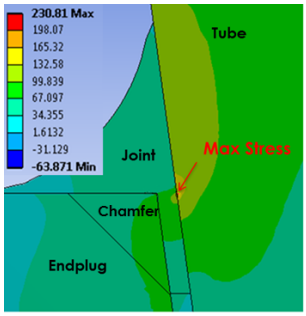

Fig. 3-36 (Right). Principal stresses calculated from FEA at a loading of 2000 N.

As seen in Fig. 3-37, addition of a chamfer to the endplug causes a ~40% drop in the calculated max tensile stress in an epoxy based joint versus a non-chamfered endplug for the same mesh size. This is a significant drop in stresses in the joint and represents a large potential increase in overall joint strength. In order to validate the model, endplugs were manufactured with the added chamfer and experimentally tested using EPPO, Table 3-6. The results of the experimental data show a 44% increase in measured strength due to the addition of the chamfer. The experimentally measured 44% increase is very similar to the calculated increase of 40% and suggests the model accurately predicted the benefit of the endplug chamfer.

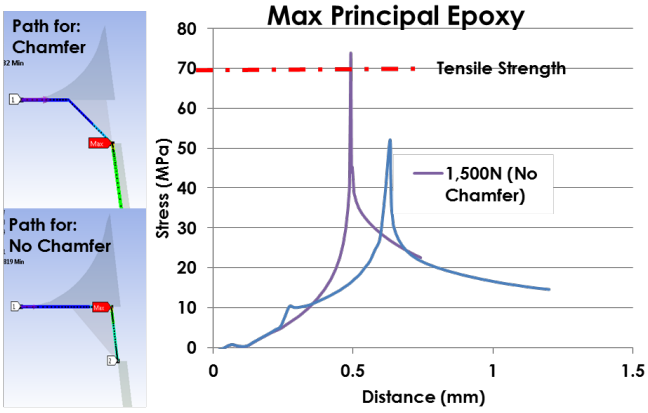

Fig. 3-37. Stresses calculated in the Epoxy from the FEA both with and without an endplug chamfer along the designated pathways.

3.4. Internal Pressurization vs. EPPO

It is expected that the primarily failure mechanism for cylindrical joint bonded to SIC based tubing will be due to axial stress. However, for completeness, the mixed mode hoop/axial stress state that is present due to internal pressurization of a fuel rod was investigated. For this study correlation and comparison of axial force only testing, represented by the EPPO test, versus internal pressurization, represented by pressure burst testing took place. The goal of this task was to show that material that tests well in pressure burst testing will also test well in EPPO testing, and that the two tests exhibit similar trends to each other. Several cases ended up existing where some variations between the EPPO and pressure burst test existed, and limitations of the test were defined based on this data.

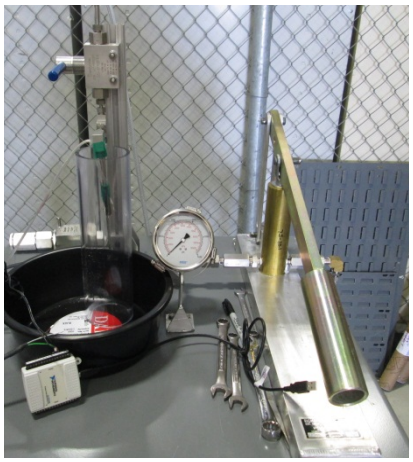

Fig. 3-38. In-house built high pressure burst rig.

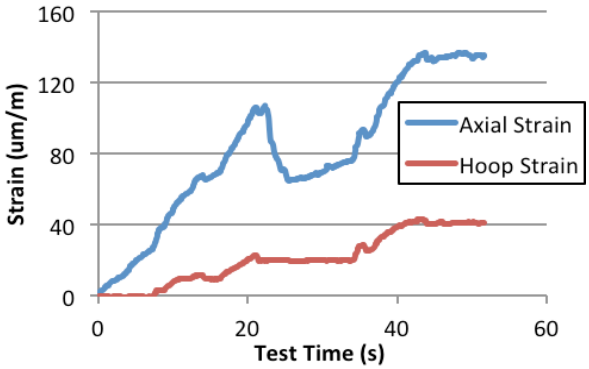

Fig. 3-39. Hoop and axial strains during hydrostatic burst testing of a monolithic tube with epoxy joint.

3.4.1. Experimental

Experimental correlation testing took place at GA using in house built test rigs. Internal pressurization testing took place through a hydrostatic burst test rig capable of pressures up to 12,500 psi, (Fig. 3-38). Hoop and axial strain data were monitored during testing, Fig. 3-39. EPPO data is cumulative from the first 14 months of testing. Three adhesives were investigated: United Resin Corp TuffBond Epoxy, Morgan Ceramics Incusil Braze, and GA Hybrid Joint Material. Both monolithic and composite SiC tubes were investigated. Accumulated test data can be seen in Table 3-7.

Table 3-7. EPPO test data versus pressure burst data for three different joint materials

Adhesive	Tube	EPPO Load (N)	Burst Pressure (psi)	EPPO Equivalent Internal Pres. (MPa)	Burst Internal Pressure (MPa)
Incusil	monolithic	749	751	24.4	5.2
Incusil	composite	880	2026	28.7	13.9
Epoxy	monolithic	1589	5322	51.8	36.7
Epoxy	composite	2609	4722	85.0	32.6
GA-Hybrid	monolithic	1356	1525	44.2	10.5
GA-Hybrid	composite	2092	2247	69.6	15.5

For the case of monolithic specimens when using Tuffbond epoxy, internal pressure results are relatively close between the EPPO test and the pressure burst test. Monolithic SiC has a very high elastic modulus (440 GPa) and is an extremely stiff material. In such a case, during internal pressurization negligible hoop stress will be imparted onto the tube and it becomes nearly a pure axial failure mode. Experimental data shows that in the course of the test, hoop strain on the tube is approximately three times smaller compared to the axial strain, (Fig. 4). In this test case it can be expected that results from the EPPO will match closely with results from internal pressurization.

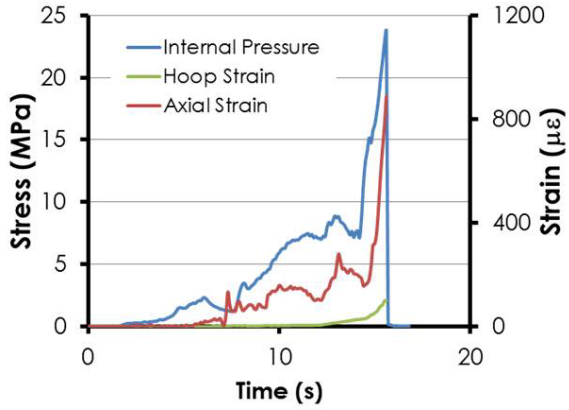

Fig. 3-40. An example of a pressure burst test on a GA hybrid joined composite tube specimen showing internal pressure and measured strains at the OD of the composite.

For the case of the composite specimens, the data is more complicated. Some specimens during hydrostatic burst testing failed sue to leaking through the wall of the composite. Leaking through the wall of the composite was particularly an issue with very strong joint materials such as the epoxy. This leaking is likely a result of the composite being stressed past the proportional limit stress during testing and internal cracking allowing a pathway for release of hydrostatic pressure. In this test case it becomes important to define a valid hydrostatic burst test as one where failure occurs at the joint and not the composite.

For the GA hybrid joints, lower pressure burst strength are obtained versus what might be expected based on the stiffness of the ceramic tubes and the relatively high ratio of axial to hoop strain measured during experimental testing, Fig. 3-40. These differences are attributed to nature of the ceramic joint material, which is more prone to individual defects, which act as crack

initiation sites. Cracking begins before the actual complete failure of the specimens and appears to more rapidly propagate in the case of the pressure burst test.

To further explain the data in Table 3-7, data for the apparent burst strength tested using the Endplug Pushout test (EPPO) and Pressure Burst tests are presented in chart form. Fig. 3-41 is for a series of different joint materials on monolithic tubes while Fig. 3-42 is for composite tubes. These charts show that results for the EPPO test tends to giver larger strengths than the pressure burst test for a given joint type. This is due to the EPPO test applying solely axial force to the joint specimen versus the pressure burst test which has a mixed mode hoop/axial stress distribution. The additional hoop stress appears to cause earlier failure in the joint during pressure burst testing and one of the reasons the EPPO test is considered a comparative tool only, similar to flexural testing of composites. For both test methods the relative order of joint strength is the same: Incusil Braze<GA-Hybrid Joint<Tuffbond Epoxy. This is true for both the joints performed on composites as well as for the joints performed on monolithic tubes. Based on this data, joint strengths obtained from the EPPO test appear to correlate well to the pressure burst test, even though they do not give the same results. This makes the EPPO test ideally suited for comparing different joint types and an effective tool for evaluation of joint materials in realistic geometries.

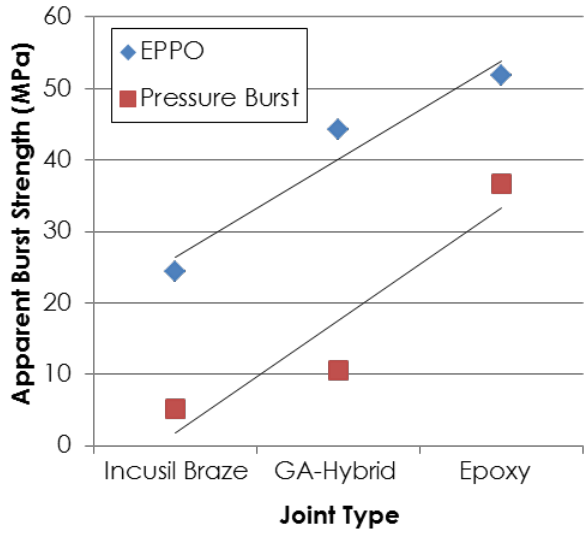

Fig. 3-41. Measured apparent burst strength from EPPO and pressure burst testing comparing a series of joints on a monolithic tube.

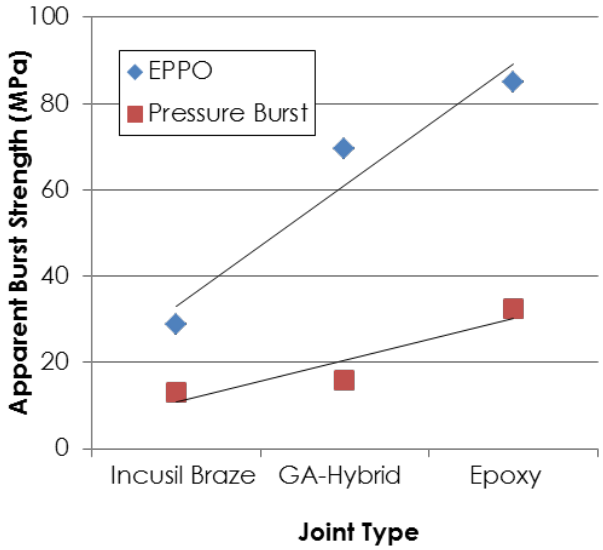

Fig. 3-42. Measured apparent burst strength from EPPO and pressure burst testing comparing a series of joints on a composite tube.

3.4.2. Internal Pressurization vs. EPPO – Finite Element Modeling (FEM)

To supplement experimental work, a more detailed evaluation of the EPPO test versus pressure burst testing was performed using FEM. The previously developed model, featuring a 2d axisymmetric model of a tube and a joined endplug meshed in ANSYS, was used for this work, (Fig. 3-43).

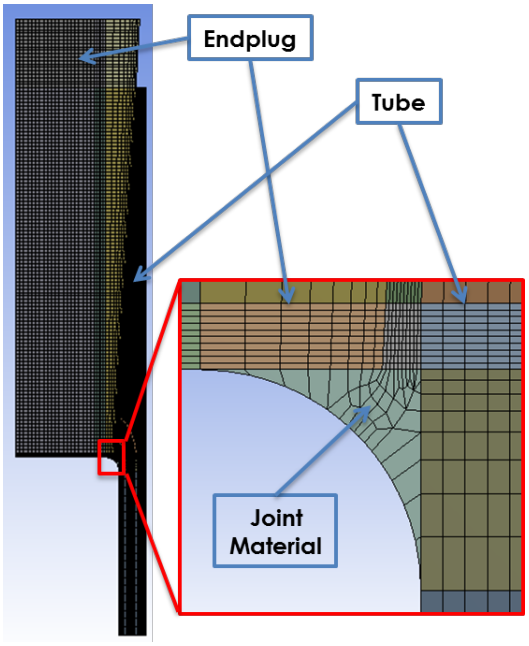

Fig. 3-43. Tube and endplug geometry, meshed in ANSYS.

Several key input parameters were identified to explore in the FEM effort. The modulus and thickness of the adhesive layer were investigated as these will factor into how hoop strain in the wall of the tube transmits to stresses in the joint layer. For the tube, the modulus and thickness was investigated. Increasing the modulus of the tube, and possibly the wall thickness, should result in convergence between the EPPO results and pressure burst test results.

Maximum calculated Von Mises stress in the joint material was used to compare the EPPO vs. pressure burst test. This stress was calculated at an EPPO load of 1000 N. For the burst test model, 1000N is equivalent to 23.5 MPa of internal pressure and this pressure was applied. As seen in Fig. 3-44, the resulting stress in the joint tends to be at a maximum in two areas, along the line of the endplug/adhesive interface, henceforth called the inner path, and along the adhesive/tube interface, henceforth called the outer path. In particular the area of highest stress has been calculated to typically be at the tip of the endplug. This stress concentration can be seen in Fig. 3-45 where a trace of the stress along the inner path is shown. This type of stress distributions holds true for both internal pressurization as well axial load only.

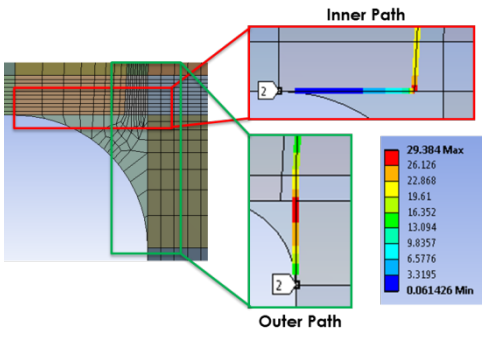

Fig. 3-44. The stress distribution and location of the inner and outer path.

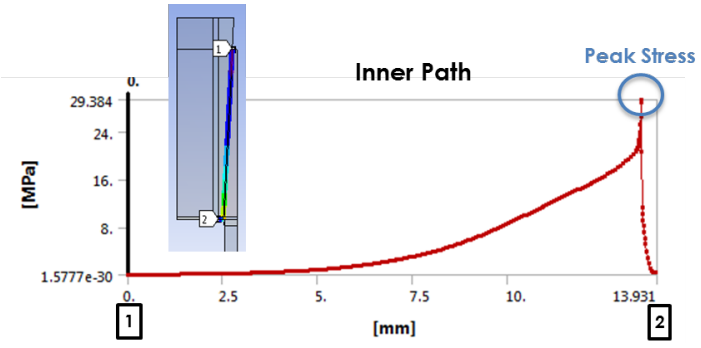

Fig. 3-45. Von Mises stress as a function of distance along the inner path of the endplug.

Wall Thickness: The effect of wall thickness has been evaluated for both the typical monolithic and composite tube used in the study with epoxy as the joint material, (Fig. 3-46). In this plot, only the maximum Von Mises stress for the inner path stress is shown as stress is larger at the inner path than the outer path. From this plot it is clear that internal pressurization induces larger stresses in the adhesive versus the case of axial loading only. This data suggests that the specimen would fail at lower internal pressure when tested using burst test versus when tested using EPPO testing. However, the axial loading seems to have a very similar trend in joint stress compared to internal pressurization. While the two tests are not expected to give the same failure strengths as wall thickness is changed, it does appear that they will trend with each other and specimens that test well using pressure burst testing should also test well using EPPO.

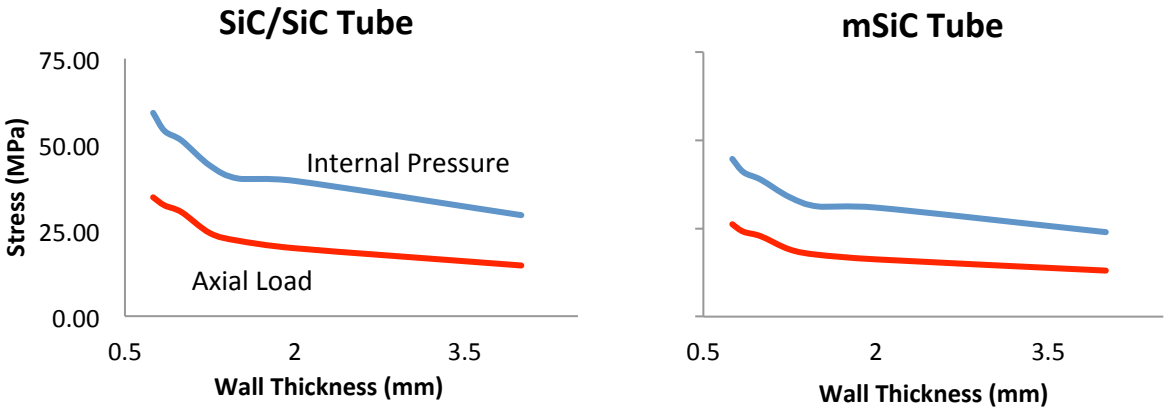

Fig. 3-46. Von Mises stress as a function of wall thickness of the tube for the inner path.

Modulus of Tube: As the modulus of the tube increases and the tube becomes stiffer it is expected that the contribution to failure from hoop stress should eventually reach zero, at which point internal pressure and axial only loads should give similar results. Modulus of the tube versus Von Mises stress was plotted in the FEM using composite tube geometry for the three different adhesives studied, (Fig. 3-47). In all cases, it does appear that the plots converge towards each other, although at very high values for elastic modulus. The overall tests trend well with each other.

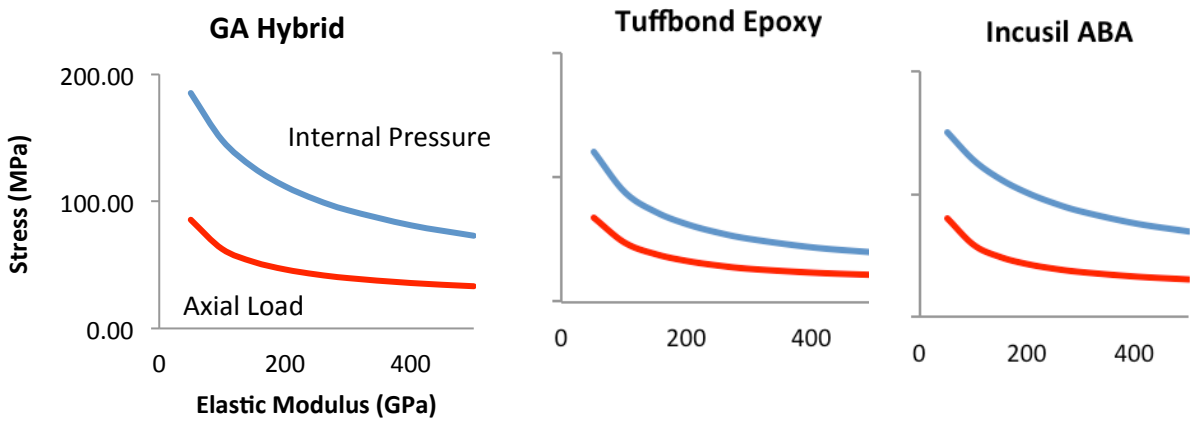

Fig. 3-47. Von Mises stress as a function of modulus of the tube for the inner path of three different adhesive types.

Modulus of Adhesive: For this analysis typical composite tube geometry and properties were used. The Poisson's ratio of the adhesive was fixed at 0.30. Plot of maximum Von Mises stress in the adhesive versus elastic modulus of the adhesive can be found in Fig. 3-48. Both the inner path and the outer path are shown in this figure due to the crossover point at 150 GPa. The crossover point suggests that for very stiff joint materials the stress acting on the endplug is effectively transmitted to the outer wall/joint interface. Again we see that internal pressurization tends to induce higher stresses in the joint than EPPO and the tests trending with each other. This trending suggests that for a variety of different adhesive compositions it can be expected for adhesives that test strong using the EPPO test to also test well during pressure burst testing.

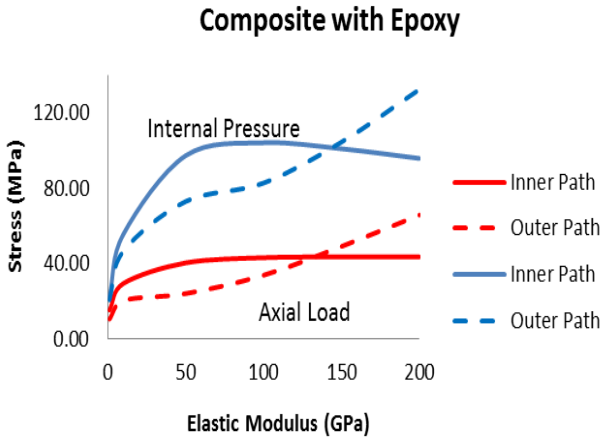

Fig. 3-48 (Left). Von Mises stress as a function of joint elastic modulus for both inner and outer path.

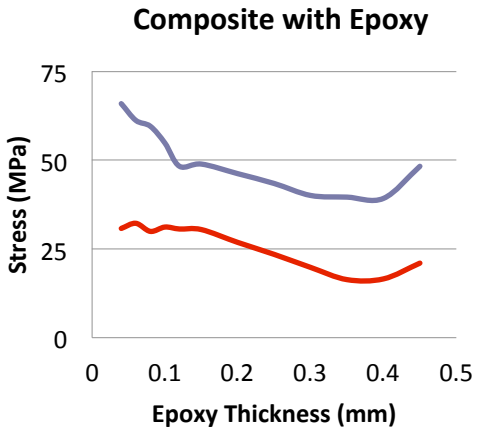

Fig. 3-49 (Right). Von Mises stress as a function of joint thickness for the inner path.

Adhesive Thickness: FEM was used to look at change in the adhesive layer thickness for the composite tube geometry using the Tuffbond epoxy, Fig. 3-49. Only the inner path is shown as it leads to the highest stresses in the joint layer. Except at very thin layers of epoxy the overall trends correlate quite well with each other.

3.4.3. Correlation Conclusions

Based on the FEM, in almost all cases the results of the end plug pushout test track with the results of the pressure burst test. Caution will need to be exercised in interpreting the data at very thin adhesive thicknesses and if the elastic modulus of the tube differs between specimens. Based on these results, specimens tested using EPPO testing will typically fail at higher equivalent internal pressures than when tested using the pressure burst test. However, the two tests do trend with each other and specimens that test at high strengths in pressure burst testing can be expected to also test high in EPPO testing. This data suggests that the EPPO test provides a good approximation of failure due to internal pressure.

Experimental data suggests that the general conclusions reached in the FEM study are correct. The experimental data showed that when using very stiff wall materials the EPPO and burst testing give relatively close results. In addition, experimental data shows the same strength trends between the two tests as was calculated in the FEM results. However, the experimental data provided additional results that should be kept in mind. Residual stress due to processing appears to have a significant effect on strengths and might not affect the EPPO test in the same manner it affects the pressure burst test. In addition, when performing pressure burst testing it is necessary to define failure criteria specifically as failure of the joint to get the best correlation with EPPO test. While there are important caveats to keep in mind, the correlation between these tests appears strong. It should be noted that there does not appear to be an easily obtained mathematical solution to this correlation, meaning the EPPO test cannot be used for fundamental shear or tensile strength measurements. However, based on this data the EPPO is particularly powerful tool when used as a comparison tool between different specimens and can be assumed that its results will correlate well with pressure burst testing.

3.5. High Temperature Testing

With a complete room temperature test method in place the emphasis was shifted to high temperature method development. The focus during this development was on the need for an appropriate gripping solution for a variety of temperature ranges. The passive method for bonding of the specimen into the test fixture was used, so suitable adhesives needed to be identified. For temperature up to 300 °C a similar adhesive as used in room temperature was used. A high temperature high strength epoxy, Masterbond EP46HT, was identified and testing took place in LWR relevant temperature range. At temperatures beyond this, the Morgan Ceramics Incusil Braze identified during earlier work in the project was used. This braze can be used for temperature up to about 650 °C. For even high temperatures, new brazes were explored. The test fixtures can only be used at temperatures up to about 850 °C, and this was the max test temperature explored for this work. While higher temperatures can be reached through the use

of ceramic fixturing, these fixtures are expensive and time consuming to have fabricated and were beyond the scope of the planned work.

While room temperature methodology was largely unaltered, several materials choices were made in order to accommodate high temperatures. Instead of hardened steel for the test fixtures, the high temperature super alloys Hasteloy X and Inconel 718 were used. The use of a compliant layer between the specimen and push rod is still required, but suggested material was changed to copper or silver foil, with sillver foil being preferred. This change was necessary due to graphite, the room temperature choice, oxidizing at the proposed test temperatures. The room temperature studies showed copper to be slightly less efficient at correcting for misalignment issues than graphite, but still a large improvement over no compliant layer. As lubricant between the collet and base fixture Boron Nitride spray coating was adopted versus teflon spray, used at room temperature.

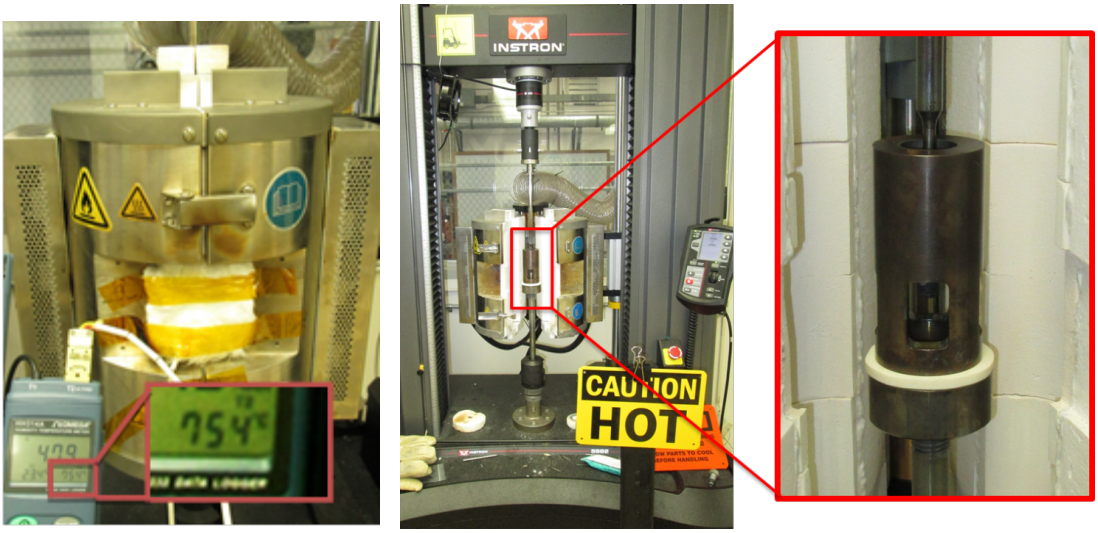

Fig. 3-50. High temperature test of a brazed incusil joint specimen just after testing at 300 °C

3.5.1. Test Temperatures

For high temperature EPPO testing it is important to be able to test at temperatures relevant to a variety advanced reactor concepts. A target temperature of 800 °C was set as the highest test temperature of this study due to the relevance to high temperature gas reactors and that being the max temperature the current superalloy fixture can be used with. Due to the difficulties of bonding SiC to metals, high temperature adhesives are limited to the class of brazes designated as “active” brazes. Active brazes contain metals that react with SiC that helps the braze wet and bond to SiC. These brazes make use of silver and copper as the primary metal filler due to the “softness” of the metal and the ability to bridge the coefficient of thermal expansion (CTE) between SiC and the steel or nickel Alloy. These brazes typically have liquidus points in the 750-900 °C range and use temps of up to 800 °C. Several active brazes were evaluated in order to increase maximum test temperature and a braze from Lucas Milhaupt containing 70% silver, 28% copper, and 2% titanium was chosen as the best candidate for testing

in the 700-800 ºC range. Note that at the higher end of this range the braze softens somewhat and loses some strength, so typical testing was done at 750 ºC, Fig. 3-50.

Silicon-chromium based brazes can be used up to temperatures approaching 1200 ºC. While it is not intended to test at these high of temperatures due to the requirement of expensive, long lead time ceramic fixtures, the use of these brazes for high temperatures has been established in the literature[9] and provides a braze for extreme temperature testing as might be expected to be seen in loss of coolant accidents.

Based on this information, and in combination with known reactor relevant temperature regimes, three test temperatures were targeted. Test temperatures of 300 °C were chosen as a demonstration of advanced LWR relevant temperatures. For this temperature regime high temp epoxies can be used to bond the specimen to the fixture. A test temperature of 600 °C was chosen due to relevance to molten salt and liquid sodium reactors which typically operate in the 550-700 °C range. For this temperature regime Incusil braze was used to bond the specimen to the fixture. A test temperature of 750 °C was chosen due to relevance towards high temp gas reactors such as GA's Energy Multiplier Module which typically operate in 750-850 °C range. For this temperature regime Lucas Milhaupt braze was used to bond the specimen to the fixture. Data is reported for valid tests only.

3.5.2. High Temp Strain Gauges

A method for application and setup for high temperature strain gauges on tubular specimens has been developed, Fig. 3-51. A multistep application of ceramic adhesive is used to apply the gauge to the specimen, Fig. 3-52. Test temperatures of up to 1000 ºC can be utilized with this method.

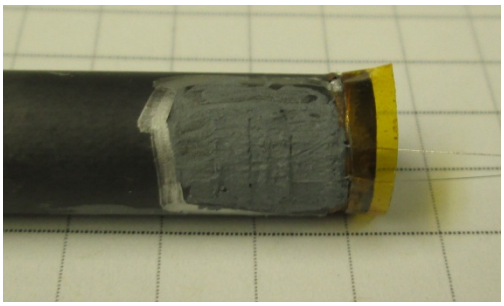

Fig. 3-51. High temperature strain gauge embedded in ceramic cement

A very thin layer of ceramic adhesive is applied as a bond coat (a) and cured. The strain gauge with carrier is applied and a thin layer of adhesive is applied to the exposed wire (b). This is cured at low temperatures and the carrier removed (c). The remaining exposed wire is coated with adhesive and a final cure of the adhesive performed (d). The strain gauge is now ready for use.

[9] B Riccardi et. al "High Temperature Brazing for SiC/SiC Ceramic Matrix Composites", in *Advanced SiC/SiC Ceramic Composites: Developments and Applications in Energy Systems*, Volume 14, John Wiley & Sons, Inc., Hoboken, NJ, USA.

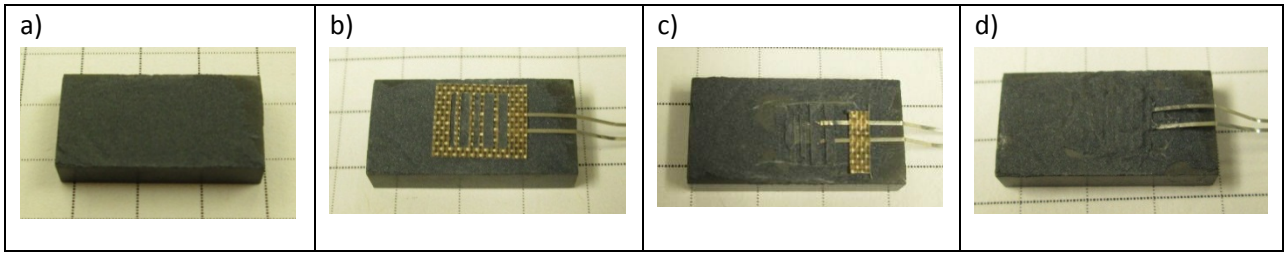

Fig. 3-52. Methodology for the application of strain gauges

In order to get accurate strain data a temperature compensating dummy gauge is utilized during testing to account for thermal induced strains, changes in lead wire resistance as a function of temperature, and changes in resistance of the strain gauge itself. To measure purely mechanical strains the dummy gauge is mounted onto a second tube identical to the first and heated alongside the test specimen, however the dummy gauge is not mechanically loaded. Data from the dummy gauge, seen in Fig. 3-53, is subtracted from data collected from the actual specimen during testing to obtain mechanical strain. However, it should be pointed out that with long enough dwell times at the target temperature the strain tends to go to a near equilibrium value and little change is seen over time.

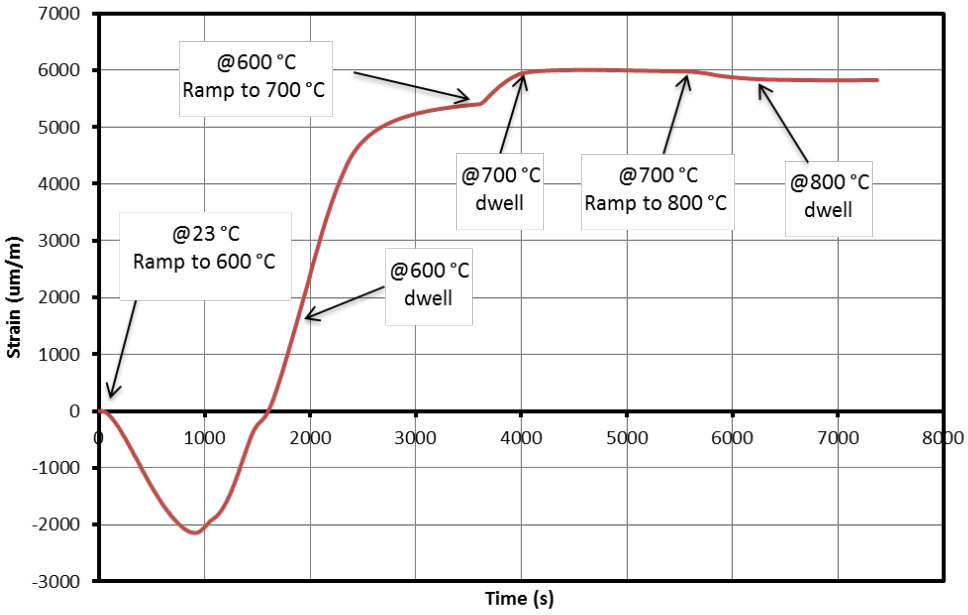

Fig. 3-53. Plot of strain versus time as measured by a temperature compensating dummy gauge as it is taken from room temperature to 800 °C

An example of the mechanical strain data for high temperature testing (600°C), properly compensated for temperature effects, can be seen in Fig. 3-54. High temperature strain gauges are subject to additional noise relative to their room temperature counterparts, but are still valuable for providing information on strain at the OD of the tube and for checking the alignment

of the specimen. In Fig. 3-54, the two strain readings at the left and right side of the specimen are nearly identical once load is applied, verifying the alignment of the specimen and ensuring a valid test is performed.

Due to the cost and lengthy procedure for application, unlike room temperature testing not all specimens were instrumented. While the strain on the outside of the tube is potentially useful information, the true purpose of the strain gauges is to evaluate bending during testing. Thanks to the alignment criteria developed earlier during room temperature method development, not all specimens require strain gauges in order to still be considered valid.

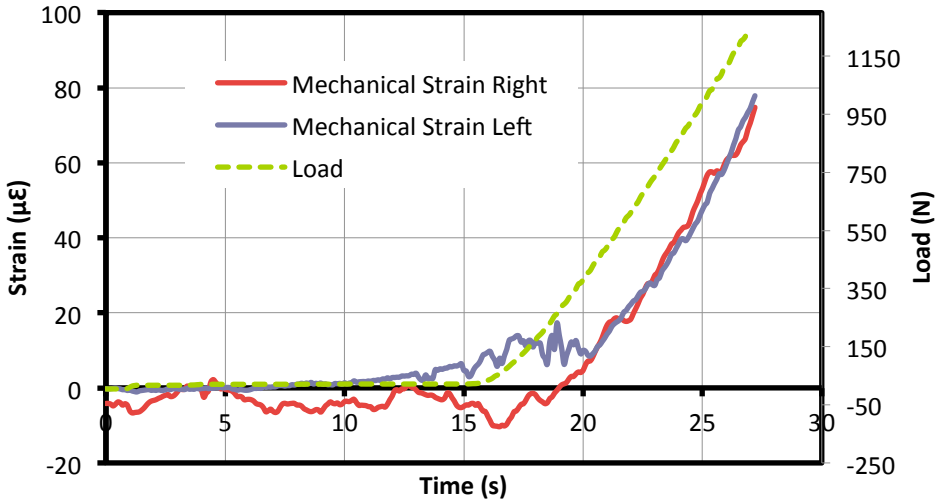

Fig. 3-54. Strain and load versus time for an Incusil brazed joint tested at 600 °C

3.5.3. Alternative Heating Methods

Typical high temperature test methodology uses a split tube furnace that uniformly heats the entire specimen and fixture to the desired test temperature. This method ensures repeatable, high quality results and was the primary development path for use in high temperature testing. However, target test temperatures are limited to the use temperature of your fixture material (<800 °C for metal fixtures) and your ability to bond the specimen to the fixture at high temperatures (commercial brazes top out at temperatures of ~800 °C). In addition, this type of test fixture can take over an hour to fully equilibrate once the target test temperature is reached.

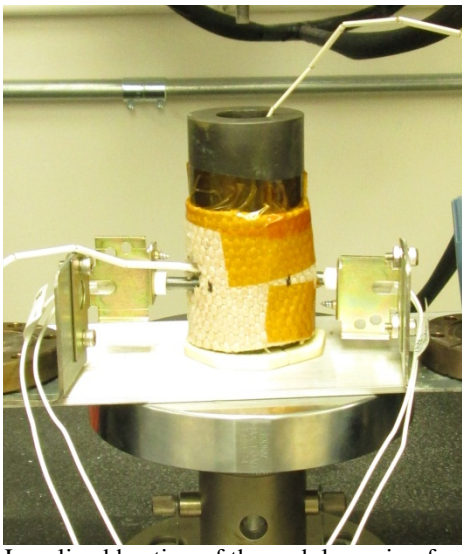

Fig. 3-55. Localized heating of the endplug using furnace ignitors.

An alternative method of heating was explored in which the joint itself was locally heated using silicon nitride based furnace ignitors, whose elements are typically very small (1/4" diameter x 2" long), Fig. 3-55. These ignitors heat very rapidly and can provide sustained temperature over 1500 °C. The ignitors are placed adjacent to the endplug inside of the test fixture thereby directing the heat to the joint itself and not through the test fixture. Insulation was added to protect the base metal fixture and to minimize heat loss. High temperature epoxy was used to bond the collets to the test specimen.

This method was used to test specimens up to 800 °C and in some cases was successful in gathering data similar to measured values using the clam shell furnace approach. For instance, the strength of a Lucas Milhaupt brazed joint at 600 °C was measured as 997 N, similar to that found for the clam shell method, 1045 N. However, two issues were encountered during testing. The first being temperature at the collet began to exceed 300 °C, and failure in the epoxy was observed. This was particularly an issue as GA tried to push the test temperature above 600 °C. The second issue was a larger than expected amount of test specimens were deemed non-valid due to failure away from the endplug region. During localized heating, thermal gradients in the tube are causing additional stress in the tube wall and causing failure in the tube as opposed to the joint. At this point, additional development is required for localized heating methods before it can be accepted as a valid alternative heating method in EPPO testing.

3.5.4. Versatility

In order to show the versatility of the high temperature test, several different adhesives, joint geometries, and tube types have been measured at several different temperatures, seen in table 3-8.

Table 3-8. High temperature and room temperature data for several joint types

Joint	Tube	Joint Geometry	Test Temp (°C)	Load at Temp (N)	Load at Room Temp (N)
Incusil	Monolithic	Scarf	300	1315 ± 358	749 ± 211
Incusil	Monolithic	Scarf	600	1337 ± 422	749 ± 211
Incusil	Composite	Scarf	600	2532 ± 645	880 ± 266
GA-HSiC	Composite	Scarf	600	1751 ± 162	1811 ± 265
GA-Glass	Monolithic	Butt	600	829 ± 138	998 ± 125
LM-Braze	Monolithic	Scarf	600	1414 ± 182	672 ± 158
GA-HSiC	Composite	Scarf	750	1551 ± 102	1811 ± 265
LM-Braze	Monolithic	Scarf	775	713 ± 148	672 ± 158

Incusil based joints on a monolithic tube were tested at 300 °C, Fig. 3-56. To bond the collets to the test specimen at 300 °C Masterbond EP46HT epoxy has been successfully used. Note that excessively long dwell times at temperatures can lead to failure of the epoxy and testing occurred as soon as the specimen equilibrated at target temperature. The results show an improved strength over room temperature testing, Table 3-8. This improved strength is likely due to relief of thermal induces residual stress in the joint. Standard deviation appears to be higher than room temperature tests, although in all cases it is within the range of 25-35% of the average.

Fig. 3-56. Incusil joined composite tube post testing at 600 °C.

For higher temperatures, Incusil Braze was used to bond the collets to the test specimen. An in situ firing process was developed where the braze is taken above the liquidus point in air in order to bond the specimen to the collets and dropped back down below the solidus point to the target test temperature. This is done in a single step to try and decrease residual stress caused by difference in the coefficient of thermal expansion (CTE) in the gripping region. By avoiding taking the specimen all the way back to room temperature, thermal induced residual stress is minimized and a stronger bond at the gripping region is obtained. This is particularly important for monolithic tube specimens where the residual stress significantly weakens the material at the collet/tube interface. A commercially available silver brazing flux is used during the process to protect the metal from oxidation. Some oxidation and weakening of the braze itself is expected to take place, but due to the large surface area of the collet this has not been a problem during testing.

The test data at 600 °C for composite and monolithic tubes with brazed, glass, and ceramic joints are seen in Table 2. Due to relief of processing stress at high temperatures, brazed based joints such as Incusil, Fig. 6, performed much better at higher temperatures. However, as in the case of the LM-Braze at 775 ºC, the braze tended to soften as it approached its liquidus

temperature and began to lose strength compared to the 600 ºC measurement. In the case of the Incusil braze the high temperature test results showed significantly larger standard deviations then room temperature testing, but this trend did not continue with the LM-Braze, nor when glass or ceramic brazes were tested suggesting this larger standard deviation at high temperatures is an artifact of the joint type and not the test itself. Ceramic and glass based joints appear to maintain the majority of their strength at elevated temperatures, as can be seen in GA fabricated Al_2O_3-Y_2O_3-SiO_2 based glass joints (GA-Glass) and SiC based ceramic joints (GA-HSiC), Fig. 3-57.

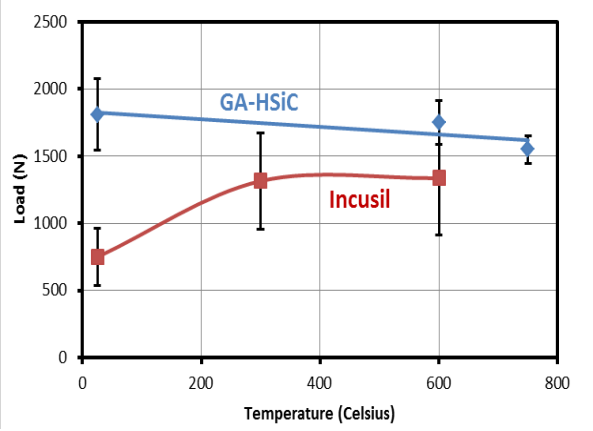

Fig. 3-57. Load vs Temp for Incusil joint on monolithic tube and GA-HSiC on composite tube.

3.5.5. Statistically Significant High Temperature Data Set

Similar to what was done at room temperature, a statistically significant set of specimens was tested at elevated temperature on the GA-HSiC joint material bonded to monolithic tube, Fig. 3-58, using the high temperature EPPO test method. The full data set can be found in appendix B.

Fig. 3-58 (Left). A set of 26 monolithic SiC Tube, CD SiC Endplug, and GA-HSiC joint specimens awaiting high temperature testing.

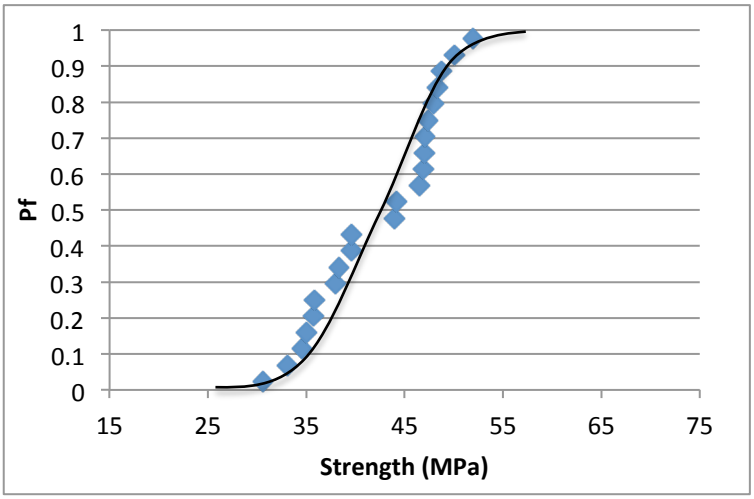

Fig. 3-59 (Right). Strength versus Probability for GA-HSiC joints tested at 600 ºC.

A total of 26 specimens were tested at 600 ºC. Four of these tests were considered invalid due to alignment or test errors giving a test efficiency of 85%, which is similar to that observed at room temperature. For the valid set of 22 specimens average load was 1640 +/- 245 N, characteristic burst pressure was 46.2 MPa and Weibull modulus was 7.8, Fig. 3-59. Weibull

modulus of 7.8 is well within the range typical for ceramics and ceramic composites as observed during flex testing. The full data for these tests can be found in Appendix B.

Comparing the Weibull modulus for this set of data to alternative test methods can provide insight into the possibility of data scatter due to test error. During previous testing of the joint material using torsion testing, a Weibull modulus of 6.0 was obtained. For room temperature EPPO testing the measured modulus was 4.4. Interestingly, both these moduli are lower than the measured modulus at high temperature. However, it is believed that these differences are due to improvements in fabrication of the joint and not due to test errors. Both the torsion and room temperature EPPO test data were taken over a year ago and since that time improvements in the fabrication process of GA-HSiC joint material have led to a decrease in measured porosity by several factors. For ceramic materials porosity level tends to be closely coupled with strength and data spread. In addition, issues with high temperature test methodology tend to lead to larger spread in the data, and decreased Weibull modulus, while the opposite trend is observed in this data.

In order to obtain a better understanding of the Weibull data obtained, XCT was used to measure the porosity in the joint, and how well the endplug mated to the tube. XCT analysis shows that while there is still residual porosity present in the joint material, the majority of this porosity tends to be small, having a volume of 0.01 mm^3 or less, and appears to be distributed uniformly through the joint, Fig. 3-60. For ceramic based joints it is expected for the Weibull modulus to be dictated by joint uniformity both on the micro and macro level as well as any scatter due to test inconsistencies. The observed XCT image and measured porosity is consistent with a joint that has a relatively high modulus. Actual EPPO testing gave a modulus of 7.8, which is consistent with the XCT imaging and suggests that the test itself is not introducing additional scatter in the data.

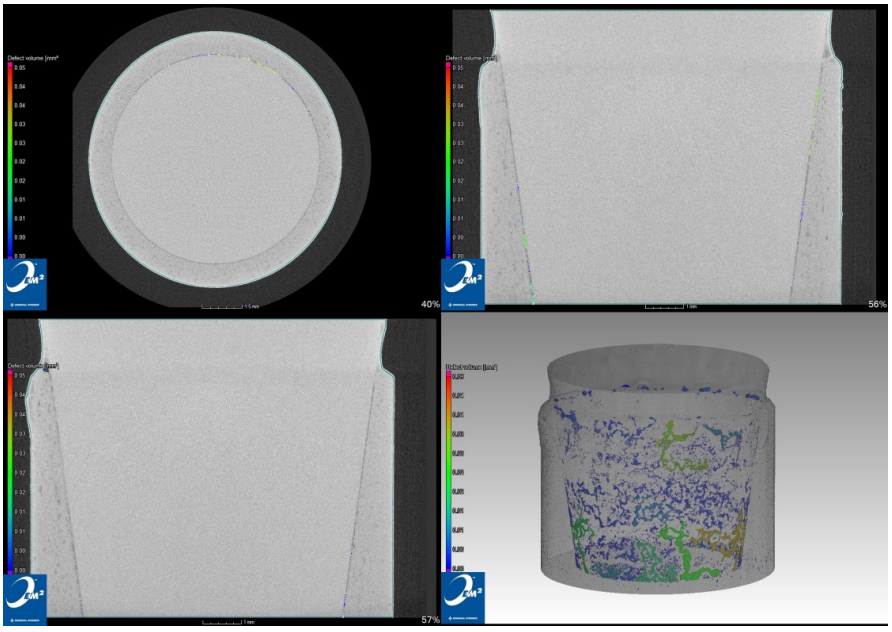

Fig. 3-60. Porosity analysis via XCT on a GA-HSiC joint using a Nikon XT H 225.

Two typical fracture patterns were observed during testing. In type A the fracture takes place entirely in the tube near the tip of the endplug, Fig. 3-61 (Left). The cleavage plane is in line with the push surface of the endplug. In type B, a mixed mode failure is seen where cracking propagates through the joint as well as in the tube, Fig. 3-61 (Right). In type B, failure appears to be predominantly in the joint, as very little substrate remains on the joint interface. Both of these failure types are considered valid tests as failure took place in the endplug region, away from the split collets.

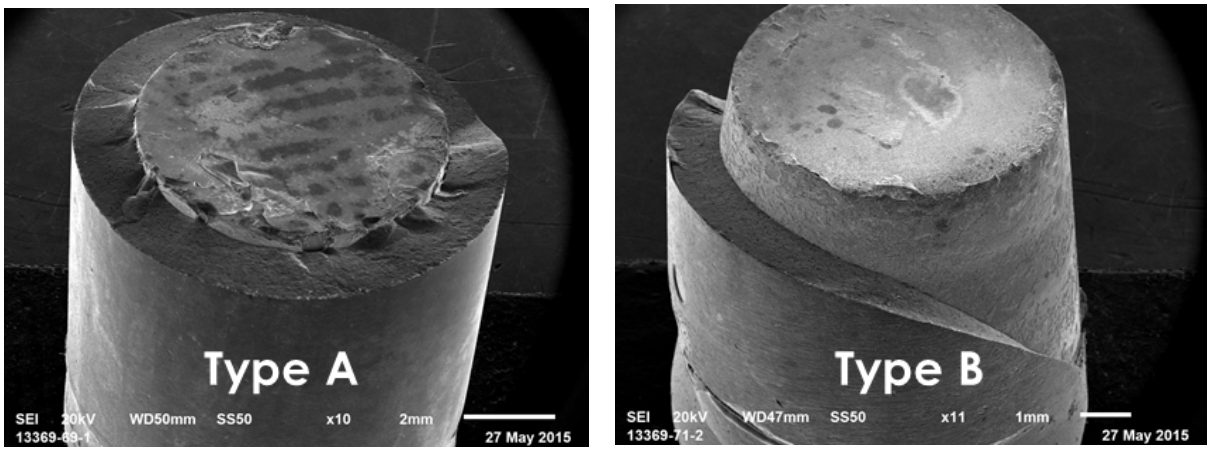

Fig. 3-61. (Left) Type A fracture in tube **(Right)** Type B mixed mode tube/joint fracture.

3.5.6. Finite Element Modeling

3.5.6.1. MODELING FAILURE OF SPECIMENS

In order to more fully understand the observed Type A and Type B failure modes discussed in section 3.5.5, a FEA was performed. As previously discussed, there is a stress concentration point in endplug-tube bonding. This stress concentrator helps to explain the Type A fracture pattern observed during testing. The location of maximum stress in the tube, matches very closely with the fracture location observed experimentally. For a load of 2000 N (apparent burst pressure of 50 MPa), this corresponds to a stress of 231 MPa which begins to approach the measured tensile strength of the Hexoloy tube (280 MPa), Fig. 3-62. Due to uncertainties associated with mesh and input properties it seems likely that the model is predicting lower stresses than what may actually be experienced during testing, but is correctly predicting the dominant stress concentration location.

Type B failure mode can be better explained by looking at the shear stress in the joint material. A plot of the maximum shear stress in GA-HSiC along the length of the joint can be seen in Fig. 3-63. The maximum stress in the joint is located adjacent to the stress concentrator in the monolithic tube and at 2000 N of load shear stress is calculated to be over 100 MPa. Hourglass torsion testing of the GA-HSiC joint material has given characteristic shear strength of approximately 80 MPa. Based on the FEA, it is expected that at high loading, the joint shear stress can be exceeded and partial failure in the joint material will occur.

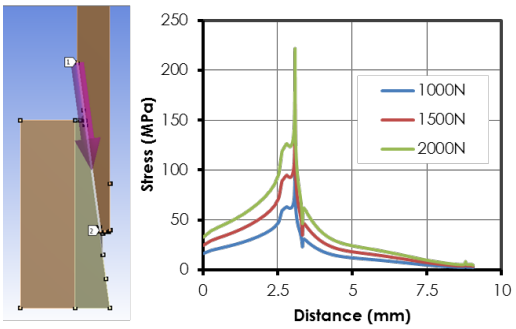

Fig. 3-62 (Left). Plot of principal stress in the monolithic tube along the designated pathway.

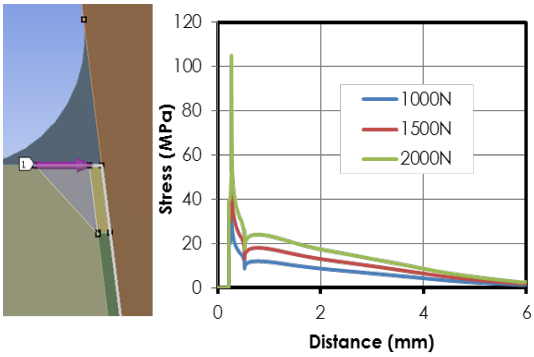

Fig. 3-63 (Right). Plot of shear stress in the GA-HSiC joint along the designated pathway.

3.5.6.2. High Temperature Modeling of Brazes

One of the challenges with the use of metal based brazes both for the bonding of the collets to the SiC tube as well as for bonding of a SiC endplug to a SiC tube is the residual stresses that build up in the joints due to mismatches between metal and ceramic thermal expansion. In the high temperature method it was necessary to set the braze in situ during testing to avoid fracturing specimens from residual stress. In order to get a better understanding of the magnitude of this stress, FEA was used.

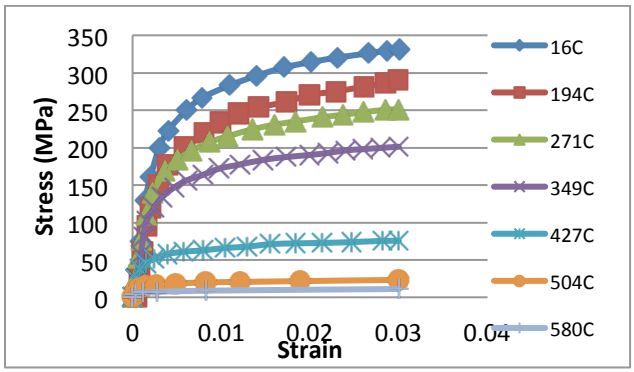

Fig. 3-64. Temperature dependent stress strain plot for Incusil Braze.

Temperature dependent properties are required for this calculation including data on CTE. For SiC, mechanical properites are assumed to remain constant with temperature and a CTE of 4.4×10^{-6} C^{-1} is used. For the Incusil braze, temperature dependent properties were obtained from the literature, Fig. 3-64. A zero stress temperature condtion for the model was set at 605 ˚C. The zero stress temperature occurs at the solidus point, when the braze material is fully transitioned to a solid in the brazing process. For these calculations, it has been assumed that the temperature decreases uniformly throughout the part.

Using this data as input to the model, the shear stress for the brazed joint can be calculated and is plotted in Fig. 3-65. As expected, the residual stresses at the joint increase as the braze temperature decreases. The lowest residual shear stress occurs at higher temperatures since they are closest to the zero stress state. If the specimen is left to cool down all the way to room temperature, large residual shear stresses are left in the joint resulting in lower measured loads in the EPPO test. This effect was observed experimentally and is reported on in the Quarter 1, 2015 report. While this modeling was specifically done on the joint itself, it can be assumed that

a similar stress buildup will be observed in the brazed bond between the collets and ceramic tube used for gripping of the specimen. This underscores the necessity of choosing a braze whose liquidus to solidus transition point is just over the target test temperature so that residual stress is minimized and failure occurs in the endplug joint instead of in the grip region.

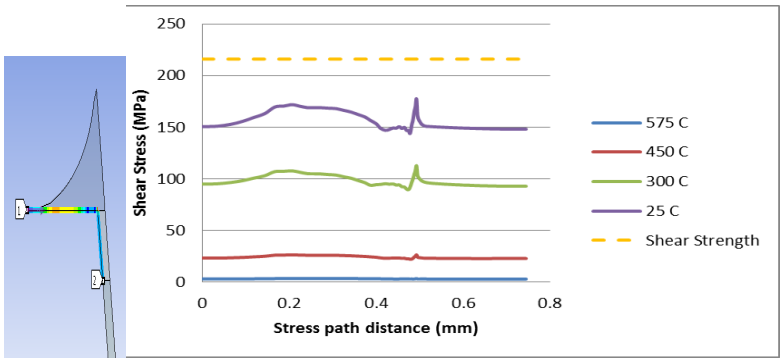

Fig. 3-65. Plot of shear stress in the Incusil joint along the designated pathway.

3.6. ASTM Standard Development

Using the accumulated data obtained during the period of performance, and ASTM standard has been drafted and is found in Appendix C for high temperature testing of cylindrical geometry joints. This standard was drafted with assistance from Steve Gonczy of Gateway Materials Corporation. Dr. Gonczy is primary author of seven ASTM C28 test standards and helped coauthor numerous additional standards. Dr. Gonczy assisted GA with writing of the ASTM standard to ensure it meets the rigors and format required by ASTM.

A work item has been assigned by the ASTM C28 ceramics committee and they have been notified of the intent to submit. GA has actively attended C28 committee hearings during the period of performance and interacted with the relevant players to assure the standard meets requirements. GA is currently allowing ceramic testing experts and end-users to review the draft of the standard and provide input before final submission. GA will be submitting the standard for balloting by the ASTM C28 ceramics committee before the end of the year.

In only about a quarter of the cases are new standards like the endplug pushout test approved on first ballot. Instead, it is typical first ballot standards receive feedback from the community and is improved upon and resubmitted. It is GAs intention to support the standard through the balloting process. If approved, a round robin study will need to commence to demonstrate the standard can be used effectively by a variety of labs with a variety of users and equipment. While this round robin was outside the scope of the proposed work, GA is willing to provide the equipment and test specimens if adequate outside funding for the endeavor is obtained.

4. PRODUCTS DEVELOPED/TECHNOLOGY TRANSFER

4.1. Conferences

George M. Jacobsen, Christina A. Back "DOE Advanced Reactor Research and Development: Development of ASTM Standard for SiC/SiC Joint Testing" 2013 ANS Winter Meeting, Washington, D.C.

Hesham E. Khalifa, George M. Jacobsen, Christian P. Deck, Christina A. Back "Robust, Radiation Tolerant Joining of SiC Structures for Nuclear Applications" CMCEE 2015, Vancouver, B.C., Canada.

George M. Jacobsen , Hesham E. Khalifa, Yi Kearns, Christian P. Deck, Christina A. Back "High Temperature Testing of Geometrically Relevant, Nuclear Grade Silicon Carbide Joints" ANS Winter Meeting, 2015, Washington, D.C.

4.2. Papers

A journal article is currently being written describing the development of the test method and comparison of burst testing to EPPO testing. It has yet to be decided where the article will be submitted, but GA will provide a copy for approval to the DOE program manager prior to submittal.

4.3. Test Standard

The ASTM standard is the primary technology transfer that occurred as a result of this award. This standard reflects the lessons learned during the period of performance and is being submitted through the ASTM ceramics committee. Upon approval, the standard will provide the nuclear community a universally available test standard for cylindrical joint testing. The pre-submittal draft can be seen in Appendix C.

4.4. Collaborations Fostered

As previously mentioned, GA worked closely with Steve Gonczy of Gateway Materials Corporation during drafting of the standard. Steve has a wealth of information on testing and standardization of ceramic composite materials and is expected to be a valuable resource as GA continues to advance ceramic testing technology and standardization for nuclear applications.

In addition, in cooperation with DOE-NE sponsored accident tolerant fuel initiative, collaboration with Thomas McKrell at MIT took place. GA had MIT perform EPPO testing as part of a more comprehensive composite testing program. This occurred late in the contract and provided an opportunity for an outside laboratory to verify the procedure developed by GA and provide input into the test standard from an outside perspective.

5. COMPUTER MODELING

An overview of the input parameters, boundary conditions, geometries, and assumptions for the FEM is provided below. Further information about how this modeling was used and verification/validation of FEM can be found in the relevant subsections of section 3.

For the computer modeling discussed in the project activities section the commercially available software Solidworks 2014[10] and ANSYS 2014/2016[11] was used. These programs were run on desktop computers with typical quad core i7 processors and a minimum of 8 GB or ram. Input data was obtained from the literature[12],[13], or from internal testing performed at GA during the EPPO contract.

In general a 3D model for the tube, joint and end plug was created in SolidWorks 2014. A nominal joint thickness of 50 microns was used. The tube OD is 9.5 mm with a wall thickness of 1.7 mm. The Solidworks file was imported into ANSYS and evaluated as an axissymetric model with boundary conditions shown in Fig. 5-1 for the tube and endplug. Composite tubes were modeled using a Bilinear Isotropic Hardening (BISO) module of ANSYS. The boundary conditions used for modeling of the tube can be found in Table 5-1.

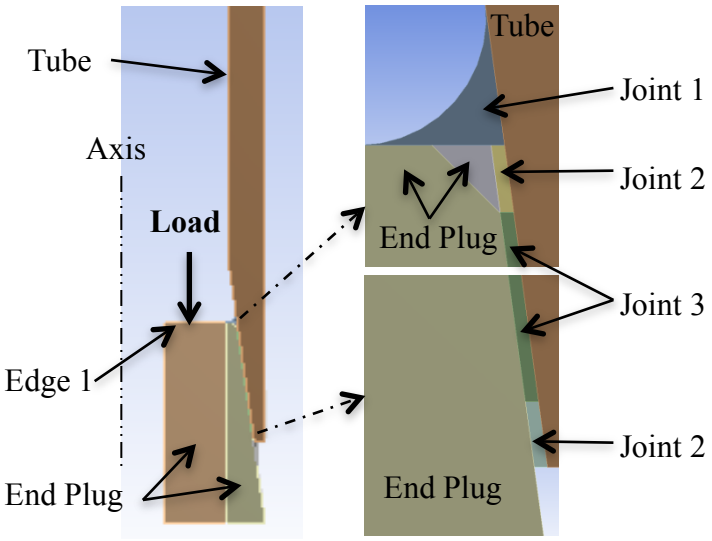

Fig. 5-1. The axisymmetric boundary conditions where the joint region was treated as a uniform material (epoxy/braze) and a three part material for GA-HSiC.

[10] SolidWorks 2014 SP 4.0, Dassault Systèmes, Vélizy, France, (2014)

[11] ANSYS APDL/ANSYS Workbench Release 14.5, ANSYS, Inc, Canonsburg, Pennsylvania, United States, (2014)

[12] Snead et. al. "Handbook of SiC Properties for Modeling", *J. Nuc. Mat.*371, 329-377, (2007)

[13] Katoh et. al. "Continuous SiC Fiber Matric Composites for Nuclear Applications" , J. Nuc. Mat., 448, 448-476, (2014)

A uniform load was applied to Edge 1 of the end plug for the EPPO test, while load replicating internal hydrostatic pressure was applied for burst testing. The tube was supported by a frictionless edge along the top of the tube. Mesh size was based on a balance of processing time versus accuracy/resolution. Very fine meshes produce more resolution and a more accurate value for the stress concentration point, see Fig. 5-2, but were time intensive to calculate solutions. Ultimately, a mesh size was chosen that allowed a run time of no more than 1 hour while still providing needed accuracy. Finer incremental meshing beyond the mesh size chosen resulted in little change to the calculated stress (<2%).

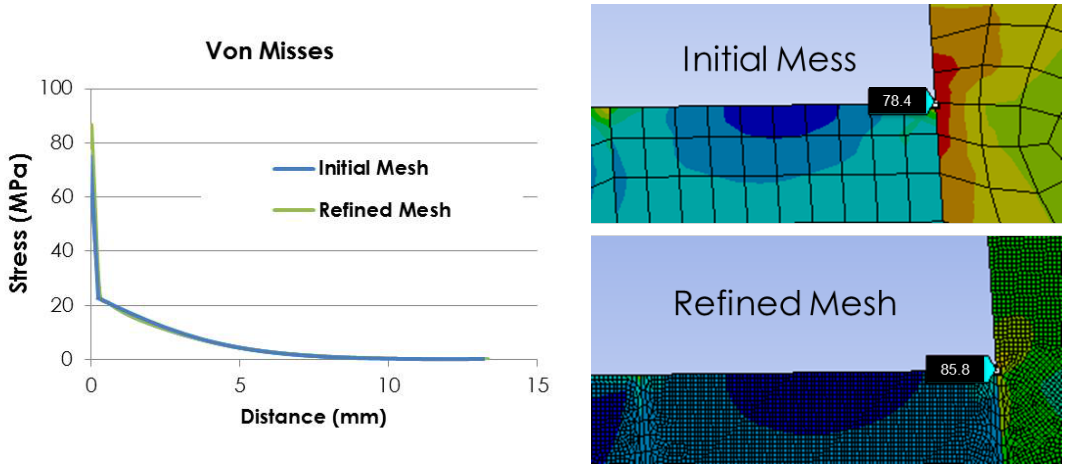

Fig. 5-2. Calculated Von Mises stresses for an initial course mesh and a refined, decreased size mesh.

Boundary conditions for different joint materials explored are listed in Table 5-2. For GA-hybrid material the joint was divided into three sections based on experimental observation of joint density. Material properties were treated as constants with increasing temperature when high temperature modeling was performed, with the exception of the brazes where temperature dependent properties were used as described in section 3.5.6.2.

Table 5-1. Boundary conditions for tube axisymmetric model

Component	Young's Modulus (GPa)		Poisson's Ratio	Tensile Strength (MPa)		CTE (C^{-1})
Monolithic Tube	440		.21	275		4.4E-6*
Composite Tube	Elastic = 290	Plastic = 30	0.17	PLS=95	UTS=215	4.4E-6*
End Plug	440		.21	275		4.4E-6*

*Constant from 605˚C to 25˚C.

Table 5-2. Boundary conditions for joint in axisymmetric model

Joint Type	Sections	Young's Modulus (GPa)			Poisson's Ratio			Tensile Strength (MPa)	Shear Strength (MPa)	CTE (C^{-1})
GA HSiC	3	1=300	2=150	3=100	1=0.21	2=0.15	3=0.14	15	75	4.4E-6*
Tuff Bond Epoxy	1	10			0.35			72	31	N/A
Incusil Braze	1	76			0.36			Variable	273	Variable

* Constant from 605˚C to 25˚C.

During modeling several key assumptions were made regarding material behavior. These assumptions are outlined below with a relative evaluation of their importance.

1. Tube, endplug, and joint material are treated as isotropic. For monolithic materials this is a valid assumption but for composite material there is known variations depending on fiber architecture. While "balanced" architectures were primarily used during composite work, it is expected that stress/strains may show some variations in axial versus hoop directions that are not accounted for in the model.

2. Joint material behavior is treated as uniform or discrete uniform sections. Variations in joint material are known to exist based on dimensions, processing conditions, applied pressure, and alignment. However, these difference appear to average out and this assumption seems to have limited impact on results.

3. A 2d axisymmetric model was used for almost all of the FEM due to the implied symmetry of the test specimen. This assumption was tested in the course of the FEM versus a full 3d model and variations were small compared to other factors like mesh size.

4. Except for the case of the high temperature braze work, all modeling was performed at room temperature with no processing stresses present in the specimens. In some case processing stresses are known to be present while in other cases actual experimental testing that the FEM was compared against was performed at high temperature. In these cases a qualitative assessment was made on what expected contributions may be due to unaccounted for stresses. Unless specifically noted in the relevant text in section 3, these stresses were determined to be small relative to expected stresses as a result of the EPPO.

APPENDIX A: ROOM TEMPERATURE REPEATABILITY TEST DATA

lab notebook pg	13380-23 through 13380-35											
Date	6/20/2014											
Tube Manufacturer/Type	Hexoloy SiC											
Tube Specs	Grade SE monolithic SiC, LWR sized											
End Plug Manufacturer/Type	GA SiC											
Endplug Specs	TEP SiC, 7.75 degree scarf angle											
Joint Manufacturerer/Type	GA SiC											
Joint Specs	Hybrid Polymer/CVI joint											
Temperature (°C)	26											
Humidity (%)	40-70											
Atmosphere	air											
Crosshead Rate (mm/min)	1.5											
Compliant Layer	1/32" Graphoil											
Push Rod Diameter (mm)	5.75											
Test ID	Specimen ID	Total Length (mm)	Tube OD (mm)	Tube Wall (mm)	Tube length (mm)		Endplug length (mm)	EndPlug D1 (mm)	EndPlug D2 (mm)	Endplug Angle		Joint length - XCT (m
13380-23-1		52.91	9.67	1.74	51.10		10.18	8.57	6.12	7.75		8.76
13380-23-2		53.24	9.74	1.67	51.65		9.90	8.94	6.32	7.75		8.32
13380-23-3		51.04	9.69	1.80	50.34		9.96	9.42	5.98	7.75		8.97
13380-23-4		52.84	9.61	1.61	50.29		9.75	9.30	6.64	7.75		7.42
13380-23-5		52.17	9.67	1.67	52.09		9.92	8.38	5.98	7.75		8.42
13380-23-6		54.51	9.60	1.64	50.87		9.92	8.58	6.16	7.75		6.76
13380-23-7		53.82	9.53	1.55	51.59		9.97	8.99	6.26	7.75		7.73
13380-23-8		54.45	9.80	1.89	50.56		11.39	9.57	6.52	7.75		7.63
13380-23-9		52.66	9.51	1.83	50.53		9.65	8.70	6.23	7.75		8.22
13380-23-10		52.04	9.72	1.65	51.33		10.10	9.39	6.84	7.75		8.78
13380-28-1		54.29	9.86	1.70	52.05		10.88	9.42	6.38	7.75		8.27
13380-28-2		54.71	9.63	1.57	53.54		10.84	8.91	6.15	7.75		9.15
13380-28-3		52.81	9.58	1.56	52.34		10.55	9.31	5.79	7.75		8.41
13380-28-4		54.17	9.80	1.68	52.09		10.60	9.35	6.45	7.75		8.31
13380-28-5		53.68	9.71	1.63	51.33		9.95	9.25	6.25	7.75		7.50
13380-28-6		52.18	9.64	1.69	51.83		10.21	8.74	6.35	7.75		9.13
13380-28-7		54.25	9.90	1.65	51.83		10.73	9.13	6.44	7.75		8.15
13380-28-8		54.40	9.69	1.69	51.61		10.20	9.60	6.65	7.75		7.98
13380-28-9		53.26	9.62	1.69	52.26		10.01	8.98	6.43	7.75		8.89
13380-28-10		54.54	9.84	1.64	52.02		10.44	9.23	6.35	7.75		7.53
13380-32-1		53.21	9.75	1.63	51.72		9.65	9.00	6.49	7.75		8.30
13380-32-2		54.32	9.70	1.70	51.78		10.34	9.34	6.56	7.75		8.11
13380-32-3		54.24	9.65	1.67	51.88		10.29	9.23	6.44	7.75		7.92
13380-32-4		52.28	9.61	1.61	50.67		10.31	9.23	6.38	7.75		8.81
13380-32-5		51.03	9.67	1.67	49.39		9.93	9.16	6.45	7.75		8.37
13380-32-6		53.46	9.59	1.65	51.82		9.88	9.44	6.73	7.75		8.24
13380-32-7		54.51	9.53	1.55	52.18		9.44	9.29	6.71	7.75		6.68
13380-32-8		54.55	9.68	1.70	51.87		9.94	9.48	6.75	7.75		7.11
13380-32-9		54.06	9.66	1.66	51.77		9.89	9.36	6.61	7.75		7.95
13380-32-10		53.65	9.75	1.63	51.81		9.72	9.41	6.77	7.75		7.32

Joint D1 - xct (mm)	Joint D2 - xct (mm)	Joint Area - Geometry (mm	Joint Area - XCT (mm^2)	Load (n)	Apparent Burst Strength	Apparent Strength - Geometry(Mpa)	Apparent Strength - XCT (Mpa)	Valid Test	Notes
6.16	8.63	260.16	203.51	1655	56	6.36	8.13	Yes	
6.20	8.62	238.85	193.68	1859	62	7.78	9.60	Yes	
6.16	8.49	268.94	206.42	1267	43	4.71	6.14	Yes	
6.64	8.60	209.16	177.63	623	18	2.98	3.51	Yes	
6.29	8.76	278.96	199.05	2044	66	7.33	10.27	Yes	
6.70	8.60	259.13	162.46	1478	42	5.70	9.10	Yes	
6.28	8.54	235.49	179.95	1222	39	5.19	6.79	Yes	
6.40	8.69	223.71	180.86	363	11	1.62	2.01	No	misalignment over threshold
6.28	8.44	221.07	190.06	888	29	4.02	4.67	Yes	
6.34	8.56	189.52	205.49	1428	45	7.53	6.95	Yes	
6.43	9.01	228.01	200.57	931	29	4.08	4.64	Yes	
6.22	9.09	226.69	220.05	959	32	4.23	4.36	No	misalignment over threshold
6.27	8.57	237.74	196.04	1474	48	6.20	7.52	Yes	
6.31	8.84	261.50	197.76	1551	50	5.93	7.84	Yes	
6.42	8.69	252.85	178.01	1599	49	6.32	8.98	Yes	
6.28	9.00	251.86	219.14	1485	48	5.90	6.78	Yes	
6.37	8.82	198.99	194.46	1820	57	9.15	9.36	Yes	
6.45	9.16	209.48	195.67	1634	50	7.80	8.35	Yes	
6.36	9.00	233.30	214.49	1839	58	7.88	8.57	Yes	
6.82	8.86	232.42	185.46	1003	27	4.32	5.41	Yes	
6.43	8.79	228.01	198.43	1603	49	7.03	8.08	Yes	
6.33	8.85	226.69	276.51	684	22	3.02	2.47	No	misalignment over threshold
6.44	8.86	237.74	272.18	996	31	4.19	3.66	Yes	
6.45	8.94	261.50	306.61	1494	46	5.71	4.87	No	misalignment over threshold
6.31	8.65	252.85	282.98	296	9	1.17	1.05	No	Crack observed in specimen ne
6.52	8.91	251.86	286.43	882	26	3.50	3.08	Yes	
6.46	8.40	198.99	223.75	938	29	4.71	4.19	Yes	
6.82	8.91	209.48	251.91	1129	31	5.39	4.48	Yes	
6.50	8.81	233.30	274.01	1322	40	5.67	4.82	Yes	
6.80	9.00	232.42	260.07	1223	34	5.26	4.70	Yes	

APPENDIX B: HIGH TEMPERATURE REPEATABILITY TEST DATA

lab notebook pg	13369-62 through 13369-80
Date	5/20/2015
Tube Manufacturer/Type	Hexoloy SiC
Tube Specs	Grade SE monolithic SiC, LWR sized
End Plug Manufacturer/Type	Morgan SiC
Endplug Specs	CVD SiC, 7.75 degree scarf angle, ground by prematech
Joint Manufacturer/Type	GA SiC
Joint Specs	GA-HSiC: Hybrid Polymer/CVI joint
Nominal Test Temp(°C)	625
Humidity (%)	46
Atmosphere	air
Crosshead Rate (mm/min)	1.5
Compliant Layer	1/64" Silver
Push Rod Diameter (mm)	5.75

	Test ID	Specimen ID	Joint Area - Geometry (mm^2)	Joint Area - XCT (mm^2)	Specimen Temp (°C)	Load (N)	Nominal Burst Strength (MPa)	Apparent Strength - Geometry (Mpa)	Apparent Strength - XCT (Mpa)
1	13369-62-1	130423-33-1	190.02	223.21	607	1510	37.9	7.95	6.76
2	13369-63-1	130423-37-5	180.58	185.55	609	1535	39.5	8.50	8.27
3	13369-63-2	130423-33-3	183.03	157.10	602	1693	44.0	9.25	10.78
4	13369-65-1	130423-33-5	174.04	136.79	604	2016	50.1	11.58	14.74
5	13369-65-2	130423-33-6	179.54	148.06	608	1891	48.7	10.53	12.77
6	13369-66-1	130423-33-9	176.35	152.91	609	1836	48.0	10.41	12.01
7	13369-66-2	130423-33-8	186.96	134.46	617	84	2.2	0.45	0.62
8	13369-66-1	130423-33-10	173.82	92.00	610	1406	35.0	8.09	15.28
9	13369-66-2	130423-37-1	171.45	191.79	616	1720	44.2	10.03	8.97
10	13369-69-1	130423-37-2	184.08	199.96	611	1998	51.9	10.85	9.99
11	13369-69-2	130423-37-3	177.46	172.00	619	1806	46.5	10.18	10.50
12	13369-70-1	130423-37-6	183.85	170.36	609	1376	35.9	7.48	8.08
13	13369-70-2	130423-37-7	183.03	204.88	588	1823	47.4	9.96	8.90
14	13369-71-1	130423-37-10	201.82	194.29	613	1501.3	39.6	7.44	7.73
15	13369-71-2	130423-38-1	179.39	165.01	602	1357	34.6	7.56	8.22
16	13369-72-1	130423-37-8	191.99	197.38	613	1170.5	30.6	6.10	5.93
17	13369-72-2	130423-33-4	194.91	136.38	618	1146	30.0	5.88	8.40
18	13369-73-1	130423-38-3	179.54	151.52	608	1282.59	33.0	7.14	8.46
19	13369-73-2	130423-33-2	191.51	129.57	599	1784	46.9	9.32	13.77
20	13369-75-1	130423-38-4	177.83	152.39	604	1374.8	35.7	7.73	9.02
21	13369-75-2	130423-38-2	196.13	145.24	598	1102	30.5	6.03	8.14
22	13369-76-1	130423-38-6	197.09	197.69	620	1823.6	48.3	9.25	9.22
23	13369-76-2	130423-38-7	178.95	156.56	602	1833.83	47.0	10.25	11.71
24	13369-77-1	130423-37-4	185.69	202.45	598	1505	38.3	8.10	7.43
25	13369-82-2	130423-38-5	192.71	137.71	605	1336	34.6	6.93	9.70
26	13369-83-1	130423-33-7	184.18	171.40	606	1838.00	47.1	9.98	10.72

Alignment Criteria	Strain 1 (με)	Strain 2 (με)	Strain 3 (με)	Strain4 (με)	Percent Bending (%)	Valid Test (Yes/No)	Break Location	Notes
Pass						yes	tube at endplug	
Pass						yes	tube at endplug	
Pass						yes	mix of joint and tube	
Pass						yes	tube at endplug	
Pass						yes	tube at endplug	
Pass						yes	tube at endplug	
Pass						yes	primarily in joint	
Pass						no	Shattered	Error during testing resulted in fragmenting of specimen
Pass						yes	tube at endplug	
Pass						yes	tube at endplug	
Pass						yes	tube at endplug	
Pass						yes	between endplug and joint	
Pass						yes	mix of tube and in joint about 70:30 (contact:uncontat area	
Pass						yes	tube at endplug	
Pass						yes	tube at endplug	
Pass						yes	joint, with 40% contact area	
Fail	89	53	N/A	N/A	51	yes	45% broke in joint, est 45 degrees crack line	
Pass						no	In joint majority, small section in tube	Non-valid due to percent bending
Pass						yes	tube at endplug	
Fail	89	N/A	N/A	N/A	N/A	yes	tube at endplug	
Pass						yes	tube at endplug	
Fail	70	26	N/A	N/A	92	no	broke in combination of tube and joint	Non-valid due to percent bending
Pass						yes	tube at endplug	
Pass						yes	tube at endplug	
Fail	76	55	N/A	N/A	32	yes	tube at endplug	
Fail	68	46	N/A	N/A	63	no	tube at endplug	Non-valid due to percent bending
Fail	N/A	N/A	N/A	N/A	N/A	yes	failed primarily in tube, small portion in joint	

APPENDIX C: ASTM DRAFT TEST STANDARD

Designation: X XXXX-XX

Work Item Number: WK51822
Date: 10/01/2015

Date: **October, 2015**

To: **ASTM Subcommittee C28.04**

Tech Contact: **George Jacobsen, General Atomics, george.jacobsen@ga.com, 858-455-2377**

Steve Gonczy, Gateway Materials Technology, Inc. gatewaymt@aol.com, 847-870-1621

Work Item #: **WK51822**

Ballot Action: **New Standard -- Standard Test Method for the Nominal Joint Strength of End-Plug Joints in Advanced Ceramic Tubes at Ambient and Elevated Temperatures**

Rationale: **This test standard provides a detailed description of a new test method for the nominal joint strength of bonded ceramic end-plugs in ceramic tubes. This is an important test for component development, product qualification, and quality control. There are no similar test standards available.**

Standard Test Method for the Nominal Joint Strength of End-Plug Joints in Advanced Ceramic Tubes at Ambient and Elevated Temperatures

This standard is issued under the fixed designation X XXXX; the number immediately following the designation indicates the year of original adoption or, in the case of revision, the year of last revision. A number in parentheses indicates the year of last preapproval. A superscript epsilon (ε) indicates an editorial change since the last revision or preapproval.

1. Scope

1.1 This test method covers the determination of the push-out force, nominal joint strength, and nominal burst pressure of bonded ceramic end-plugs in advanced ceramic cylindrical tubes (monolithics and composites) at ambient and elevated temperatures (See Figure 1). The end-plugs can have a variety of different configurations with single and mixed-mode stress states. Adhesively bonded joints use organic adhesives, solders, metals brazes, glass sealants, and ceramic adhesives (sintered powders, sol-gel, polymer-derived ceramics) as the bonding material between the end-plug and the tube The test method describes the test capabilities and limitations, the test apparatus, test specimen geometries and preparation methods, test procedures (modes, rates, mounting, alignment, testing methods, data collection, and fracture analysis), calculation methods, and reporting procedures.

In this end-plug push-out (EPPO) test method, test specimens are prepared by adhesively bonding a fitted ceramic plug into one end of a ceramic tube. The test specimen tube is secured into a gripping fixture and test apparatus and an axial compressive force is applied to the interior face of the plug to push it out of the tube. (See Figure 2.) The axial force required to fracture (or permanently deform) the joined specimen is measured and used to calculate a nominal joint

1.2 strength and a nominal burst pressure. Tests can be done at ambient and elevated temperatures, based on the temperature capabilities of the test furnace and the test apparatus.

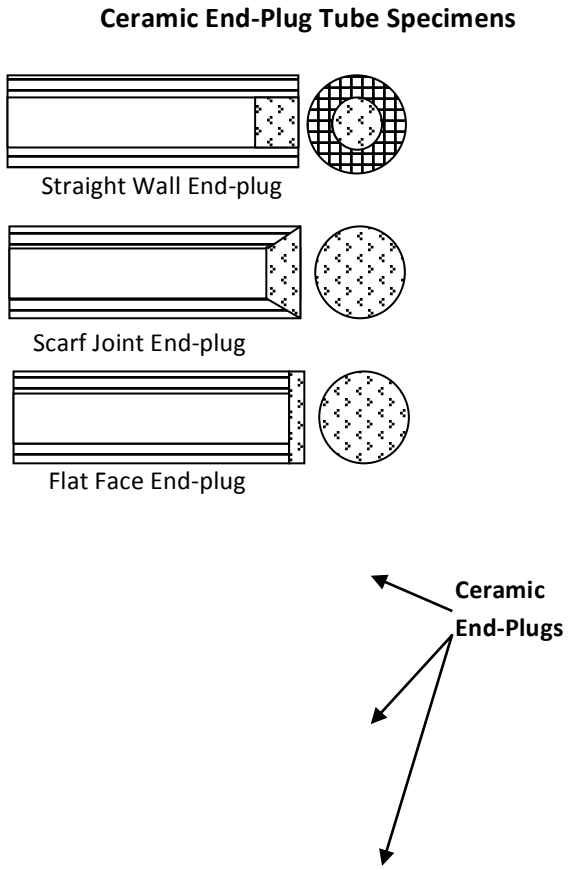

Figure 1 - Test Specimens with Different End-Plug Configurations

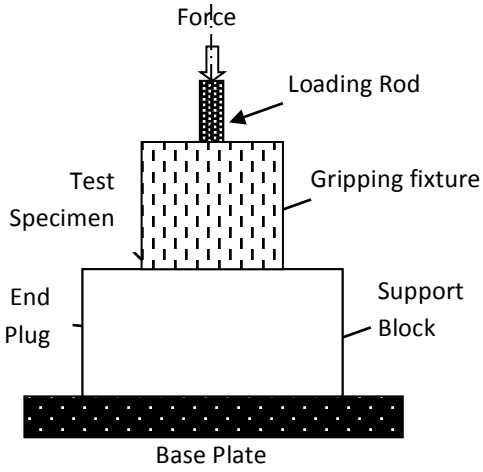

Figure 2 - End-Plug Push-Out (EPPO) Test System Schematic

1.3 This test method is applicable to end-plug test specimens with a wide range of configurations and sizes. The test method does not define a standardized specimen geometry, because the purpose of the test is to determine the nominal joint strength and nominal burst pressure of an application-specific plug-tube design. The test specimen should be similar in size and configuration with the intended application and product design.

1.4 This test method calculates a nominal joint strength which is specific to the adhesives, adherends, configuration, size, and geometry of the test specimen. The nominal joint strength has value as a comparative test for different adhesives and plug configurations in t the intended application geometry. The joint strength calculated in this test may differ widely from the true shear and/or tensile strength of the adhesive. (True adhesive shear and tensile strengths are material properties independent of the joint geometry).

1.5 In this test a nominal burst pressure is calculated and reported as an engineering corollary to the burst pressure value measured from a hydrostatic pressure test, which is a more difficult and complex test procedure. As a general rule, the nominal burst pressure measured in this EPPO test is different than the burst pressure from a hydrostatic burst pressure test, because the EPPO test does not induce the hoop stresses commonly observed in a hydrostatic pressure test.

1.6 The use of this test method at elevated temperatures is limited by the temperature capabilities of the loading fixtures, the gripping method (adhesive, mechanical clamping, etc.) and the furnace temperature limitations.

1.7 Values expressed in this test method are in accordance with the International System of Units (SI) and Practice IEEE/ASTM SI 10 .

1.8 This standard does not purport to address all of the safety concerns, if any, associated with its use. It is the responsibility of the user of this standard to establish appropriate safety and health practices and determine the applicability of regulatory limitations prior to use.

2. Referenced Documents

2.1 *ASTM Standards:*

2.1.1 C1145 Terminology on Advanced Ceramics

2.1.2 C1322 Practice for Fractography and Characterization of Fracture Origins in Advanced Ceramics

2.1.3 C1469 Shear Strength of Joints of Advanced Ceramics at Ambient Temperature

2.1.4 D907 Terminology of Adhesives

2.1.5 D4896 Guide for Use of Adhesive-Bonded Single Lap-Joint Test Results

2.1.6 E4 Practices for Force Verification of Testing Machines

2.1.7 E6 Terminology Relating to Methods of Mechanical Testing

2.1.8 E105 Practice for Probability Sampling Of Materials

2.1.9 E122 Practice for Calculating Sample Size to Estimate, With Specified Precision, the Average for a Characteristic of a Lot or Process

2.1.10 E220 Test Method for Calibration of Thermocouples By Comparison Techniques

2.1.11 E230 Specification and Temperature-Electromotive Force (emf) Tables for Standardized Thermocouples

2.1.12 E251 Test Methods for Performance Characteristics of Metallic Bonded Resistance Strain Gages

2.1.13 E337 Test Method for Measuring Humidity with a Psychrometer (the Measurement of Wet-and Dry-Bulb Temperatures)

2.1.14 E1012 Practice for Verification of Testing Frame and Specimen Alignment Under Tensile and Compressive Axial Force Application.

2.1.15 SI 10-02 IEEE/ASTM SI 10 American National Standard for Use of the International System of Units (SI): The Modern Metric System

2.2 More references, as developed.

3. Terminology

3.1 *Definitions:*

3.1.1 *adherend*, n —a body held to another body by an adhesive.(D907)

3.1.2 *adhesion failure*, n— rupture of an adhesive bond in which the separation appears visually to be at the adhesive/adherend interface. (D907)

3.1.3 *adhesive,* n –a substance capable of holding materials together by surface attachment. (D907)

3.1.4 *advanced ceramic*, n—a highly-engineered, high performance predominately nonmetallic, inorganic, ceramic material having specific functional attributes. (C 1145)

3.1.5 *ceramic matrix composite*, n—material consisting of two or more materials (insoluble in one another), in which the major, continuous component (matrix component) is a ceramic while the secondary component(s) may be ceramic, glass/ceramic, glass, metal, or organic in nature. These components are combined on macroscale to form a useful engineering material possessing certain properties or behavior not possessed by the individual constituents. (C1145)

3.1.6 *cohesive failure*, n—rupture of a bonded assembly in which the separation appears visually to be in the adhesive or the adherend (D907) a segmented band or sleeve put around a shaft or spindle and tightened so as to grip it.

3.1.7 *collet grip*, n —a cone shaped, segmented sleeve placed on a shaft or tube and tightened with a tapered collar, so as to grip the shaft or tube.

3.1.8 *elastic stress limit* [FL^{-2}],n—the greatest stress which a material is capable of sustaining without any permanent strain remaining upon complete release of the stress, in units of MPa. (E6)

3.1.9 *failure*, *n* -- an arbitrary point beyond which a material or system ceases to be functionally capable of its intended use. This may be defined by elastic brittle failure or by a defined amount of permanent deformation beyond the elastic stress limit.

3.1.9.1 Failure strength is commonly defined by the force parameter (force, moment, torque, stress, etc) applied to a test specimen which produces either brittle fracture and loss of load-carrying capability or permanent deformation beyond a specified limit.

3.1.10 *joining,* n—controlled formation of chemical, or mechanical bond, or both, between similar or dissimilar materials. (C1469)

3.1.11 *nominal joint strength*, S_{NJ} [FL^{-2}], n— the calculated strength at failure in units of MPa, calculated from the push-out force and the calculated adhesive bond area of the defined test specimen.

3.1.12 *nominal burst pressure,* P_{NB} [F^{L-2}], n -- a burst pressure value calculated from the push-out force and the face area of the end-plug in units of MPa.

3.1.13 *push-out force*, F_{PO} [F], n— in a push-out test with a specific specimen geometry and size, the force level at which failure occurs in units of N.

3.1.14 *shear stress* [FL^{-2}], -- the stress component tangential to the plane on which the forces act. (E6)

3.1.15 *true shear strength*, [FL^{-2}],n— the maximum uniform shear stress which a material is capable of sustaining in the absence of all normal stresses. (D4896)

4. Summary of Test Method

4.1 This test method is used to determine the push-out breaking force, the nominal joint strength, and the nominal burst pressure of adhesively bonded ceramic end-plugs in advanced ceramic cylindrical tubes (monolithics and composites) at ambient and elevated temperatures. Test specimens are prepared by bonding a fitted ceramic plug into one end of a ceramic tube. The test specimen tube is secured into a loading fixture and an axial compressive force is applied to the interior face of the end-plug to push it out of the tube. The axial force required to fracture (or yield) the specimen joint is measured and used to calculate a nominal joint strength and a nominal burst pressure. Tests are done at ambient temperatures and at elevated temperatures, based on test furnace and test fixture temperature capabilities.

4.2 Typical end joint test specimens and a typical test system are shown schematically in Fig. 1 and Fig. 2, respectively. Selection of the test specimen geometry and size depends on the functional design of the application-specific tube and the size limitations of the available test material.

4.3 The force application arrangement of this test method is direct axial compression on the end face of the plug, where the predominant forces (shear, tensile, and mixed mode) occur in the circumferential adhesive bond section between the plug and the tube.

5. Significance and Use

5.1 Advanced ceramics are candidate materials for high temperature structural applications requiring high strength along with wear and corrosion resistance. In particular, ceramic tubes are being considered and evaluated as hermetically tight fuel containment tubes for nuclear reactors. These ceramic tubes require end-plugs for containment and structural integrity. The end-plugs are commonly bonded with high temperature adhesives into the tubes. The strength and durability of the specimen joint are critical engineering factors and the joint strength has to be determined across the full range of operating temperatures and conditions. The test method has to determine the breaking force, the nominal joint strength, the nominal burst pressure, and the failure mode for a given tube/plug/adhesive configuration.

5.2 The end-plug push-out test provides information on the strength and the deformation of specimen joints under applied shear, tensile, and mixed-mode stresses (with different plug geometries) at various temperatures and after environmental conditioning.

5.3 The end-plug test specimen geometry is a direct analog of the functional plug-tube application and is the most direct way of testing the tubular joint for the purposes of development, evaluation, and comparative studies involving adhesives and bonded products, including manufacturing quality control. This test method is a more realistic test for the intended geometry than the current shear test of ceramic joints (C1469) which uses an asymmetric 4-point shear test on a flat adhesive face joint.

5.4 The EPPO test method may be used for joining method development and selection, adhesive comparison and screening, and quality assurance. This test method is not recommended for adhesive property determination, design data generation, and/or material model verification/validation.

6. Interferences

6.1 The end-plug push-out (EPPO) test in its basic form is a variation of the common single-lap joint shear test geometry, based on the rotation of a single-plane lap joint to form a cylindrical lap joint. So the complexities of the single lap-joint (as described in C4896) are carried over to the EPPO test.

6.2 As described in C4896, there are many factors (geometric, adhesive properties, adherend properties, force levels) which can affect the stress levels in the adhesive bond section and the failure strength values in a given experimental adhesive bond lap-type test. All of these factors interact to determine the actual stress levels at different points in the specimen joint section. For full engineering analysis of the joint system and the test results, all of these factors should be carefully controlled and measured during testing.

6.2.1 The strain and stress conditions in the adhesive bond section will vary spatially, based on variations in the bond morphology and properties and the stress-strain interaction with the adherends. Critical factors are -- adhesive bond length and thickness, adhesive shear and tensile moduli and Poisson's ratio, adherend thickness, adherend shear and tensile moduli and Poisson's ratio, and interface surface conditions.

6.2.2 Depending on the type of adhesive and the process conditions, the adhesive bond may contain residual stresses and critical flaws which may affect the experimental strength. This is a particular concern with many of the high temperature adhesives commonly used to bond advanced ceramics. In many cases the residual stresses and critical flaws will increase with larger bond section sizes and bond thicknesses

6.3 Force misalignment in the load system can produce extraneous bending stresses in the adhesive joint which will give erroneous test results. The misalignment can develop from misaligned end-plugs in the tube specimens, out-of-tolerance test specimens (straightness and concentricity, out-of-tolerance test specimens and misfit of end-plugs, misalignment of the specimen in the grip fixture, and misalignment load train components.

6.4 A common variable in adhesives is the different modes of joint failure– brittle elastic versus ductile-plastic -- for different types of adhesives and at different temperatures for a given adhesive. For each adhesive system and test condition, the failure criteria has to be appropriately defined to determine the point at which the adhesive functionally fails under load.

6.5 The gripping mechanism must be sufficiently strong at the test conditions so that the test specimen is securely held in the grip section and failure occurs in the end-plug section, not in the grip section of the test specimen. Grip failure is more likely at elevated temperatures, because of degradation of the grip adhesive at elevated temperatures and because of differential thermal expansion stresses between the grip fixture and the specimen. **Slippage and/or breakage in the grip section produces an invalid test.**

6.6 The adhesive properties can change with temperature and with time, either under specimen conditioning or in aggressive test environments. In particular, ceramic and glass adhesives can fail by slow crack growth under moisture and/or elevated temperature conditions,

which may produce a different flaw population and microstructure and/or a change in failure mechanisms.

6.7 At elevated testing temperatures, differential thermal stresses caused by different thermal expansion coefficients between the end-plug, the adhesive, and the adherend can introduce extraneous stresses which may produce premature adhesive failure.

7. Apparatus

7.1 Testing Machine -- Specimens shall be tested in compression loading with any suitable testing machine provided that uniform rates of direct loading can be maintained. The force measuring system shall be free of initial lag at the loading rates used and shall be equipped with a means for retaining readout of the maximum force as well as a force-time or force-displacement record. Machines used for axial compression testing shall conform with and have an accuracy in accordance with Practice E 4.

7.2 Force Measurement Devices-- The measurement devices used in determining the force shall be accurate within ±1% at any force within the selected load range of the testing machine as defined in Practice E 4. Force calibration shall be performed in compression for universal machines.

7.2.1 Test Apparatus Fixture -- The test apparatus shall be designed and fabricated so that the compressive force is applied to the test specimen axially, uniformly, and with negligible friction. The test apparatus shall apply an axial compression force to the interior face of the end-plug without inducing excessive bending stresses or transverse shear stresses in the test specimen. Force application can be accomplished with a universal testing machine with appropriate gripping and loading fixtures. A typical test apparatus consists of a base plate, a support block, a gripping fixture, and a loading rod. A schematic of a test apparatus is shown in Fig. 2.

7.2.2 The test apparatus components shall be machined and fitted to maintain alignment, or the test apparatus may incorporate alignment fixtures (ball and socket, centering devices, etc.) for manual and/or self-alignment.

7.2.3 The test apparatus shall be built with adequate materials and sized large enough to contain the test specimen and to support the applied forces without deformation or damage to the apparatus at the test temperatures. At ambient temperatures the fixture materials are commonly high strength, high hardness steel. At elevated temperatures (>500°C) high nickel alloys or high strength ceramics (aluminum oxide, silicon carbide) may be necessary for strength, hardness, and stability at the test temperature.

7.3 It is not the intent of the test standard to require specific loading and alignment fixtures for testing. Different test apparatus configurations can be designed and used for testing. The primary requirement is that the test fixture (as designed and fabricated) securely grips the test specimen and that the force is applied axially and uniformly with less than +/-10% extraneous bending stresses in the test specimens. An example of an axial test apparatus for small ceramic tube specimens (10 mm diameter and 50-70 mm long) is described in Appendix X1.

7.4 Gripping Fixtures, Support Blocks, and Base Plates and Alignment Devices

7.4.1 A gripping fixture is necessary to secure the test specimen in the test apparatus without slipping or breakage while force is applied. The gripping fixture also aligns the test specimen in the load train. Gripping fixtures for tube specimens are grouped into two classes -- mechanical

grip fixtures (mechanical clamps, collets, and collars) and adhesive bonding into grips. See Appendix X2.

7.4.1.1 The brittle nature of advanced ceramics requires a uniform force application between the grip fixture and the gripped section of the test specimen. Line or point contacts and non-uniform forces can produce stress concentrations and Hertzian type stresses leading to crack initiation and fracture of the test specimen in the gripped section. The selection of a gripping method depends on the strength, rigidity, and brittleness of the ceramic tubes. Mechanical grips are permitted if they can secure the test specimen without slipping or breakage in the grips at the test conditions. If the tubes are small, thin-walled, brittle, and rigid, adhesive gripping methods may be more successful than mechanical gripping.

7.4.1.2 For adhesive gripping at ambient temperatures, high strength epoxy adhesives are generally suitable for securing the test specimen in the grips. High temperature epoxies can typically be used at temperatures below 250°C, provided enough enough grip length is provided. At elevated test temperatures (typically greater than 250°C for ceramics), appropriate high temperature bonding adhesives (metal solder, metal braze compounds, ceramic cements, sealing glasses) should be selected that have sufficient bond strength at the desired test temperature. (See Appendix X2.)

7.4.1.3 A critical test design factor is the selection of the grip bond length. The bond length must be long enough to avoid failure in the grips and produce failure in the end-plug adhesive. Appendix X2 provides a calculation of a minimum bond length for an expected push-out force and a grip adhesive with a defined shear strength.

7.4.2 The gripping fixture, support block, and base plate shall be sized and constructed to securely grip and align the test specimen. All the components shall be strong, rigid, and hard enough to support the applied forces without deformation or damage at the test temperatures. High strength steel, high nickel alloys, aluminum oxide, and silicon carbide may be used as required for the designated test temperature.

7.4.3 Alignment -- The test apparatus shall be designed and constructed to keep extraneous bending stresses and strains around the circumference of the test specimen at less than +/- 10% difference from the mean stress around the circumference. Misalignment bending stresses can develop with non-uniform test specimens (variations in tube diameter, concentricity, and straightness; non-parallel end-plug faces. See section 10.3.2) and from misalignments in the load train.

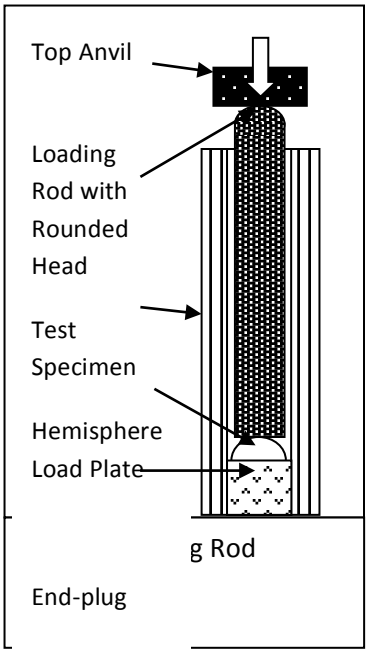

7.4.3.1 Flat bearing surfaces on the base plate, the support block, and the grip fixture shall have flat and parallel surfaces to within 0.002 m/m and shall be fitted together (with or without alignment fixtures) to maintain the required axial and lateral alignment.

7.4.3.2 Alignment features in the test apparatus can use conical or spherical seats to maintain axial and lateral alignment of the gripping fixture in the support block.

7.5 Loading Rod -- The loading rod shall be straight, rigid, and strong enough to apply the force directly to the plug face

without bending, deformation, or damage. The loading rod shall be long enough to reach the bottom of the test specimen with direct contact to the upper loading anvil. Adequate precautions should be taken to avoid/minimize friction between the loading rod and the interior of the test specimen tube. The material for the loading rod shall be appropriate for the test temperatures (high strength steel, high nickel alloys, aluminum oxide, silicon carbide, per 7.2.3)

7.5.1 The loading rod may use hemispherical or rounded features/fixtures or other alignment aides at the top and bottom to maintain axial alignment of the applied force. The flat face of the hemispherical load plate should seat on the end-plug to avoid point contact stresses on the end-plug. (See Figure 3)

7.5.2 A compliant layer (copper or graphite sheet) may be used between the face/tip of the loading rod and the interior face of the end-plug to reduce or eliminate stress concentrations and misalignments.

7.5.3 An example of a test apparatus developed in 2013-2015 for silicon carbide composite tubes (10 mm diameter and 40-70 mm long) for the nuclear industry is shown in Appendix X1.

7.6 Cross-Head Displacement Measurement -- The cross-head displacement should be measured and recorded as record of the force-time response of the test specimen. Cross-head displacement of the test machine should not be used to define displacement or strain in the end-plug test section.

7.7 Strain gages are not used in this test method to measure adhesive strain in the end-plug bond section during testing. Strain gages on the test specimen tube may be used to assess bending stresses and strains produced by misalignment (Section 12.3.3) If used, strain gages shall be selected and used per E251.

7.8 Data Acquisition – At the minimum, make an autographic record of the maximum applied force; however, it is desirable to also make a record, where applicable, of applied force and crosshead displacement, as a function of time. Use either digital data acquisition systems of analog chart recorders for this purpose, although a digital record is recommended for ease of later data analysis. Recording devices shall be accurate to 1.0% of full scale. Data acquisition rates will depend on the loading rates used to conduct the test. A data acquisition rate of at least 20 Hz should be used, and the acquisition rate should be fast enough to capture the maximum force within 1%.

7.8.1 Force- time or force-cross-head displacement plots should be recorded, documented and used to assess the mode of fracture.

7.9 Dimension Measuring Devices -- Micrometers, calipers, and optical microscopy used for measuring linear dimensions shall be accurate and precise to at least one half the smallest unit to which the individual dimension is required to be measured. For testing small diameter (< 20 mm) test specimens, the measuring devices should have an accuracy of 0.01 mm.

7.10 Elevated Temperature Testing

7.10.1 This test method is applicable to elevated temperature testing with the use of suitable furnace equipment and temperature control and measurement. The test temperature shall be selected based on the functional temperature requirements of the ceramic application.

7.10.2 Furnace Configuration -- The furnace system shall be constructed and have a temperature control system to maintain a constant temperature in the end-plug test section during each testing period. The steady state variation in temperature with time during the test shall be no greater than ±5°C or ±1% of the test temperature, whichever is larger. The furnace system shall be configured so that spatial thermal differences along the length of the end-plug test section of the specimen are no greater than ±5°C or ±1% of the test temperature (whichever is larger).

7.10.2.1 The furnace system can be configured in a variety of ways depending on the size and configuration of the test specimen and the test apparatus. A box furnace can be used that surrounds the entire test apparatus with the loading rods and support fixtures extending through the floor and ceiling of the box furnace. Depending on the test temperatures, load train components in or close to the hot zone may require active cooling. An alternative configuration is to use small resistance heating elements in close proximity to the end-plug section with appropriate insulation to retain the heat in the end-plug test section.

7.10.2.2 Heating can be done with any suitable heating method (indirect electrical resistance heating elements, direct induction, indirect induction through a susceptor, radiant lamp, or direct resistance in the test specimen) that maintains proper temperature conditions.

7.10.3 The furnace may have an air, inert, or vacuum environment, as required. If an inert or vacuum chamber is used, and it is necessary to direct the force through a bellows, fittings, or seal, it shall be verified that losses or errors in force measurement do not exceed 1 % of the expected failure forces.

7.10.4 Temperature Measurement --The temperature measurement device for the test specimen shall have a resolution of 2°C or better. If temperature is measured with a thermocouple, the specimen temperature shall be monitored with the thermocouple tip located no more than 1 mm from the end-joint section of the specimen. Either a fully sheathed or exposed bead junction may be used. If a sheathed tip is used, it must be verified that there is negligible error associated with the sheath.

7.10.4.1 A separate thermocouple may be used to control the furnace chamber if necessary, but the specimen temperature shall be the reported temperature of the test.

7.10.4.2 The thermocouple(s) shall be calibrated and used in accordance with Test Method E220 and Tables E230.

7.10.4.3 The temperature measurement shall be accurate to within ±5°C. The accuracy shall include the error inherent to the thermocouple as well as any errors in the measuring instruments.

7.10.5 System Equilibrium—The time for the system to reach thermal equilibrium at test temperature shall be determined for the test temperature to be used. This shall be performed for both hot-furnace loading or cold-furnace loading, to support specimen heat-up per Section 12.4.2.

7.10.6 At a minimum for elevated temperature tests, record temperature as single measurements at the initiation and completion of the actual test. However, temperature can also be recorded continuously, similar to force and strain except the record can begin at the start of the heating of the furnace (including ramp-up to test temperature).

8. Calibration and Standardization

8.1 Calibration of equipment (force measurement, strain measurement, thermocouples, etc.) shall be provided by the supplier against standards traced to the National Institute of Standards

and Technology (NIST). Recalibration shall be performed with NIST-traceable standards on all equipment on a six-month interval or whenever accuracy is in doubt.

8.2 Reference materials -- There are currently no standard reference materials for this type of test.

9. Hazards

9.1 Precaution -- During the conduct of this test method, the possibility of flying fragments of broken test material is quite high. The brittle nature of advanced ceramics and the release of strain energy contribute to the potential release of uncontrolled fragments upon fracture. Means for containment and retention of these fragments for safety as well as later fractographic reconstruction and analysis is highly recommended.

9.2 Precaution -- Elevated temperature testing often produces the possibility of fire, burns, and electrical shorts. Furnaces shall be properly designed, assembled, and operated to minimize those hazards.

9.3 Precaution -- Exposed fibers at the edges of fiber reinforced composite test specimens present a hazard due to the sharpness and brittleness of the ceramic fiber. Inform all persons required to handle these materials of such conditions and the proper handling techniques.

10. Test Specimens, Preparation, Sampling

10.1 The geometry of an end-plug push-out (EPPO) test specimen is dependent on the purpose of the test and the design configuration and geometry of the end-use component. Generally, the dimensions (length, diameter, wall thickness, end-plug geometry, etc.) of the end-plug test specimen will reflect the size and dimensions of the end-use component. If it is desired to evaluate the effects of geometry and the adhesive processing, then the size of the test specimen and resulting bond geometry will be selected to accurately assess the test variables. In addition, grip methods will influence the final length and design of the test specimen geometry. These different test objectives will produce a wide range of test specimen diameters and length and preclude the use of a single, standardized test specimen geometry.

10.1.1 In general only a single variable should be evaluated in a given test series; i.e., if evaluating the effect of different adhesives, a single bond geometry should be chosen and standardized between tests.

10.1.2 Any test specimen geometry is acceptable if it meets the gripping, fracture location, bending limits , and temperature profile requirements of this test method. The test apparatus shall be designed and constructed to grip and secure the defined test specimen geometry at all test conditions.

10.1.3 The geometry of the test specimen for elevated temperatures testing will depend on the type and configuration of the furnace, the requirements of temperature uniformity, and ambient temperature test specimen geometry. For example, thermal gradients may introduce additional stress gradients in test specimens which may already exhibit stress gradients at ambient temperatures due to geometric transitions. Therefore, analyze untried test configurations simultaneously for both loading-induced stress gradients and thermally-induced temperature gradients to ascertain any adverse interactions.

10.1.4 10.1.5 An example of a test specimen geometry and test apparatus developed in 2015 for silicon carbide composite tubes for the nuclear industry is shown in Appendix X1.

10.2 A major factor in the design of the test specimen is the configurational fit between the end-plug and the tube. Critical factors are the bond geometry (for example, straight wall plug, scarf joint plug, flat face plug -- See Figure 4), the bond length and area, and the adhesive bond thickness between the tube ID and the plug OD. The test specimen bond geometry will likely match the bond configuration of the end-use component.

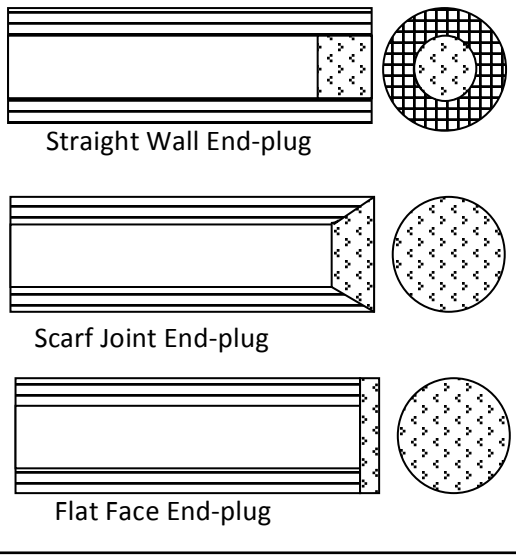

Fig. 4 - End-plug Geometries

10.3 As a starting point for tolerances, the test specimen should match the dimensional tolerance requirements of the end-use component.

10.3.1 The test designer shall define dimensional tolerances for the end-plug and the joint section of the tube that ensure uniform and consistent fit of the end-plug in the tube. The parallelism tolerance of the two end-plug faces should be defined so that the inner end-plug face is perpendicular to the loading rod axis in the test apparatus to within +/- 5 degrees.

10.3.2 The test designer shall also consider misalignment stresses and grip fitting in the test specimen based on variations in outer diameter (OD), inner diameter (ID), straightness, and concentricity of the test specimen tube geometry. The designer shall define additional dimensional tolerances for the test specimen that minimize misalignment stresses.

10.3.3 The presence of excess adhesive on the interior face of the end-plug may interfere with the alignment of the loading rod and introduce bending stresses. The bonding process should include steps to minimize adhesive on the interior face. The interior face should be checked after bonding for excess adhesive. Test specimens with adhesive on the interior face should be discarded or the excess adhesive should be removed.

10.4 Adhesive Bond Processing --The adhesive bond material and processing method shall be selected to support the test objectives and/or match the end-use application. A test specimen adhesive preparation procedure shall be defined and documented, describing the adhesive bond material, specimen and bond geometry, specimen and end-plug preparation steps, adhesive assembly/ alignment steps, processing methods and conditions, and machining/finishing steps.

10.4.1 The test designer shall define and document a quality evaluation procedure for the test specimen, defining the critical specimen parameters (dimensions, tolerances, fit, surface condition, etc), the methods of measurement, and the pass-fail requirements for the selected parameters.

10.4.2 Prior to bonding, measure, record, and ensure that the dimensions of the specimen tubes and the end-plugs meet defined dimensional requirements (OD, ID, straightness, parallelism, etc)

10.4.3 Prepare all test specimens with bonded end-plugs per the defined test specimen preparation and adhesive bonding procedure.

10.4.4 Depending on the condition of the test specimen OD, the grip section of the test specimen may be finished, smoothed, or turned to produce a uniform diameter and suitable surface finish for the gripping fixture to effectively secure the specimen.

NOTE -- Machining of the ceramic should be performed with appropriate media and fluid cooling to minimized surface damage and machining stresses. Grip section machining may be done before or after end=plug insertion.

10.4.5 Nondestructive evaluation (radiography, computerized tomography, ultrasonics, thermal imaging, etc.) may be used to assess the alignment and fit of the end-plug and the condition of the adhesive joint (gaps, porosity, thickness uniformity, etc).

10.4.6 Perform and record all quality evaluation tests and the results of any nondestructive evaluations and include them in the final report.

10.4.7 For environmental conditioning, see Section 11.

10.5 The test specimens shall be properly packaged and stored to minimize environmental exposure and bond degradation, caused by moisture, heat, or cold.

10.6 Test specimens may be selected from as-fabricated components for the purposes of quality control, if the test is designed for the as-fabricated geometry. Specimen sampling from a production lot shall be done per E105.

10.7 Definitions of Valid, Invalid and Censored Tests - A valid test is a test in which failure (fracture or permanent deformation) occurs by adhesive or cohesive failure within the end-plug length of the test specimen. Breakage may occur in or run into the tube section and include partial fracture in the tube section if it is within the bond-endplug length. An invalid test is a test in which slippage or breakage failure occurs in the grip section of the test specimen or a test in which maximum percent misalignment bending is 10% of the average stress (See Section 12.3.3 and Appendix X3.1) A censored test is a test in which failure occurs by breakage outside of the end-plug section, but along the test specimen length within a 1X diameter distance from the end-plug section. (See Figure 5)

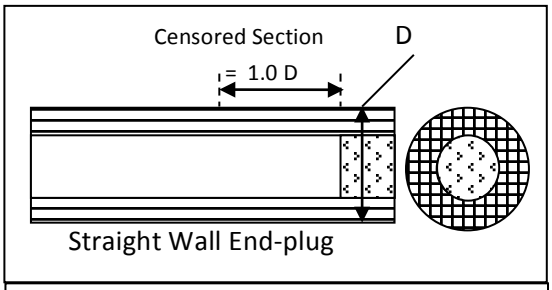

Figure 5 -- Censored Test Section

10.8 Required Number of Valid Tests -- Five (5) tests shall be a minimum number of valid tests for determining a base-line average. Ten (10) tests is recommended as a minimum number of valid tests for determining an average with a standard deviation calculation. For full statistically significant data, the procedures outlined in Practice E122 should be consulted.

11. Specimen Conditioning

11.1 Finished test specimens may be conditioned at different temperatures and environments for defined periods of time to assess temperature and environmental effects on the joint strength and durability. Any conditioning treatments should be fully defined for time, temperature, and environmental conditions. Test specimens should be weighed, measured for dimensions, and visually examined before and after conditioning to assess physical changes in the test specimens.

12. Test Procedure

12.1 Test Specimen Measurement and Examination

12.1.1 Check the interior face of the end-plug for excess adhesive that will interfere with the loading rod. Remove the excess adhesive or set the test specimen aside if excess adhesive cannot be removed.

12.1.2 Measure and record the OD and straightness of the test specimens to ensure that the specimen meets the defined dimensional requirements.

12.1.3 Visually examine the outside surface of the end-plug and the outside surface of the test specimen for surface variations and anomalies. Record the type and location of any observed anomalies.

12.1.4 If possible, measure the flatness and alignment of the interior face of the end-plug with the concentric axis of the test specimen to meet a +/- 2° alignment tolerance. This may be done by contact probes or by radiography. This can also be measured via the outer face of the endplug if a tight parallelism tolerance is verified between the two endplug faces.

12.1.4.1 Adhesive Gripping of the Specimen -- If adhesive grip bonding is used, the end-plug test specimen/s should be fitted, aligned, and bonded into the gripping fixture per the grip adhesive manufacturer's process instructions. The defined bonding process (curing, heating, sintering, melting, heat-treating) should be followed and controlled to produce a test specimen securely fitted and aligned in the gripping fixture. (See Appendix X2.)

12.1.4.2 If possible, measure the angular alignment of the fitted test specimen in the gripping fixture to ensure that test specimen is aligned and concentric with the gripping fixture to within +/- 3°.

12.2 **Preparation of the Test Apparatus System**

12.2.1 Based on the expected failure mode of the end-plug adhesive at the test temperature, define a failure criteria for the test -- Elastic brittle fracture for brittle adhesives and/or the limit of permanent deformation for ductile/plastic adhesives. (See Figure 6)

12.2.1.1 The EPPO test is commonly done with displacement control. Set a constant cross-head speed, so that specimen failure occurs within 10-60 seconds. The required cross-head speed will depend on the specimen size, the bond geometry, and the nominal joint. Preliminary tests may be necessary to determine the appropriate cross-head speed.

12.2.1.2 Slower or faster test rates may be used to evaluate strain rate effects on the joint strength.

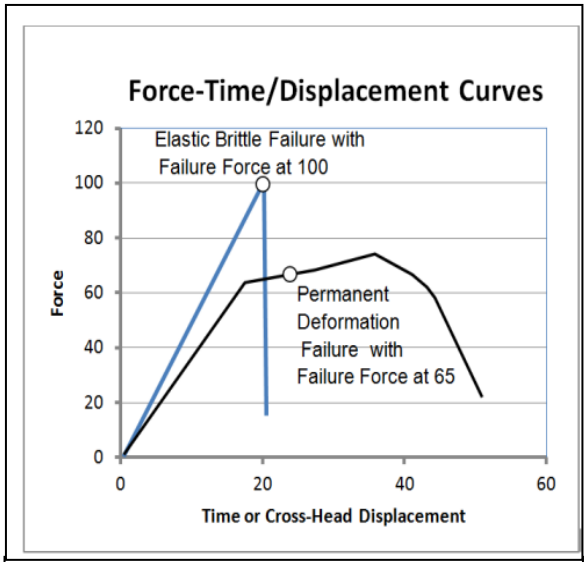

Fig 6-- Force-Time Curves for Brittle Failure and Deformation Failure

12.2.2 Set up and align the testing apparatus in the universal testing machine.

12.2.3 Set-up, turn on, and check the universal test machine control system, the force and strain measurement systems, and the data acquisition system. Set the defined test mode and test rate on the test machine.

12.2.4 Measure and record the ambient temperature and relative humidity (E337) in the laboratory at the start and end of the test sequence.

12.2.5 For elevated temperature testing, install, set-up, turn on, and check the operation and control of the furnace system with the test apparatus installed.

12.3 **Test Specimen Mounting and Alignment**

12.3.1 If mechanical gripping is used, align, fit, and secure the test specimen into the gripping fixture. Ensure that the test specimen is aligned and concentric with the gripping fixture to within +/- 3°.

12.3.2 Fit and align the gripping fixture (with the test specimen) and the loading rod into the test apparatus (in the test furnace for elevated temperature testing).

12.3.3 Alignment Measurement - The alignment of the test specimen in the test apparatus can be experimentally checked by loading a strain-gaged test specimen and checking the strain at 4 points around the circumference of the specimen tube. (See Appendix X3.) The maximum allowable percent misalignment bending among the four strain gages is 10% , as measured and calculated in Appendix X3.

12.3.4 Alignment measurements should be conducted at the beginning and end of a series of tests with a measurement at the midpoint of the series recommended; whenever the grip fixtures

and load train fixtures are changed or installed on a different test machine; whenever a different operator is conducting a series of tests; or when damage or misalignment is suspected.

12.3.4.1 If experimental conditions, time, and cost permit, all test specimens may be strain-gaged for alignment check (See Appendix X3) and checked for misalignment in the initial stages of each temperature test. Test specimens that exceed the misalignment limit should be realigned or discarded.

12.3.5 Safety shields should be placed around the specimen and test fixture to contain and collect fracture fragments.

12.4 **Test Initiation**

12.4.1 The test load train should be preloaded to approximately 5% of the expected push-out force to seat the components of the test apparatus, remove slack, and check for grip slippage.

12.4.2 For elevated temperature testing, begin furnace heat-up with specimen temperature recording. Heat the specimen at a defined heating rate to the designated test temperature and hold at the designated constant test temperature until the specimen reaches thermal equilibrium. During heat-up adjust the preload to maintain constant force on the test specimen and compensate for thermal expansion stresses.

12.4.3 Start data acquisition and start force application at the defined displacement rate. Load the test specimen to the defined failure criteria, as shown by either brittle fracture failure or by a predetermined permanent deformation beyond the elastic stress limit with increasing compliance and/or maximum force. See Figure 6.

12.5 **Test Completion**

12.5.1 Record the force-time/displacement data and record the force at failure (push-out force).

12.5.2 After specimen failure, stop the action of the test machine and the data acquisition. Retract the cross head to its starting position. For elevated temperature tests, allow the furnace to cool.

12.5.3 Collect and remove any specimen fragments from the test apparatus. Remove the specimen from the gripping fixture. Save the specimen and the fragments for failure analysis.

12.5.4 A valid test is a test in which the test specimen breaks in the end-plug section, as described in 10.7. An invalid test is a test in which the test specimen breaks in the grip section. A censored test is a test in which the test specimen breaks with a defined distance from the end-plug section.

12.5.5 To complete a required sample set for a statistical average, one replacement test specimen should be tested for each invalid test specimen.

12.5.5.1 The specimen fracture surface should be visually examined to determine if the location of failure is in the end-plug section, necessary for a valid test. Visual examination may show if the failure mode is adhesive at the bond line or is cohesive in the adhesive bond material, the end-plug, or the ceramic tube. Microscopic examination may be necessary to determine adhesive failure or cohesive failure in the adhesive. For failure in advanced ceramic tubes and ceramic-based joints, post-fracture analysis can be performed using the guidelines in ASTM C1322.

13. Calculation of Results

13.1 The **Push-out Force (F_{PO})** in Newtons is the measured force at failure, either the brittle failure force or the defined permanent deformation force.

13.2 The **Adhesive Bond Area** (A_A) is the calculated area of the adhesive bond surface specific to the end-plug configuration. For each different configuration the adhesive bond area is calculated from the bond geometry. Surface area equations for bond areas of straight wall, scarf joint, and flat face bonds are given in Annex A1.

13.3 The **Nominal Joint Strength** (S_{NJ}) in MPa is calculated for valid tests as --

$$S_{NJ} = F_{PO} / A_A \quad (1)$$

where

F_{PO} = the measured push-out force at failure (Newtons)

A_A = the adhesive bond surface area (mm^2) specific to the end-plug bond geometry

13.4 The **Nominal Burst Pressure,** P_{NB} in MPa is calculated as

$$P_{NB} = F_{PO} / A_F = F_{PO} / (\pi (d/2)^2) \quad (2)$$

where

F_{PO} = the measured push-out force at failure (Newtons)

A_F = the interior face area of the end-plug (mm^2)

d = the diameter of the interior face area of the end-plug (mm) or the inner diameter of the ceramic tube (mm)

13.5 Statistics -- For each test specimen set, calculate the average, standard deviation, and the coefficient of variation for the selected test data -- F_{PO}, S_{NJ}, and P_{NB} .

$$mean = \overline{X} = \frac{\sum_{i=1}^{n} X_i}{n} \quad (3)$$

$$standard\ deviation = s.d. = \sqrt{\frac{\sum_{i=1}^{n} \left(X_i - \overline{X}\right)^2}{n-1}} \quad (4)$$

$$Percent\ Coefficient\ of\ Variation = CV = \frac{100\ (s.d)}{\overline{X}} \quad (5)$$

Xi = the measured value and n = the number of valid tests.

13.6 The force-time or force displacement curve should be plotted out and analyzed for the mode of failure (brittle failure or permanent deformation failure) as illustrated in Figure 5. The force-time/displacement curves may also show signs of system alignment compliance and specimen slippage in the grips.

14. Report -- The report shall include the following information for the test set. Any significant deviations from the procedures and requirements of this test method shall be noted in the report.

14.1 Name of laboratory, location, date of test, and test operators

14.2 **Test Materials and Test Specimens**

14.2.1 Description of the end-plug material and the ceramic tube material -- source, material description, method of fabrication, material specifications and designations, lot #, date of fabrication, and any other necessary information.

14.2.2 Description of the End-plug geometry and ceramic tube geometry (include engineering drawing, if available) with dimensions and tolerances.

14.2.3 A calculation of the adhesive bond area for the test specimens.

14.2.4 Preparation, machining, and conditioning of the joining surfaces for bonding.

14.2.5 Description of the end-plug adhesive material and bonding process -- source, composition, chemistry, method of fabrication, tooling, and conditioning.

14.2.5.1 Machining and finishing of the grip section of the test specimen.

14.2.5.2 Specimen conditioning parameters, if any, and specimen storage conditions.

14.3 **Equipment and Test Parameters**

14.3.1 Type and configuration of the test machine (include drawing or sketch, if necessary). If a commercial test machine was used, the manufacturer and model number are sufficient for describing the test machine

14.3.2 The force capacity and accuracy/resolution of the load cell with manufacturer and model number.

14.3.3 Description of all the test apparatus components (include an engineering drawing, if available) in terms of geometry and material.

14.3.4 Detailed description of the gripping fixture with geometry and dimensions.

14.3.5 Detailed description of the grip adhesive and bonding procedure for specimen gripping, if used.

14.3.6 The method of the data collection, specifying the data collection rate, accuracy, and resolution.

14.3.7 Method and date of calibration of the force and strain measurement systems.

14.3.8 Description of the alignment check procedure and the results of the alignment check.

14.3.9 Test Parameters – mode of control, cross-head displacement rate, pre-load force, selected test temperatures.

14.3.10 The definition of the failure criteria for this adhesive system under these test conditions.

14.3.11 Ambient humidity and temperature in the laboratory during the tests.

14.3.12 If used, a description of the furnace system (configuration, heating method, temperature control and measurement) and the heating protocol.

14.3.13 Any variations in the test procedure, compared to the specification.

14.4 **Test Results**

14.4.1 Mean, standard deviation, COV, and valid test count for the Push-out Force (F_{PO}) for all valid tests at each reported test temperature.

14.4.2 Mean, standard deviation, COV, and valid test count for the calculated Nominal Joint Strength (S_{NJ}) , for all valid tests at each reported test temperature.

14.4.3 Mean, standard deviation, COV, and valid test count for the calculated Nominal Burst Pressure (P_{NB}), for all valid tests at each reported test temperature.

14.4.4 Number of valid, invalid, and censored tests at each reported test temperature.

14.4.5 Selected test temperature/s and measured humidity.

14.5 **Data for Individual Specimens**

14.5.1 Measured end-plug dimensions (diameter and length) and cylinder dimensions (OD, ID, and length) for each specimen.

14.5.2 Measured dimensional variations in the end-plug and cylinder each test specimen.

14.5.3 Any observed joint or surface anomalies and NDE results prior to testing.

14.5.4 Test temperature

14.5.5 Push-out Force (F_{PO}), calculated Nominal Joint Strength (S_{NJ}) and calculated Nominal Burst Pressure (P_{NB}) and classification as a valid, censored, or invalid test.

14.5.6 Force- displacement/time curves, if available.

14.5.7 Mode of fracture and appearance of each specimen after fracture ,

14.5.8 Any fractographic observations and the method of fractographic analysis.

15. Precision and Bias

15.1 An "analysis of errors" study shows that the measurement of the end-plug diameter is the dominant source of measurement error, because of the use of diameter squared in the calculation of surface area. All other measurement errors produce linear errors in the calculations.

15.2 Repeatability studies are strongly affected by material variations in the adhesive bonding of test specimens. Single laboratory repeatability studies are in progress

15.3 A full ILS study is planned for ambient temperature testing, based on the availability of funding, sufficient test specimens, and test apparatus sets.

16. Keywords

16.1 adhesive bonding, end-plug push-out test, nominal joint strength, nominal burst pressure, ceramic composite, ceramic joint,

ANNEX (Mandatory Information)

ANNEX A1 -- Calculation of Adhesive Bond Surface Area in the EPPO Test Specimen

A1.1 The calculation of the nominal joint strength requires a measurement of the surface area of the adhesive bond of the end-plug. The adhesive bond area is calculated for the specific end-plug configuration, assuming basic symmetrical geometry. The equations for the adhesive bonding areas of three basic end-plug geometries are given in Table A1.

Table A1 -- Adhesive Bond Surface Area Calculations for Three Types of End-Plug Geometries

Geometry and Bond Surface Area	Surface Area Equation
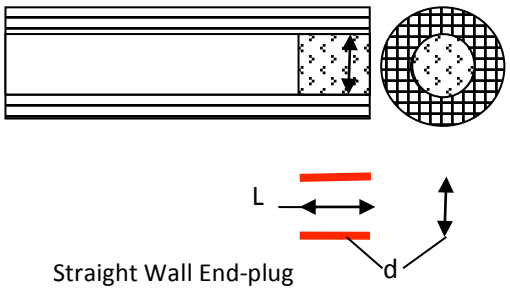 Straight Wall End-plug Flat Face End-plug	$A_A = L \times \pi d$ Where L = the length of the end-plug d = the inner diameter of the specimen tube and the diameter of the inner face of the end-plug
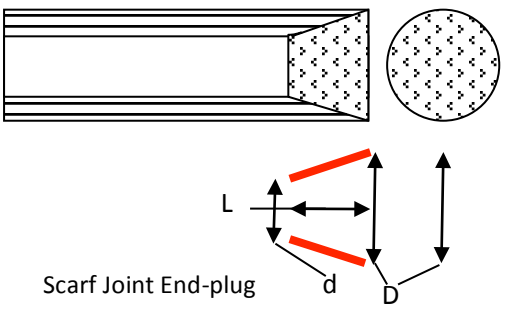 Scarf Joint End-plug	$A_A = (\pi (D + d) / 2) \times [((D-d)/2)^2 + L^2]^{1/2}$ Where D = outer diameter of the end-plug at the scarf joint (mm) d = the inner diameter of the specimen tube (mm) and the inner diameter of the end-plug at the scarf joint (mm) L = the length of the scarf joint or the end-plug (mm)
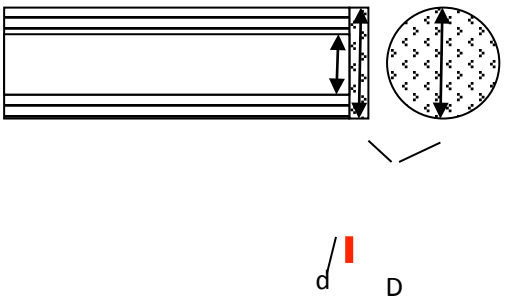	$A_A = \pi [(D/2)^2 - (d/2)^2]$ Where D = outer diameter of the specimen tube (mm) d = the inner diameter of the ceramic tube (mm)

APPENDIX (Non-mandatory Information)

Appendix X1 -- Example of a Test Specimen Geometry and a Test Apparatus

X1.1 In 2013-2015 the Department of Energy funded a research project with the General Atomics Corporation to develop an end-plug push-out test for ceramic tubes (both monolithic ceramics and ceramic matrix composite (CMC) materials.) The ceramic tubes are being developed as cladding materials for nuclear fuel, replacing zirconium alloys. The objective of the project was to develop, validate, and document an experimental test method for determining the mechanical strength of different end-plug geometries and different adhesives in ceramic tubes at ambient and elevated temperatures.

X1.2 Two types of ceramic materials were used as specimen tubes -- a) silicon carbide fiber-silicon carbide matrix composite tubes, consisting of Tyranno SA3 SiC fibers in a chemical-vapor-infiltrated silicon carbide matrix and b) sintered monolithic silicon carbide tubes. End plugs were monolithic silicon carbide produced by sintering or hot pressing. Two different plug geometries were evaluated -- scarf joints and face joints. Two types of end-plug adhesives were evaluated -- a high strength epoxy for room temperature test development and a proprietary high temperature ceramic adhesive for functional testing. Earlier tests on the high temperature ceramic adhesive using torsion testing showed adhesive bond strengths on the order of 75 MPa.

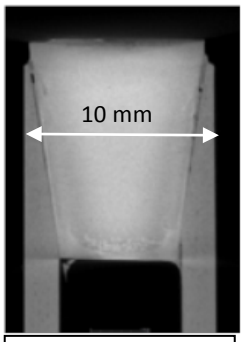

Fig. X1.1 XCT of End-Plug Fit

X1.3 Test Specimen Geometry - Specimen tubes were approximately 10 mm in outer diameter with an interior diameter of ~7 mm and a wall thickness of ~1.5 mm and a tube length of 45 to 60 mm. The length of the scarfed end-plug fit into the specimen tube was ~7-12 mm. Different scarf angles were explored, ranging from 3°-8°. (See Figure X1.1)

X1.4 Test Apparatus -- The test apparatus consists of a support block, a loading rod, and a split conical collet with the test specimen. The test apparatus is shown in Figure X1.2.

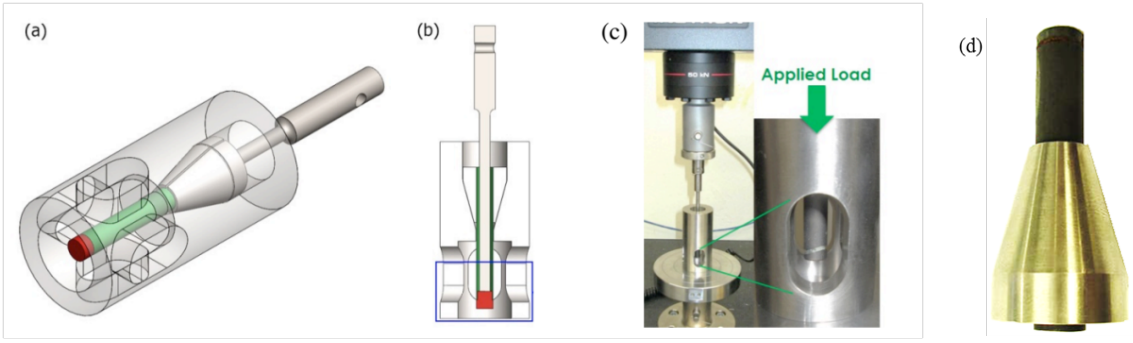

Figure X1.2 -- End-plug push out test, (a) isometric view, (b) section view showing loading rod insertion into specimen tube, (c) assembled fixture in use, and (d) test specimen bonded into split conical steel collet.

The test specimen tube is adhesively bonded in the split conical collet with a 25 mm grip bond length. The conical collet fits into the support block, where the taper of the collet serves to self-align the test specimen as well as to apply a small amount of normal force to the tube to aide in

grip strength. The support block has cutouts in the lower section so the end-plug section of the test specimen can be observed and strain gaged. U-joints are included in the load train to minimize misalignment. For testing the loading rod is inserted into the open end of the specimen tube. The entire test fixture can be fitted into a high temperature furnace.

X1.5 Test Methodology -- A compressive force is applied through the loading rod to the interior face of the end-plug until failure occurs. A crosshead speed of 1.5mm/min is used during testing. Force and cross-head displacement are measured and recorded as a function of time. (See Fig X1.3) Tests were done at room temperature, 300°C, 600°C, and 750°C in air.

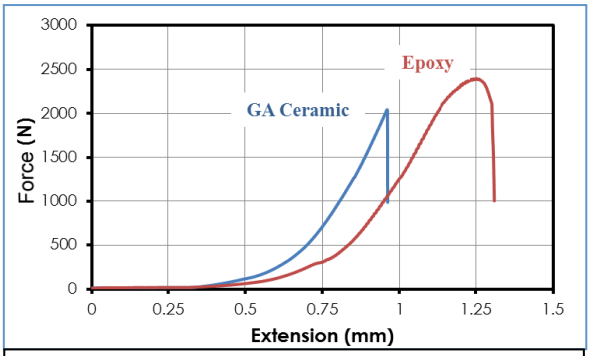

Fig. X1.3 Force- Extension Plots for End-Plug Push Out Tests

X1.6 Gripping Methodology-- Mechanical action grips (wedge grips and collet grips) were initially evaluated for these ceramic specimens, but they commonly failed by specimen slippage and failure in the grips. Adhesive grip bonding was more successful. For room temperature testing a high strength epoxy was used to bond the specimen tube into the split collet. For high temperature testing, metal brazes, sealing glasses, and ceramic adhesives were evaluated.

X1.7 Quality Assurance -- X-ray computed tomography (XCT) was used to image the end-plug fit into the ceramic tube, checking for alignment and fit and adhesive uniformity and voids. (Fig. X.1.1)

X1.8 Alignment Issues and Bending Stresses -- In the test development effort, significant effort was put forth in identifying potential causes of misalignment and how to minimize the resulting stresses. Strain gages around the outer circumference of the end plug section were utilized to measure percent bending during testing. The principle source of these misalignment strains were -- off-angle and off-center loading rod, off-axis misaligned interior face of the end-plug, residual adhesive on the face of the end plug, and out-of-tolerances and poor fit of the test specimen in the grip fixture. The tolerances for misalignment cited in the standard were derived from this testing, and recommendations on compliant layers, U-joints, and hemispherical alignment devices were developed.

X1.9 Nominal joint strengths and nominal burst pressure were successfully obtained for all geometries and material types at room and high temperature with a test efficacy of approximately 85% . A typical example of the force versus extension plots obtained during room temperature testing can be seen in Fig.X1.3. A complete analysis of the test methodology, the resulting data, and a discussion of the test results can be found in the reference literature (1, 2, 3).

X2. Appendix X2 -- Types of Gripping systems

X2.1 In the EPPO test the test specimen tube is secured in a gripping fixture and the gripping fixture is seated on or into the support block. Two types of grip fixtures are commonly used for gripping cylindrical test specimens -- mechanical grip fixtures and adhesive bonded grip fixtures.

X2.2 *Mechanical grip fixtures* – Mechanical grips use the direct application of a force normal to the grip surface of the tube test specimen. These mechanical grips commonly use three types of devices to clamp onto the test specimen -- jaw chuck clamps, collet chucks, and clamping shaft collars (See Figure X2.1). All these gripping devices use radial mechanical force to produce static friction forces which keep the test specimen from slipping out of the grip. The gripping device also act as mechanical stop to hold the test specimen on/in the support block.

Jaw Chucks	Collet Chuck	Shaft Collars

Fig. X2.1 -- Gripping Devices for the EPPO Test

X2.2.1 Jaw chuck clamps use three, four, or six jaws in a self-centering adjustable plate or body to grip the test specimen at 3, 4, or 6 points around the circumference.

X2.2.2 A collet chuck consists of a flexible segmented collet with a cylindrical inner surface and tapered outer surface which is radially compressed in a matching tapered receiving sleeve by the collet cap which pull or pushes the collet into the sleeve. The compression of the collet segments clamps onto the test specimen positioned in the center of the collet. A collet chuck applies clamping force more uniformly around the entire outer surface of the test specimen, as compared to jaw chucks which commonly apply line contacts.

> NOTE -- For collet chucks close tolerances are required for the diameter of the grip section of the test specimen, because of low diametral tolerance in the collet. Actual specimen diameter tolerances will depend on the exact configuration and acceptance dimensions of the collet. A uniform diameter of the tube specimen may be produced by direct machining/turning of the grip section.

X2.2.3 Clamping shaft collars are one- or two-piece sleeves where screws compress the collar around the test specimen. Two-part shaft collars provide more even pressure distribution around the circumference of the test specimen, compared to one-piece split collars. Longer collars provide more grip surface.

X2.2.4 Three important aspects of mechanical grip interfaces are uniform contact force around the test specimen (minimizing point and line stresses), sufficient grip length, and an effective coefficient of friction over the grip/specimen mating surface.

X2.3 *Adhesive bonded grip fixtures* —Adhesive bonded grip fixtures are fitted sleeves, collars, or blocks with a precisely machined internal central bore in which the tubular test specimen is adhesively bonded to secure the specimen into the grip fixture (See Figure X2.2). The bonded grip fixture can be a single piece or a split fixture. Two-part split fixtures (along the length of

the fixture) are more easily assembled with uniform adhesive distribution. Specimen removal is also easier for split fixtures.

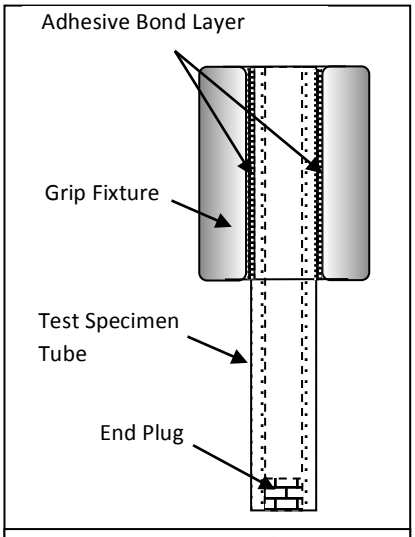

Fig. X2.2 - Schematic of Adhesively Bonded Grip Fixture and Test Specimen

X2.3.1 Both the inner bore of the grip fixture and the OD of the grip section of the test specimen must be precisely machined to provide enough space for the adhesive layer and to keep the test specimen centered and aligned.

X2.3.2 A suitable adhesive should be selected based on the fixture material, the test specimen material, and the selected test temperature. For adhesive gripping at ambient temperatures for the EPPO test, high strength epoxy adhesives are generally suitable for securing the test specimen in the grip fixture. A commonly used adhesive is a two-part room-temperature curing, tough, high strength [20-35 MPa (3-5 ksi)] epoxy. High temperature epoxies can typically be used at temperatures below 250°C, provided enough grip length is provided. At elevated test temperatures (typically greater than 250°C for ceramics), appropriate high temperatures bonding materials (metal solder, metal braze compounds, ceramic cements, sealing glasses) should be selected for gripping that have sufficient bond strength at the desired test temperature.

X2.3.3 The specimen tube must fit snugly in the grip with a thin (~0.1-0.2mm) space for the adhesive, providing uniform bonding contact between the gripped section of the test specimen and the surface of the grip fixture. Bonding can be done on the OD of the specimen for a sleeve grip configuration. Grips with center cores can have bonding on both the OD and the ID of the test specimen.

X2.3.4 The length of the bonded grip section of the test specimen must be long enough to distribute the shear forces across a large bonding surface and keep the shear stress below the failure strength of the adhesive. Insufficient bonding surface in the grips will produce adhesive failure in the grip before specimen failure. As a rule of thumb the bond shear forces which develop from the maximum tensile force in the specimen should produce shear stresses <50% of the nominal shear strength of the grip adhesive. The required length of the bonding grip surface length for tube can be estimated with the following equation.

$$\text{Grip Bond Length} = L_{bond} = (K \times F_{PO}) / [S_{GA} \times (\Pi\ D_{bond})] \quad \text{(X2.1)}$$

Grip Adhesive Shear Strength (S_{GA}) = ($K \times F_{PO}$) / (Grip Bond Area)

Grip Bond Area (OD Bond) = Bond Length (L_{bond}) x Bond Circumference ($\Pi\ d_O$)

Grip Bond Area (Two Sided -- OD and ID Bond)

= Bond Length (L_{bond}) x [Outer Circumference ($\Pi\ d_O$) + Inner Circumference ($\Pi\ d_i$)]

L_{bond} = Required length/depth of the bonding grip section (mm)
K = Selected Safety Factor (2 for 50% reduction)
F_{PO} = Expected push-out force of the end-plug bond (N)
S_{GA} = Shear strength of the grip adhesive (MPa)
D_{bond} = Effective diameter of the bonding zone
[d_o for bonding on the OD circumference;
(d_o + d_i) for bonding on the outer and inner circumferences] Diameters in mm

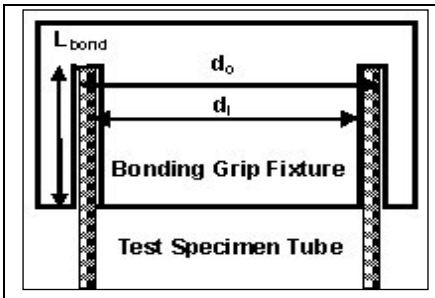

Fig. X2.3 - Schematic of Bonding Grip Fixture

X2.3.5 Elevated temperature adhesives (brazes, sealing glasses, ceramic cements) commonly require a high temperature process step, which can produce residual stresses between the test specimen and the grip fixture after cooldown from the process step. These residual stresses can cause premature failure of the adhesive or the test specimen in the grip section. The residual stresses develop of differences in the thermal expansion coefficients between the specimen material and the grip material. This is a particular issue when ceramic test specimens are bonded into metal fixtures.

X2.3.6 Removal of the test specimen from the grips commonly requires thermal or chemical degradation the adhesive bonding the specimen into the grips.

X3. Appendix X3 -- Verification of Specimen and Load Train Alignment

X3.1 Purpose of Verification—The purpose of this verification procedure is to demonstrate that the grip system and load train couplers can be used by the test operator in such a way as to consistently meet the limit on percent bending as specified in 7.4.3 Thus, this verification procedure should involve no more care in setup than will be used in the routine testing of the actual tensile specimen. The bending under compression force should be measured using verification (or actual) specimens of exactly the same design as that to be used for the EPPO tests. For the verification purposes, strain gages should be applied as shown in Fig. X3.1. Verification measurements should be conducted at the beginning and end of a series of tests with a measurement at the midpoint of the series recommended; whenever the grip fixtures and load train fixtures are changed or installed on a different test machine; whenever a different operator is conducting a series of tests; or when damage or misalignment is suspected.

X3.2 Practice E1012 should be used as a basic guideline for assessing load-train and specimen alignment in the test system.

X3.3 When test conditions, time, and budget permit, each test specimen may be strain gaged and tested per the following instructions to check for misalignment bending stresses as a part of each individual test.

X3.4 Verification Specimen— The verification specimen should be of identical materials and geometry to that being tested with attention to all tolerances and concentricity requirements. However, in the case of CFCCs the type of reinforcement or degree of residual porosity may complicate the consistent and accurate measurement of strain. Therefore, it is recommended that an alternate material (isotropic, homogeneous, and continuous) should be used with elastic modulus, elastic strain capability, and hardness similar to the test material. The verification specimen should be carefully inspected with an optical comparator before strain gages are attached to ensure that these requirements are met. After the strain gages are applied it will no longer be possible to meaningfully inspect the specimen, so care should be exercised in handling and using it.

X3.5 For simplicity, four foil resistance strain gages should be mounted around the circumference (0°, 90°, 180° and 270°) of the verification specimen within 5 mm of the end-plug section, as shown in Figure X3.1. High temperature strain gages can be used for high temperature testing.

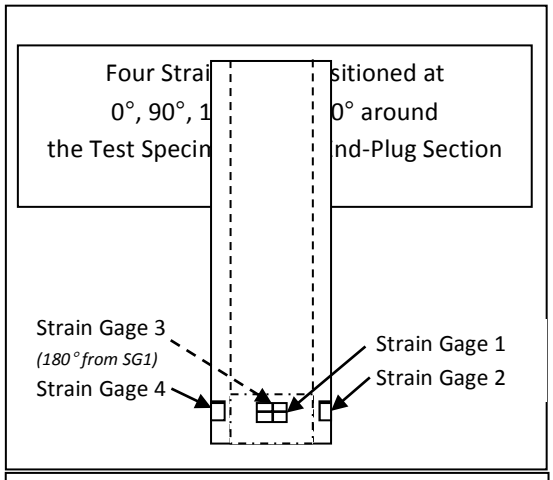

Fig. X3.1 Strain Gage Placement on EPPO Test Specimen

X3.6 Verification Procedure—Procedures for verifying alignment are described in detail in Practice E 1012. However, salient points for EPPO verification/test specimens are described here for emphasis.

X3.6.1 Assemble and align all the load-train fixtures and components in the test system frame.

X3.6.2 Connect the lead wires of the four strain gages to the conditioning equipment and allow the strain gages to equilibrate under power for at least 30

min prior to conducting the verification tests. This will minimize drift during actual conduct of the verifications.

X3.6.3 Mount the verification specimen in the grip fixture and position and align the grip fixture (with the test specimen) in the load train.

X3.6.4 Zero the strain gages of the verification specimen in the load train, without the loading rod in position.

X3.6.5 Insert and align the loading rod in the test specimen. Apply a sufficient force to the verification specimen to achieve a mean strain (among the four strain gages) equal to either one half the anticipated strain at the onset of the cumulative fracture process (for example, matrix cracking stress) in the test material or a strain of 0.0005 (that is, 500 microstrain) whichever is greater. Note that it is desirable to record the strain (and hence percent bending) as a function of the applied force to monitor any self alignment of the load train.

X3.6.6 Calculate the maximum percent bending as follows referring to Fig. X3.1 for the strain gage numbers. Percent bending in the verification plane of the end-plug section is calculated as follows (per E1012).

Average axial strain $a = (e_1 + e_2 + e_3 + e_4)/4$ (X3.1)

where:

e_1, e_2, e_3, *and* e_4 = the measured strains at the four strain gage locations; the subscript indicates the order of the strain gages around the specimen.

Local bending strain $b_1 = e_1 - a$ (X3.2)

$$b_2 = e_2 - a$$

$$b_3 = e_3 - a$$

$$b_4 = e_4 - a$$

The maximum bending strain $B = \frac{1}{2}\left[(b_1 - b_3)^2 + (b_2 - b_4)^2\right]^{\frac{1}{2}}$ (X3.3)

The maximum percent bending strain $PB = (B/a) \times 100$ (X3.4)

REFERENCES

1. Khalifa, H.E.; Deck, C.P.; Gutierrez, O.; Jacobsen, G.M.; Back, C.A. “Fabrication and Characterization of Joined Silicon Carbide Cylindrical Components for Nuclear Applications,” Journal of Nuclear Materials, 457, (2015), 227-240.

2. Khalifa, H.E.; Jacobsen, G.M.; Gutierrez, O.; Back, C.A. “Out-Of-Pile Characterization And Testing of Joined Cylindrical Components for SiC-Based Nuclear Fuel Cladding,” Transactions of the American Nuclear Society, 109, (2013), 419-422.

3. Jacobsen, G.M.; Khalifa, H.E.; Kearns, Y.; Gutierrez, O.; Deck, C.P.; “High Temperature Testing of Geometrically Relevant, Nuclear Grade Silicon Carbide Joints,” Transactions of the American Nuclear Society, (2015), in press.